SHELBURNE SUBBASIN POSTMORTEM ANALYSIS
REVIEW OF CHESHIRE L-97 AND MONTEREY JACK E-93

COMPARISON WITH OETR 2011 PLAY FAIRWAY ANALYSIS

Shelburne Subbasin Postmortem Analysis

Shell Exploration Program in Nova Scotia

In 2012 and 2013, Shell acquired 6 parcels in the Shelburne Subbasin with a ~$US1.1 billion exploration program planned over a 6 year period. A 3D wide azimuth seismic dataset was acquired in 2013 in water depths over 1500 meters. Two exploration wells were drilled in 2016 and 2017: Cheshire L-97 and Monterey Jack E-93. These were the first exploration wells on Nova Scotia's deep water margin since 2004 and the first since Crimson F81 in the Central Scotian slope area.

The objective of both wells was to test the hydrocarbon potential of offshore Nova Scotia. The wells had several targets:

- Primary target: Lower Cretaceous turbidite sandstones interpreted as being the downdip equivalent to the Missisauga deltaic sandstone observed in the up-dip shelf wells.
- Secondary target: downdip equivalent to the Mohawk/Mic Mac sandy formation which is observed on the shelf in the Glooscap and Moheida wells (PL. 1.1.4).
- Additional to the secondary target: a potential Jurassic (Tithonian) source rock identified on the 3D seismic.

The wells did not encounter the targeted reservoirs or an Upper Jurassic source rock.

The objective of this project is to reassess and compare the 2011 Play Fairway Analysis in light of Shell's well results and their impact on the understanding of the Shelburne Subbasin petroleum system. This postmortem analysis is presented as follows:

- A review of the geological models with a comparison between the initial Beicip Franlab PFA geological model (OETR, 2011) based on a literature overview and Shell's exploration hypothesis
- A comparison between stratigraphic modelling predictions from the 2011 PFA study and Shell's well results
- A review of stratigraphic plays
- A postmortem structural analysis of Shelburne Subbasin with an overview of structural traps
- A comparison between basin modelling predictions from 2011 and Shell's well results

Summary of the Main Conclusions

Geology and Stratigraphy

The geological model defined by Shell for the Shelburne Subbasin is different from what was published in the literature and what was used in the 2011 PFA. Wells Cheshire L-97 and Monterey Jack E-93 confirmed the published models (Table 1).

Shell geological model for Shelburne Subbasin	Literature and PFA 2011 geological model for Shelburne Subbasin	Well results
Sable delta sole source of clastics through the Mohican graben	Multiple entry points. Sable delta influence limited to Sable Subbasin	
Clastic dominated margin	Starved margin	Low sedimentation rates; traces of sand; no reservoirs;
MicMac/Mohawk mid-late Jurassic sandstone in deep water	Abenaki Carbonate rim limit clastic input into deep water. Predominance of carbonate and shale facies	Predominance of shale and carbonate facies
Possible Tithonian and Toarcian SR	Possible Tithonian and Early Jurassic SR	No Tithonian SR Early Jurassic not reached

Table 1: Comparison of geological models: Shell, literature + 2011 PFA, and Shell well results.

The new Shell wells are consistent with the PFA 2011 stratigraphic modelling results except for the lowermost part of the wells (Late Middle Jurassic/Early Upper Jurassic). This is due to the lack of bathymetric constraint at the time of the 2011 PFA which is the source of the discrepancy with the stratigraphic model.
A fast track analysis of 3D seismic data and review of newly obtained biostratigraphic data on a Jurassic section led to the following conclusions:

- **Observations for the Jurassic**: paleobathymetry estimates conducted on Jurassic sediments of Monterey Jack E-43 and Cheshire L-97 indicate that prior to the Late Jurassic, the Scotian Slope was shallower than previously assumed in 2011. The presence of shelfal carbonates as old as Bajocian and the occurrence of Late Triassic salt underneath them imply that a carbonate ramp system likely developed throughout the Early to Middle Jurassic interval across the Shelburne Subbasin. A calcarenite facies belt is assumed to be present in the proximal part of Shelburne Subbasin, north of Shell's exploratory wells. Calcarenitic ramp facies are usually prolific HC reservoirs especially when their porosity is enhanced through dolomitization/dissolution processes.
- **Observations for the Cretaceous:** most of the area was bypassed by sediment during the Hauterivian and Cenomanian. Sediment is stored downslope in mini-basins or far out onto the abyssal plain as turbidite fans where sandstone facies may be expected. For the Hauterivian – Albian interval, seismic data shows a sediment thickening until meeting a salt wall, but lithofacies at wells and regional correlations suggest a rather shale dominated interval. Sandy facies is expected in upper to mid slope canyon for the Tertiary section, particularly the Early Eocene and Oligocene, and potentially from the K130 interval. It appears that both wells are still within the by-pass area and silt/shale dominated zone.
- Shell's wells were drilled in too deep water to sample Eocene reservoirs and too shallow water depositionally to encounter Cretaceous deep-water reservoirs. They were not properly located and too shallow to sample Early - Mid Jurassic carbonate reservoirs.

Age	Formation	Facies	Risk	Shell Targets	Play Tested	Study
Lower Jurassic	Iroquois	Carbonate Ramp	Undefined		No	Postmortem 2019
Middle Jurassic	Mohican	Clastics	High	Mohican Formation sands	No	PFA 2011
	Baccaro	Reef	Low		No	PFA 2011
		Oolites	High		No	
		Slump	Medium		No	
Upper Jurassic	Mic Mac	Delta top	High	Mohawk/MicMac Formation sands	No	PFA 2011
Berriasian	Lower Missisauga	Delta top	High		No	PFA 2011
		Turbidite	Medium		No	
Valanginian/ Hauterivian	Middle Missisauga	Delta top	Medium	Down dip turbidite equivalent of the Missisauga Fm.	No	PFA 2011
		Turbidite	Medium		No	
Albian	Logan Canyon	Turbidite	Medium		No	PFA 2011
Albian	Cree/Marmora	Low stand fan	Medium		No	PFA 2011
Tertiary	Banquereau	Slope fan	Undefined		No	Postmortem 2019
		Drift and Channelized sand complex	Undefined		No	Postmortem 2019
		Turbidite	Undefined		No	Postmortem 2019

Table 2: Summary of studied plays from the 2011 Play Fairway Analysis and the current postmortem study.

Structural analysis

Post-drill structural analysis shows that targeted structures were misinterpreted. Both structures were interpreted as 'turtle-like' structures with 3/4-way closure. Our analysis indicates:

- **Cheshire is an "extensional anticline"** that mimics a turtle structure but is not really an inverted, early-formed mini-basin between two diapirs (salt diapir is still present below the anticline). Moreover (as shown on the structural map) no real 4-way closure exists.
- **Monterey Jack is a drape structure on top of a diapir**. The formation mechanism appears to be related to the relative collapse by salt withdrawal around an early asymmetrical salt dome. This results in an apparent drape structure with a 4-way dip closure for all horizons from Early Jurassic through the Late Cretaceous. The closed structure is no more than 12 km^2 for a vertical relief of 125 meters.

Most of the analysed data indicate that salt tectonics started very early, probably during the Early Jurassic, with salt diapir tongue deposition reaching the sea bottom. Deposition and distribution of Early Jurassic sediments were not continuous and ubiquitous since salt highs and ridges already existed. This implies that the assumption (made in PFA 2011) of a simple ubiquitous Early Jurassic source rock distributed everywhere as a continuous unit coincident with the primary salt basin is unlikely. **A more likely scenario is that any Early Jurassic source is distributed in a series of discrete mini-basins**.

Shelburne Subbasin Postmortem Analysis

Basin Modelling Postmortem Analysis

New well data (Cheshire L-97 and Monterey Jack E-43) has been compared with PFA 2011 3D model results in order to test the predictivity of the model. Temperatures and pressures are available for Cheshire L-97 only, while vitrinite was sampled in both wells. Simulated data display a good fit with observed data in both wells, which indicates an excellent predictivity of the PFA-2011 3D model (at a given depth the pressure, temperature and maturity level are well predicted).

Significant salt tectonism in the deep basin defines the restricted drainage area (<100km^2 for Cheshire L-97 & <200km^2 for Monterey Jack E-43) leading mostly to vertical migration and potential limited lateral connection between small drainage areas. Closed traps have a relatively small closure areas (often <10 km^2) too. According to the model the largest accumulations may hold 50 to 150 MMboe.

Lack of hydrocarbon (HC) accumulation in drilled wells may result from:

- A risk of **reservoir presence** and carrier beds in Cretaceous and Upper Jurassic units. Generated HCs could not concentrate in large reservoirs. Only pervasive HC accumulations in close vicinity to SR layers may be expected. This is a possible explanation of the diffuse gas observed on mud logs (small amount of in-situ generated biogenic and/or thermogenic gas in low-TOC shale intervals).
- A risk of the **presence of active source rocks (SR).** There is no direct evidence for the presence of a prolific source rock in the deep Shelburne Subbasin (potentially the Pliensbachian or Toarcian SR, not yet penetrated).
- A risk of **charge efficiency** (in addition to the SR risk) due to small drainage areas and structure sizes, poor lateral connection of drainage areas (isolated mini-basins between salt bodies) and mostly vertical migration possibly along salt diapirs (drainage <100 km^2 for Cheshire & <200 km^2 for Monterey Jack). Observed high pressure (as predicted by the model) confirms the lack of efficient lateral connection at large scale. In these conditions, a very rich source rock would be required for charging large traps.

New Evidence for Active Thermogenic Source Rock in the Shelburne Subbasin

Several elements still favor an active petroleum system in the Shelburne Subbasin:

- Presence of a thermogenic (isotopes, fluid inclusions) gas flare in a carbonate layer (Scatarie Mbr.) near the TD of Monterey Jack E-43 suggests the presence of an active source rock in the Early-Middle Jurassic (not penetrated).
- DHI and gas hydrate mapping performed on seismic data indicates a consistent fit between DHI location and the area of maximum maturity (potential Pliensbachian SR within the gas window, VR0>1.2%; Fig. 2). This correlation strongly supports the existence of at least one active petroleum system. Hydrocarbons (condensate and gas at present day) generated in potential Early Jurassic source rocks would migrate vertically up to Cenozoic sediments and would often accumulate on top of the salt diapirs.
- Several hydrocarbon seeps have been identified during seabed surveys conducted by NSDEM in the area of interest (e.g., APT 2019 – Fig. 2).

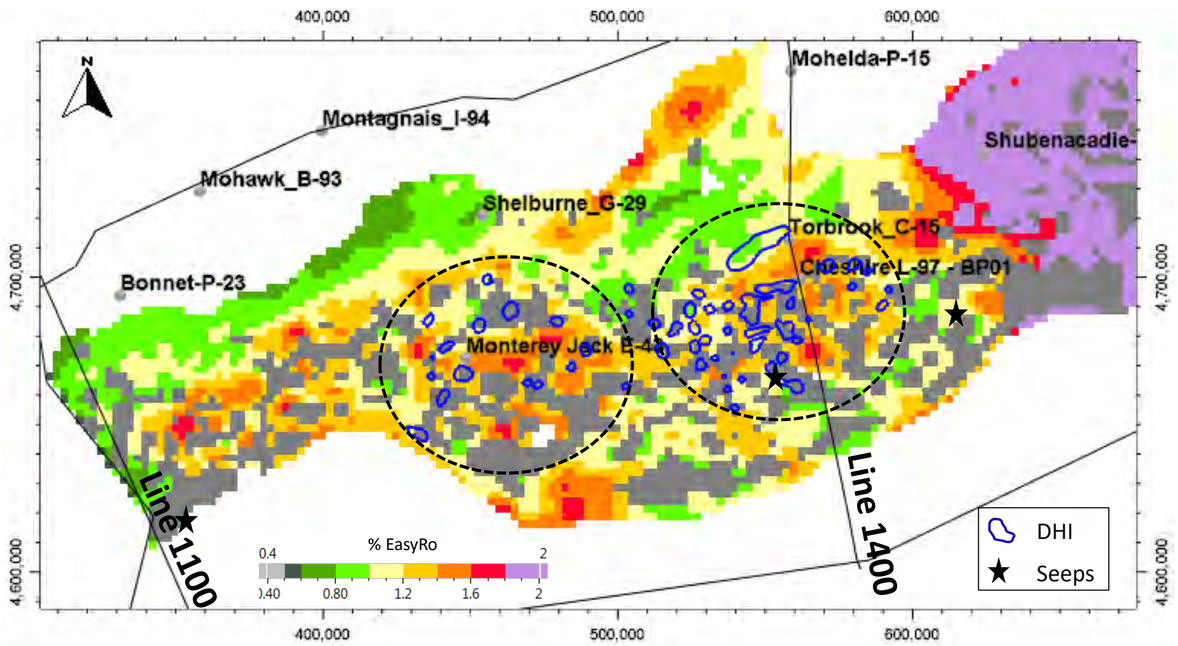

Figure 2: DHI and gas hydrate locations overlaid on top of the Pliensbachian maturity map

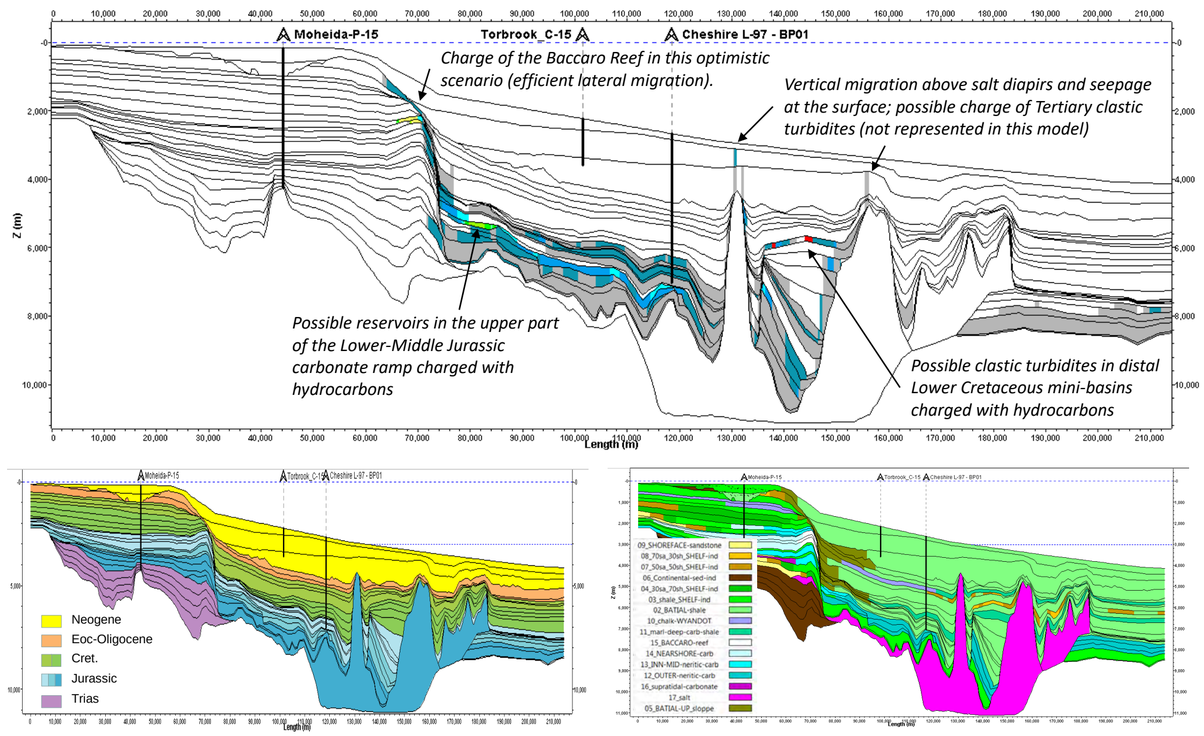

Figure 3: 2D basin modelling result on NovaSpan 1400 from the 2011 PFA predicting HC accumulation in the lower-mid Jurassic carbonate ramp play and in the lower Cretaceous turbidites in the mini-basin south of Cheshire,

General Conclusions

The Shelburne Subbasin post Shell well analysis conclusions are as follows:

- The 2011 Play Fairway Analysis appears to be regionally accurate and predictive for reservoir distribution in the Shelburne Subbasin.
- Shell's wells do not rule out any of the potential plays as the wells did not encounter the targeted reservoir and source rock. The Shelburne Subbasin petroleum potential predicted in PFA 2011 remains unchanged excepted for the lack of Tithonian source rock. Proper stratigraphic and structural traps remain untested.
- Despite the high risk of certain petroleum system elements identified in PFA 2011, the potential of several new plays should be re-evaluated based on new data.
- There is a potential **Tertiary and Lower Cretaceous clastic turbidite play**. The **Tertiary play** appears to be a good candidate for HC-bearing reservoir but this play **was not evaluated in PFA 2011**.
- There are potential reservoirs in more proximal parts of the **Lower-Middle Jurassic carbonate ramp play** (shallow marine carbonates; See PL. 1.2.5 to 1.2.7).
- Hydrocarbon accumulations are predicted in the Lower/Middle Jurassic carbonate ramp, in particular in its proximal parts where better reservoirs may be expected (in accordance with the new concepts).
- There is also a possible charge of Lower Cretaceous turbidites south of Cheshire, in the mini-basin where anomalies have been detected on the 3D seismic (see PL.1.1.6).
- Trap effectiveness (with reservoir rocks) underneath allochthonous salt bodies has not been tested and represents another potential new play

1.1 Geological Model

New Seismic Data and Well Locations

In 2012 Shell acquired 6 parcels in the Shelburne Subbasin with a $1 billion exploration program planned over a 6 year period. A 3D wide azimuth seismic dataset was acquired in 2013 in water depth over 1500 m (Figure 1.1.1). Two exploration wells were drilled in 2016 and 2017 (Tables 1.1.1 & 1.1.2): Cheshire L-97 and Monterey Jack E-93.

Well ID	Coordinate Ref. Sys.: NAD27 UTM 20N				WD	KB	TD (TVD)	Well Termination Record
	Lat	Long	X(m)	Y(m)				
Cheshire L-97	N 42° 26' 37.325"	W 62° 14' 53.096"	561,839.45	4,699,101.42	2143	32	7064,9	21-09-2016
Monterey Jack E-43	N 42° 12' 16.4285"	W 63° 37' 29.9601"	448,404,48	4,672,464.27	2119	32	6691	21-01-2017

Table 1.1.1: General well information from Shell's end of well report

Shell Well Objectives

The wells had several targets (Table 1.1.2):

- Primary target: Lower Cretaceous turbidite sandstones interpreted as being the downdip equivalent to the Missisauga deltaic sandstone observed in Sable Subbasin.
- Secondary target: Downdip equivalent to the Mohawk/Mic Mac sandy formation which is observed on the Shelf in the Glooscap and Moheida wells (PL. 1.1.4).
- Additional to the secondary target: one potential Jurassic source rock - the Tithonian SR potentially identified on the 3D seismic data.

Based on Shell's end of well reports, criteria to deepen the wells into the secondary targets were not met and so the wells were stopped within the Bajocian (Cheshire L-97) and Callovian (Monterey Jack E-43).

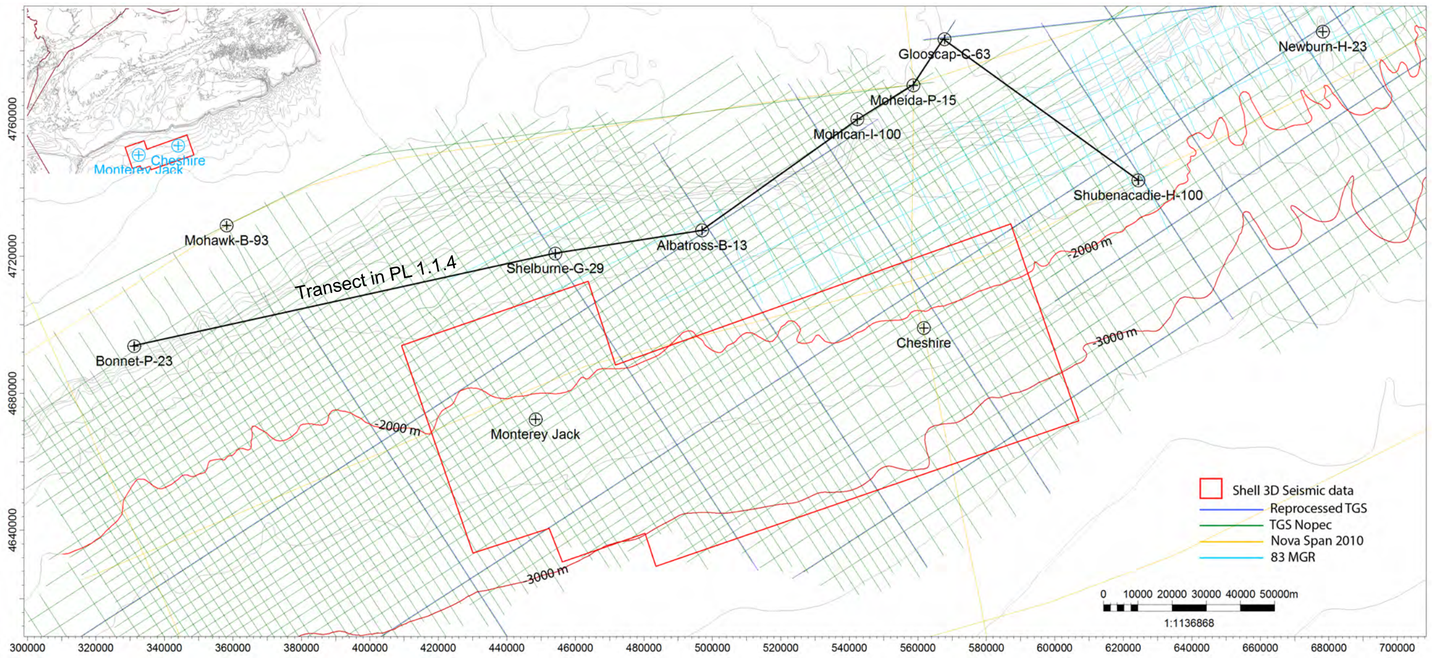

Figure 1.1.1: Location of Shell 3D seismic cube and associated wells (Cheshire L-97 and Monterey Jack E-93)

	Well tops	Age	Surface Type	Cheshire L-97	Monterey Jack E-43	Target	Lithology Expected	Lithology encountered
Tertiary	T29	Oligocene (Rupelian)	Unconformity	4115	4054			
	T50	Eocene (Ypresian)	Unconformity	4435	4366			
Cretaceous	K94	Cenomanian	Unconformity	4785	4890			
	K101	Albian	Unconformity	5000	5229			
	K130	Hauterivian	MFS	5616	5764	Down dip turbidite equivalent of the Missisauga Fm. Deltaic system in Sable Subbasin	Interbedded sandstone, siltstone and Shale	Claystone and marlstone; fine grained sandstone stringers
	K137	Valanginian	Unconformity	5863	6190			
Jurassic	J150	Tithonian	MFS	5911	6271	potential source-rock interval in the Jurassic (Tithonian) & time-equivalent Mohawk/MicMac Formation and Mohican Formation sands that are recognized on the shelf	Possible Organic-rich shale, calcareous shale and sandstone	Shale, interbedded claystone and marlstone, Limestone
	Top Callovian	Callovian	MFS	6324	6657		Interbedded sandstone, siltstone and Shale	
	J163	Callovian	MFS	6456				Marlstone, Limestone ; fine grained sandstone stringers
	Late Bajocian	Bajocian	MFS	6953				
	Early Bajocian	Bajocian	MFS	7041				

Table 1.1.2: Well geological summary information. Target and lithological information are from Shell's end of well reports. Well tops and related information are from a 2018 RPS biostratigraphic report completed for the Nova Scotia Department of Energy and Mines and an NSDEM seismic data QC.

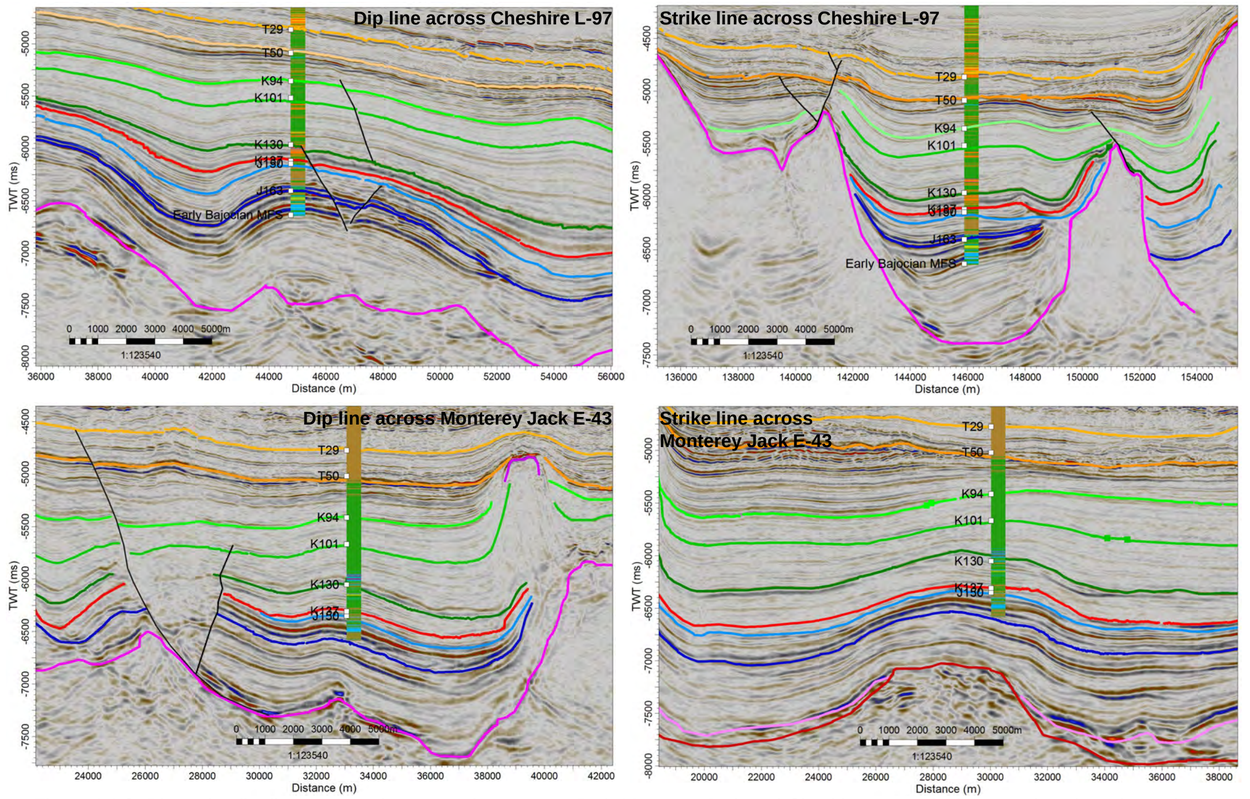

Figure 1.1.2: Dip and strike lines across the targeted structures. Both Monterey Jack and Cheshire targeted what was thought to be turtle back structures (see subchapter 1,3 for more detailed analysis). All figures are at the same scale.

Shell Exploration Failure

Cheshire L-97 and Monterey Jack E-43 were the first exploration wells on the margin since 2004 and the first since Crimson F81 on the Central Scotian Slope. Results were disappointing: the wells found no reservoirs and no upper Jurassic source rock (Figures 1.1.5a and b). This led to two questions:

- Where could sandy reservoirs be found?
- Is a Lower Jurassic or older system rock the only potential source of hydrocarbons?

Along the entire Scotian Margin, reservoir is considered the main challenge for O&G exploration. Reservoir risk assessment requires robust structural and stratigraphic models.

The hypothesis for the presence of Early Cretaceous sandstone reservoir relies on the observation made from wells that net to gross sand decreases on the shelf from the Sable Subbasin to Shelburne Subbasin. Well correlations suggest a net to gross decrease from 49% to 22% from wells Glooscap C-63 to Mohican I-100 (Figure 1.1.3), which is approximately 60 km upslope from Cheshire L-97 (Figure 1.1.1). Evidence for numerous canyons along the slope may have led to the conclusion that shelfal deltaic sands were transferred down to the basin becoming trapped within a salt induced mini-basin. A similar assumption was made for the Mid – Upper Jurassic interval, for which presence of MicMac – Mohawk sands were inferred to be present in deep water.

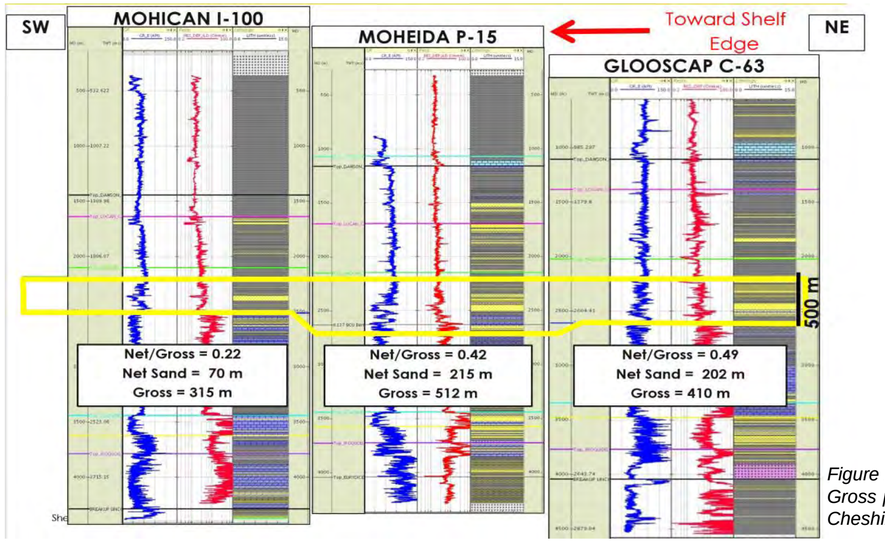

Figure 1.1.3: Lithostratigraphy and Net to Gross properties of 3 wells upslope from Cheshire L-97

Seismic Interpretation at Well Locations and Results

Lower Cretaceous and Early – Mid Jurassic targets were likely based on seismo-facies, amplitude analysis and a geological model. The high amplitude facies at Top Jurassic could have been interpreted to be a potential Jurassic source rock (Figures 5a and b). Targeted structures were thought to be turtle back-like structures (Figures 1.1.6a and b), which *a posteriori* appeared to be a misinterpretation (see sub chapter 1.3).

Instead of finding reservoirs, source rocks and evidence for hydrocarbons, the two wells penetrated thick successions of claystones, calcareous mudstones, marls and limestones (Figures 1.1.4 a and b). A few thin-bedded fine sandstones were observed within the Callovian in Cheshire L-97 (Figures 1.1.2 and 1.1.4a). Seismic facies prediction appeared to be inaccurate, particularly for the Jurassic section. The well results are consistent with previous experience in terms of reservoir risk and show that any likely source of charge most likely must be older than Middle Jurassic.

Failure of these two wells raises several questions:

- What are the implications of the discrepancies between facies prediction and well results?
- How representative are the lithologies found in the wells of the Shelburne Subbasin?
- Is the failure related to the play tested?
- How to de-risk reservoir presence in the Shelburne Subbasin?

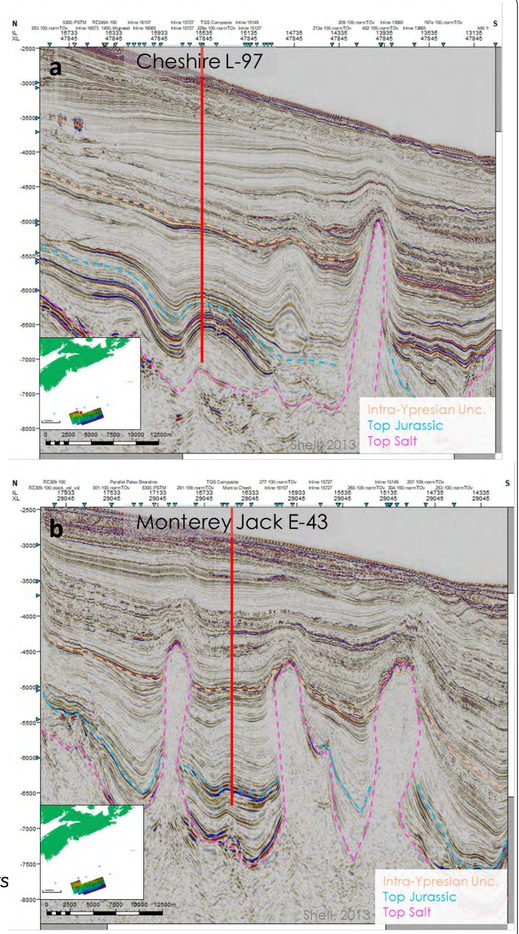

Figure 1.1.5: Seismic Dip Lines through drilling targets (a) Cheshire L-97 and (b) Monterey Jack E-43)

Figure 1.1.4 a: Cheshire L-97 stratigraphic column (from Cheshire L-97 end of well report)

Figure 1.1.4 b: Monterey Jack E-43 stratigraphic column (from Monterey Jack end of well report)

Cheshire L-97A Stratigraphic Column

TVDSS (m)	Epoch	Interval Tops	Lithology	Seismic Section Shell 40Hz Pseudo Impedance Black is Hard; Orange is Soft	Measured Depth (m)	Top Depth TVDSS (m)	Thickness TVD (m)	Offshore Nova Scotia Formation Name	Lithology Comment
2500	Pleistocene-Pliocene?	WB	Riserless	36° 28°	2,175	2,143	521	Banquereau	*Riserless Section: No samples to surface. This section is expected to be the hemipelagic wedge consisting mostly of hemipleagic mud, mudstone and claystones.*
3000		T2			2,696	2,664	644	Banquereau	*Riserless Section: No samples to surface. This section is expected to be the hemipelagic wedge consisting mostly of hemipleagic mud, mudstone and claystones.*
3500	Miocene	T6		22°	3,340	3,308	575	Banquereau	Dominated by reactive hemipelagic dark grey claystone with occasional very fine grained siltstone.
4000	Oligocene / Eocene / Paleocene	T20		18°	3,915	3,883	522	Banquereau	Very fine grained siltstone with trace glauconite, occasional very calcareous shales and marlstones, and dark grey claystones.
4500	Upper Cretaceous	T50			4,437	4,405	121	Banquereau	Dark grey claystone with occasional very calcareous shales and marlstones.
		K87			4,558	4,526	224	Dawson Canyon	Composed of mostly dark grey claystone with occasional brick red claystones.
5000	Lower Cretaceous	K94		16°	4,782	4,750	976	Naskapi Shale	Homogenous grey to dark grey claystones with trace mica. Base of interval is a tight, olive grey siltstone.
5500		K129		14°	5,758	5,726	655	Verrill Canyon	Capped by a tight siltstone and section consists of alternating calcareous shales and marlstones. Base of unit is a hard marlstone.
6000	Upper Jurassic								
6500	Middle Jurassic	J163			6,413	6,381	334	Misaine Member	Capped by shelfal claystone. Section consists of interbedded siltstone, claystone, and sandstone.
		J166+			6,747	6,715	321+	Scatarie Fm.	Grainstone, oolitic limestone, and traces of claystone, sandstone, and siltstone. Grading to packstone at the base.
7000					7,068	7,036	-	Total Depth	Alternating cycles of limestones (packstone to wackestone) and claystones.

Lithology Legend: Claystone; Siltstone; Sandstone; Marlstone; Limestone

Monterey Jack E-43A Stratigraphic Column

TVDSS (m)	Epoch	Interval Tops	Lithology	Seismic Section WG PSDM Pseudo Impedance Blue is Hard; Red is Soft	Measured Depth (m)	Top Depth TVDKB (m)	Thickness TVD (m)	Offshore Nova Scotia Formation Name	Lithology Comment
2500	Pleistocene-Pliocene?	WB	Riserless	36° 28°	2,182	2,150	613	Banquereau	*Riserless Section: No samples to surface. This section is expected to be the hemipelagic wedge consisting mostly of hemipleagic mud, mudstone and claystones.*
3000		T2			2,813	2,781	354	Banquereau	*Riserless Section: No samples to surface. This section is expected to be the hemipelagic wedge consisting mostly of hemipleagic mud, mudstone and claystones.*
3500	Miocene	T6		22°	3,167	3,144	525	Banquereau	Dominated by reactive hemipelagic dark olive grey claystone with few parts grading to siltstone.
4000	Oligocene	T18		18°	3,692	3,660	896	Banquereau	Dominated by reactive hemipelagic dark olive grey claystone with few parts grading to siltstone.
4500	Eocene / Paleocene	T50.5			4,561	4,529	96	Banquereau	Dark grey claystone with occasional very calcareous shales and marlstones.
5000	Upper Cretaceous	K82			4,657	4,625	543	Dawson Canyon	Composed of mostly dark grey claystone with occasional marlstones.
5500	Lower Cretaceous	K101		14°	5,200	5,168	476	Naskapi Shale	Homogenous grey to dark grey claystones with trace pyrite. Trace red mudstone stringers.
6000		K129			5,676	5,644	966	Verrill Canyon	Section consists of claystones and marlstones with variable amounts of calcareous content. Trace fine grained sandstone stringer. Base of unit is a hard limestone.
6500	Upper Jurassic / Middle Jurassic	J155			6,642	6,610	50+	Misaine Member	Misaine Member Shale is thin dark grey to black claystone. Section below consists of thin interbedded claystones and marlstone.
7000					6,692	6,660	-	Total Depth	

Current State of Geological Knowledge Regarding the Shelburne Subbasin

The Shelburne Subbasin is a subdivision of the southwestern part of the Scotian Margin. Rifting of the margin started in the early Triassic and opening of the Atlantic Ocean started in the early Jurassic (Figure 1.1.6).

The earliest basin infilling occurred during Triassic rifting and consists of red continental clastic sediments and evaporites (**Euridice and Argo Formation**). During the **Early Jurassic**, rift basins were gradually infilled by clastic and carbonate sediments. Fully marine conditions developed by **Mid Jurassic**, leading to a set of alluvial plains, deltaic and carbonate environments. Subsequent to the **Avalon Uplift** in the north and New England hot spot uplift in the south, the **Early Cretaceous** was dominated by deltaic progradation and shelf clastic deposits. **Late Cretaceous / Early Tertiary** sedimentary deposits were dominated by transgressive shale, sporadic influxes of deltaic sands, limestone, and chalk sequences. During the Paleo – Eocene transition, the southern part of the margin was destabilized by the Montagnais bolide impact (Deptuck and Campbell, 2012).

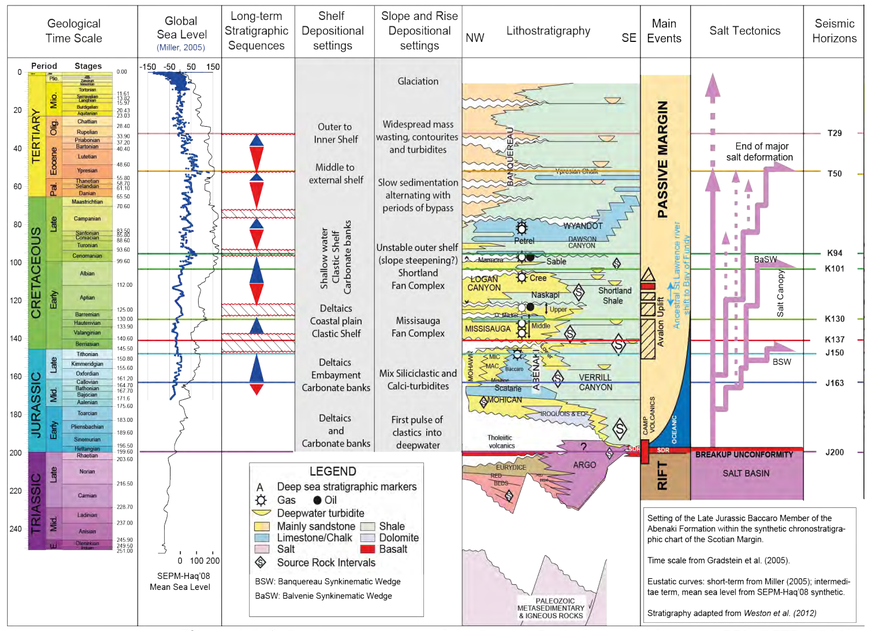

Figure 1.1.6: Stratigraphic chart of the Scotian Basin (adapted from the PFA: OETR, 2011).

Figure 1.1.7: a) generalized facies distribution of Abenaki and equivalent formations; b) facies relationships within the Missisauga Formation on the LaHave Platform (adapted from Wade and MacLean, 1990)

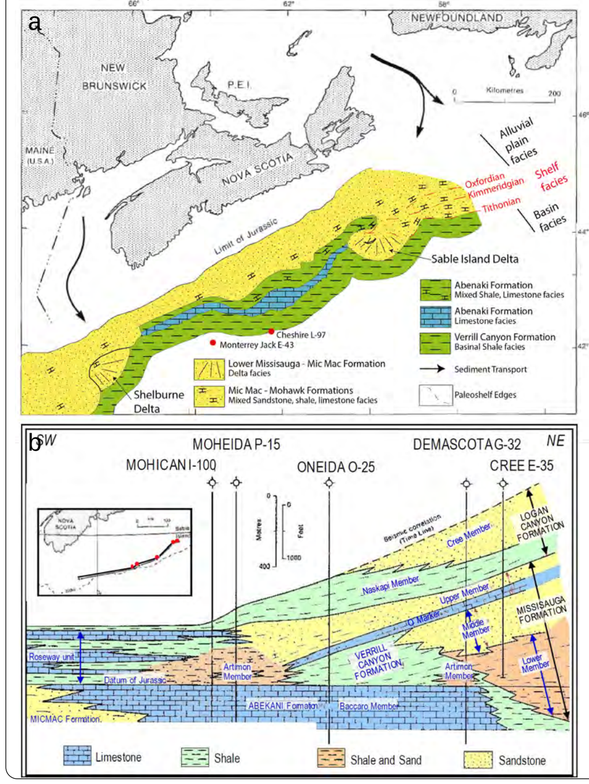

The difficulty in predicting facies distribution along the Scotian Margin is that it was a mixed clastic carbonate system for the entire Jurassic and part of the Early Cretaceous (Figures 1.1.7 a, b and 1.1.8, PL. 1.4, sub chapter 1.2).

The Sable and Shelburne deltas begin to develop early in the Jurassic in the northern and southern parts of the margin respectively (Figures 1.1.7 & 1.1.8). In the meantime thick carbonate successions developed away from these major deltas, covering most parts of the margin (Figures 1.1.7 a and b). Carbonate thickness increases southward to reach maximum thickness in the Shelburne Subbasin. These Jurassic carbonate successions correspond to the **Iroquois** and **Abenaki Formations**, the latter being divided into **Scatarie, Misaine** and **Baccaro Members** (Kidston et al., 2005; Wade and MacLean, 1990).

The **Iroquois Formation** covers the timespan between the Hettangian and Bajocian (Figure 1.1.6). It is a transgressive formation consisting primarily of dolomite deposited under slightly restricted marine conditions. Dolomite is observed until the Toarcian but can extend until the Bathonian in places (OERA, 2015). The Iroquois Formation is coeval with the lower part of the Mohican Formation due to coexisting carbonate rims and deltaic formations (Shelburne delta to the south).

Significance of Abenaki Formation:

The Abenaki Formation is a limestone-dominated unit corresponding to a prominent carbonate bank facies (Figures 8a and b). The Formation reaches its maximum extent at the transition between the Sable Subbasin and Shelburne Subbasin (Wade and MacLean, 1990) where Shell's parcels are located. It forms an outer shelf carbonate bank complex and is subdivided into three Members. Basin slopes show evidence for carbonate breccia accumulations across the Shelburne Subbasin and toe-of-slope carbonate fans (OETR, 2011; OERA, 2015).

The **Scatarie Member** covers the Bajocian – Callovian interval. Proximal facies are predominantly shallow water oolitic limestones. Near the Sable and Shelburne deltas, offshore sedimentation is predominantly a mix of calciturbidites and siliciclastic turbidites until the Callovian.

The **Misaine Member** is a shale-dominated unit deposited during the Callovian. It is the only clastic-dominated unit of the Abenaki Fm (Kidston et al., 2005; Wade and MacLean, 1990). It is a transgressive facies and overlies the Scatarie Mb. The Misaine member is composed of dark grey calcareous shales with minor laminated limestone pinching out landward over the platform with interbedded proximal sandstone. The Misaine Member is representative of the Callovian regional transgressive event and is well developed along the Jurassic shelf margin (Wade and MacLean, 1990). It's the only time interval that allows for clastics to cross the shelf where carbonate banks are present.

The **Baccaro Member**, which developed from early Oxfordian to Tithonian times, is the thickest and best developed carbonate unit of the Abenaki Formation. It is composed of numerous aggrading and prograding limestone parasequences with very minor shale and sand intervals. The width of Baccaro Member varies, but on average comprises a 15 – 20 km wide belt that follows the Jurassic hinge line and defines the seaward limit of the Abenaki platform margin (Kidston et al., 2005; Wade and MacLean. 1990).

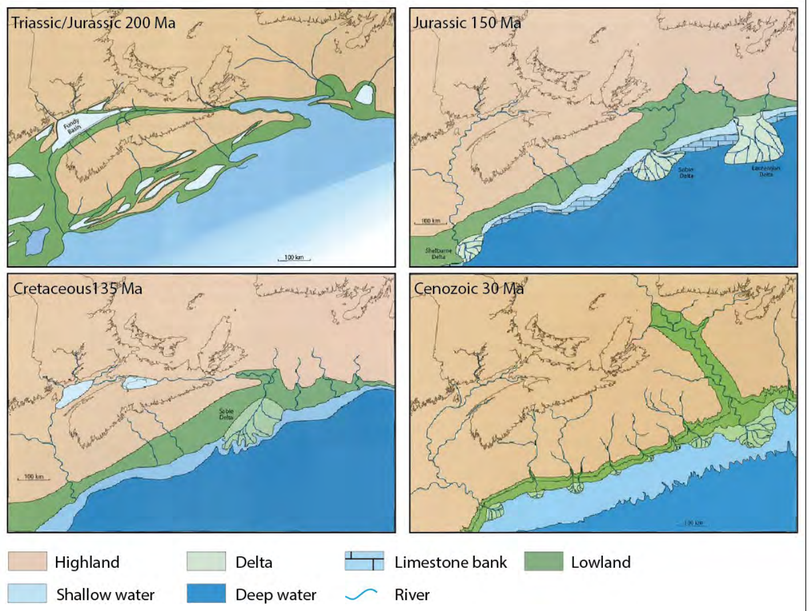

Figure 1.1.8: Regional paleogeography of the Maritimes over the last 200 million years (adapted from Fensome and Williams, 2001)

Source to sink clastic sediment

The Shelburne Subbasin covers an approximate area of 100,000 km². It is fed clastic sediment by a large drainage system from northeastern flank of the Appalachian Orogeny, extending from Massachusetts to New Brunswick (Figure 1.1.9). Secondary clastic sources from the Meguma Terrane are also recorded in wells in the northernmost part of the Subbasin (Figures 1.1.8 and 1.1.9; Chavez et al., 2018; Zhang et al., 2014). These secondary sources are small, short rivers with sufficient relief to supply a significant amount of lithic clasts. They are interpreted as being coastal rivers in an arid climate, likely to be flash flood dominated (Nagle et al., 2019).

The size of the drainage systems and organisation of related tributaries are only inferred, nonetheless shelf and deep water sedimentary records show that it provided a continuous supply of sediments that accumulated in a number of complex, interconnected subbasins.

Work on sediment provenance from mineralogical studies (Figure 1.1.9) has shown it's unlikely the Sable Delta extended out to wells in the Shelburne Subbasin. In fact, the Shelburne Delta was the main clastic supplier to the Shelburne Subbasin and supplies were limited to its southern part (OERA, 2015). In the Shell acreage, only rivers from Meguma Terrane provided clastic sediment to the subbasin (Figure 1.1.9).

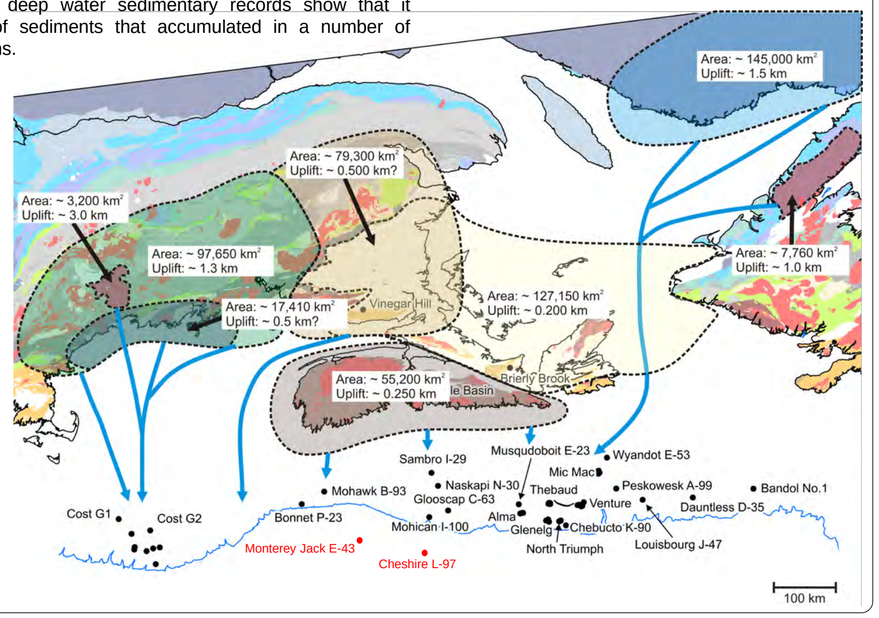

Figure 1.1.9: Map showing drainage patterns inferred from mineralogical studies by researchers at Saint Mary's University, NS (Chavez et al., 2018 modified by Nagle et al., 2019; Zhang et al., 2014)

Well Correlation Across the Shelburne Subbasin

This plate is taken from PFA 2011 (OETR, 2011). The transect highlights the lack of clastic reservoirs across the margin except in Glooscap C-63 which is located on the shelf. It is notable that all wells show a predominance of carbonate lithologies during the Jurassic except Shelburne G-29 which contains shale. This may suggest the proximity of a canyon, a clastic conduit or an embayment nearby.

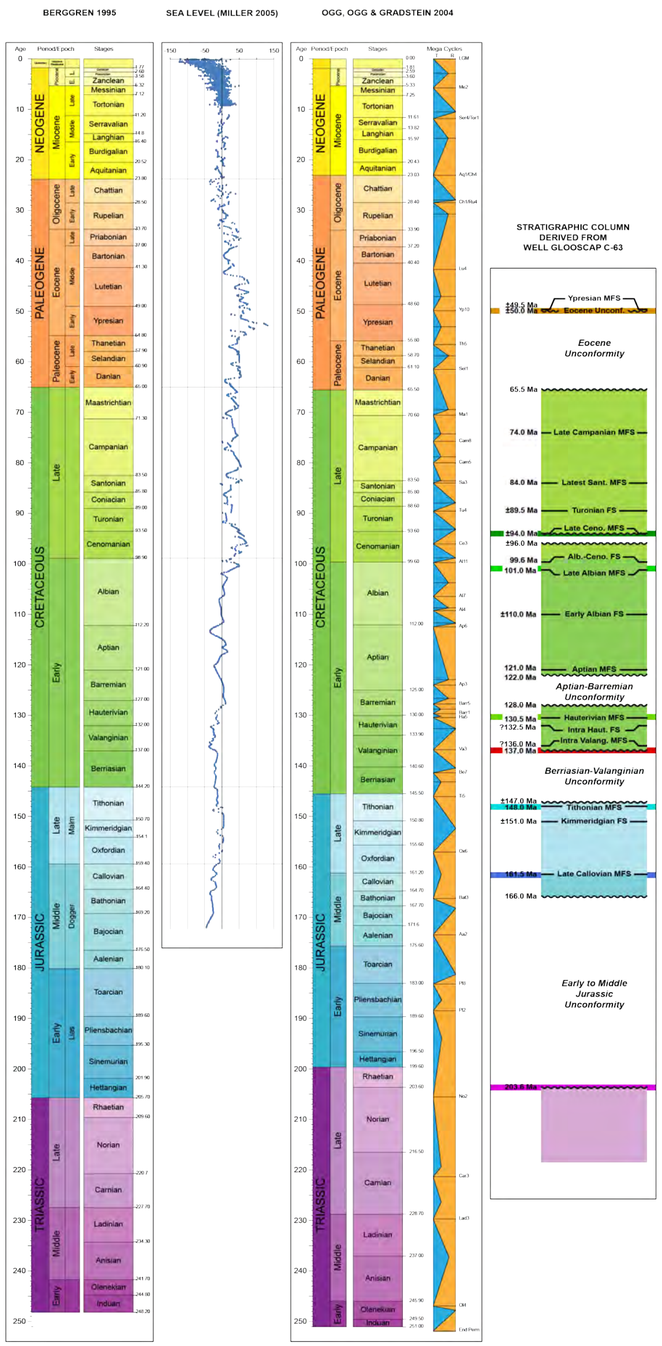

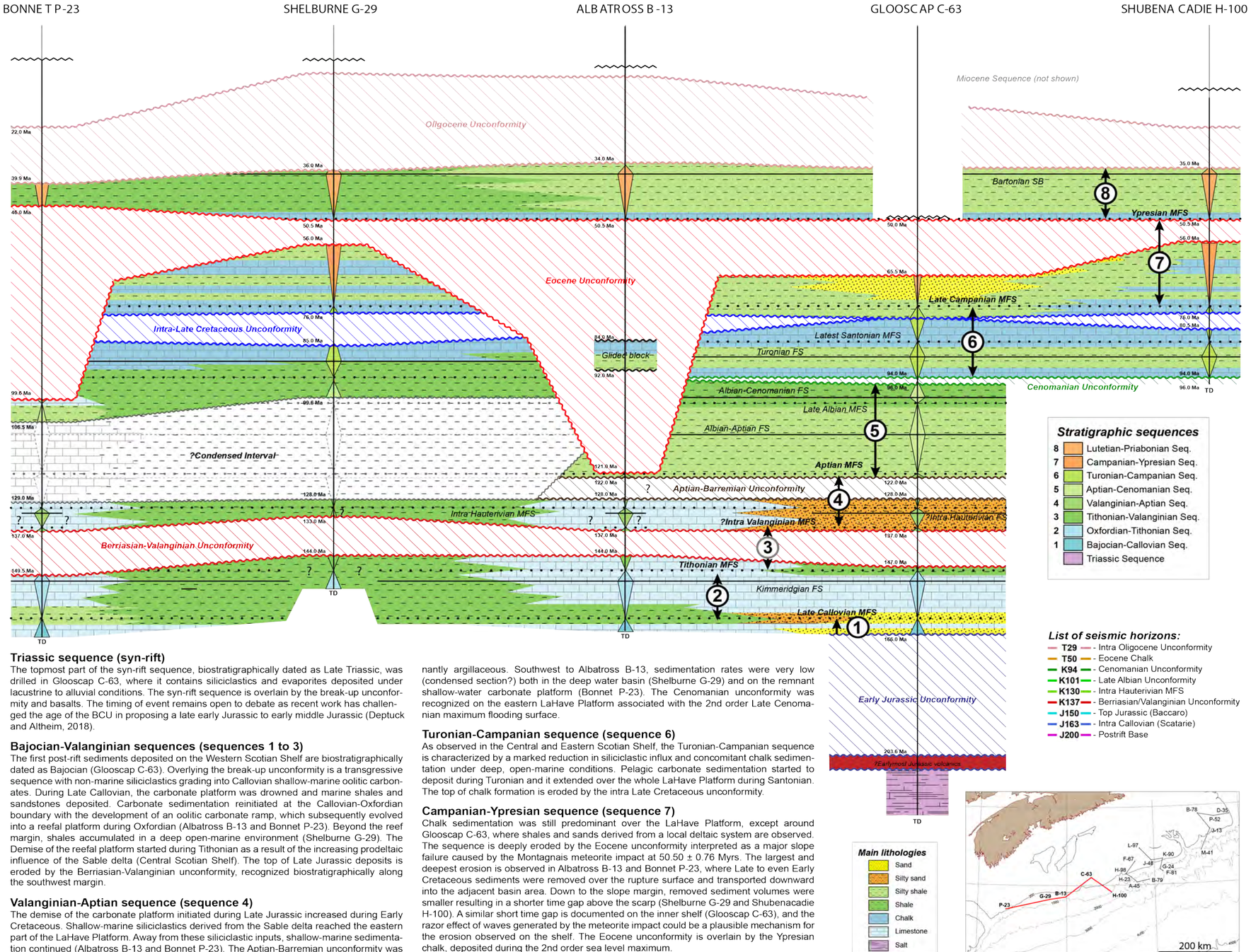

Triassic sequence (syn-rift)

The topmost part of the syn-rift sequence, biostratigraphically dated as Late Triassic, was drilled in Glooscap C-63, where it contains siliciclastics and evaporites deposited under lacustrine to alluvial conditions. The syn-rift sequence is overlain by the break-up unconformity and basalts. The timing of event remains open to debate as recent work has challenged the age of the BCU in proposing a late early Jurassic to early middle Jurassic (Deptuck and Altheim, 2018).

Bajocian-Valanginian sequences (sequences 1 to 3)

The first post-rift sediments deposited on the Western Scotian Shelf are biostratigraphically dated as Bajocian (Glooscap C-63). Overlying the break-up unconformity is a transgressive sequence with non-marine siliciclastics grading into Callovian shallow-marine oolitic carbonates. During Late Callovian, the carbonate platform was drowned and marine shales and sandstones deposited. Carbonate sedimentation reinitiated at the Callovian-Oxfordian boundary with the development of an oolitic carbonate ramp, which subsequently evolved into a reefal platform during Oxfordian (Albatross B-13 and Bonnet P-23). Beyond the reef margin, shales accumulated in a deep open-marine environment (Shelburne G-29). The Demise of the reefal platform started during Tithonian as a result of the increasing prodeltaic influence of the Sable delta (Central Scotian Shelf). The top of Late Jurassic deposits is eroded by the Berriasian-Valanginian unconformity, recognized biostratigraphically along the southwest margin.

Valanginian-Aptian sequence (sequence 4)

The demise of the carbonate platform initiated during Late Jurassic increased during Early Cretaceous. Shallow-marine siliciclastics derived from the Sable delta reached the eastern part of the LaHave Platform. Away from these siliciclastic inputs, shallow-marine sedimentation continued (Albatross B-13 and Bonnet P-23). The Aptian-Barremian unconformity was recognized on most of the LaHave Platform, but could not be biostratigraphically extended to its western end (Shelburne G-29 and Bonnet P-23).

Aptian-Cenomanian sequence (sequence 5)

The sequence was identified on the LaHave Platform up to the Albatross B-13 area. In this region, away from any significant sand sources, shallow water sedimentation was predominantly argillaceous. Southwest to Albatross B-13, sedimentation rates were very low (condensed section?) both in the deep water basin (Shelburne G-29) and on the remnant shallow-water carbonate platform (Bonnet P-23). The Cenomanian unconformity was recognized on the eastern LaHave Platform associated with the 2nd order Late Cenomanian maximum flooding surface.

Turonian-Campanian sequence (sequence 6)

As observed in the Central and Eastern Scotian Shelf, the Turonian-Campanian sequence is characterized by a marked reduction in siliciclastic influx and concomitant chalk sedimentation under deep, open-marine conditions. Pelagic carbonate sedimentation started to deposit during Turonian and it extended over the whole LaHave Platform during Santonian. The top of chalk formation is eroded by the intra Late Cretaceous unconformity.

Campanian-Ypresian sequence (sequence 7)

Chalk sedimentation was still predominant over the LaHave Platform, except around Glooscap C-63, where shales and sands derived from a local deltaic system are observed. The sequence is deeply eroded by the Eocene unconformity interpreted as a major slope failure caused by the Montagnais meteorite impact at 50.50 ± 0.76 Myrs. The largest and deepest erosion is observed in Albatross B-13 and Bonnet P-23, where Late to even Early Cretaceous sediments were removed over the rupture surface and transported downward into the adjacent basin area. Down to the slope margin, removed sediment volumes were smaller resulting in a shorter time gap above the scarp (Shelburne G-29 and Shubenacadie H-100). A similar short time gap is documented on the inner shelf (Glooscap C-63), and the razor effect of waves generated by the meteorite impact could be a plausible mechanism for the erosion observed on the shelf. The Eocene unconformity is overlain by the Ypresian chalk, deposited during the 2nd order sea level maximum.

Lutetian-Priabonian sequence (sequence 8)

This sequence, documented at the top of the biostratigraphically dated section in wells, recorded widespread open-marine shales preserved below the Oligocene unconformity.

Stratigraphic sequences

8	Lutetian-Priabonian Seq.
7	Campanian-Ypresian Seq.
6	Turonian-Campanian Seq.
5	Aptian-Cenomanian Seq.
4	Valanginian-Aptian Seq.
3	Tithonian-Valanginian Seq.
2	Oxfordian-Tithonian Seq.
1	Bajocian-Callovian Seq.
	Triassic Sequence

List of seismic horizons:

- T29 - Intra Oligocene Unconformity
- T50 - Eocene Chalk
- K94 - Cenomanian Unconformity
- K101 - Late Albian Unconformity
- K130 - Intra Hauterivian MFS
- K137 - Berriasian/Valanginian Unconformity
- J150 - Top Jurassic (Baccaro)
- J163 - Intra Callovian (Scatarie)
- J200 - Postrift Base

Main lithologies

- Sand
- Silty sand
- Silty shale
- Shale
- Chalk
- Limestone
- Salt

Shelburne Subbasin Postmortem Analysis

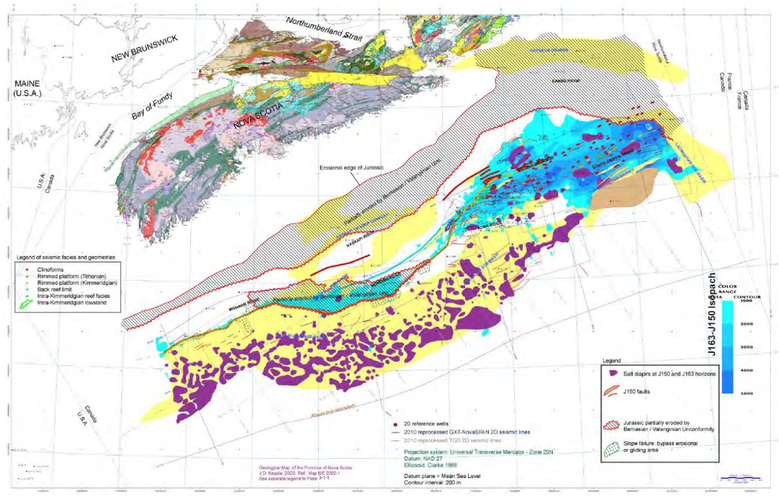

Figure 1: Schematic structural and stratigraphical framework of the unit J163 – J150

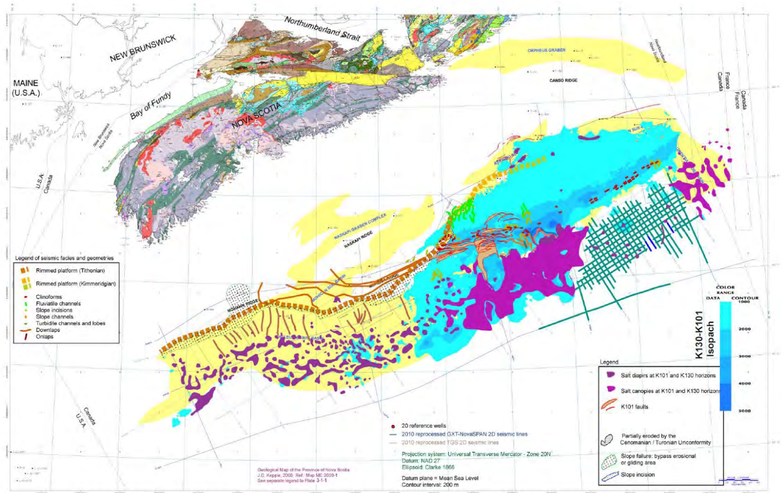

Figure 2: Schematic structural and stratigraphical framework of the unit K130 – K101

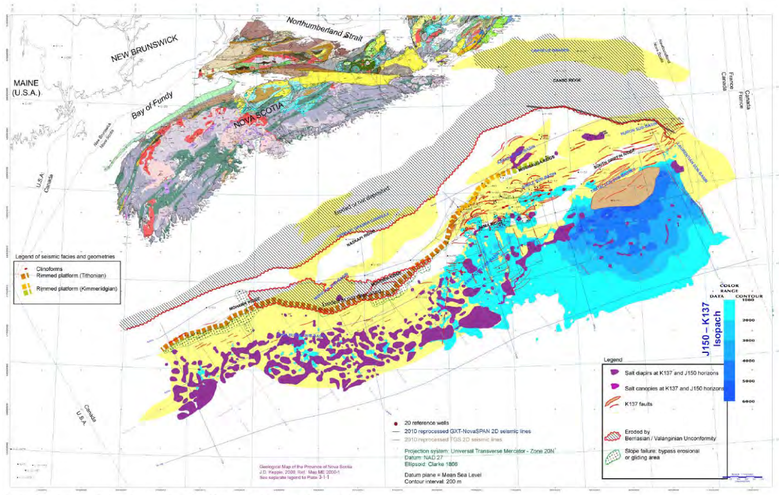

Figure 2: Schematic structural and stratigraphical framework of the unit J150 – K137

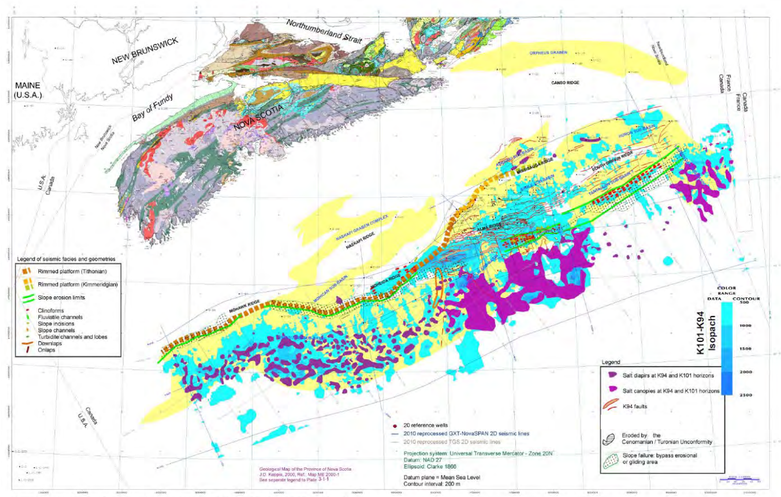

Figure 1: Schematic structural and stratigraphical framework of the unit K101 – K94

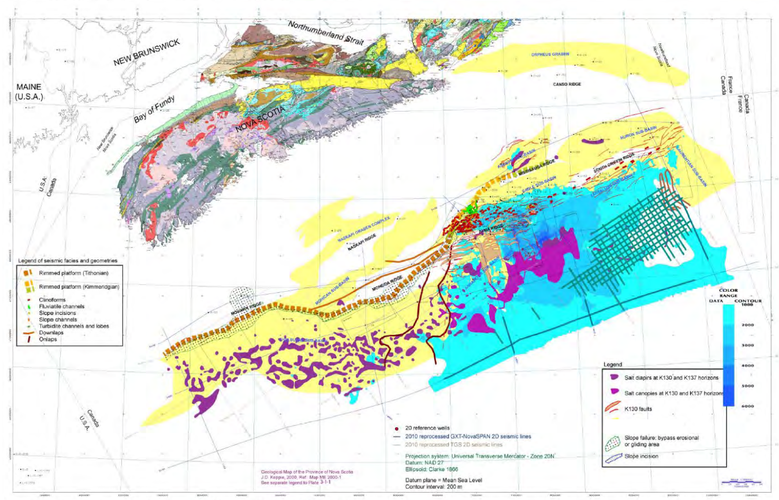

Figure 2: Schematic structural and stratigraphical framework of the unit K137 – K130

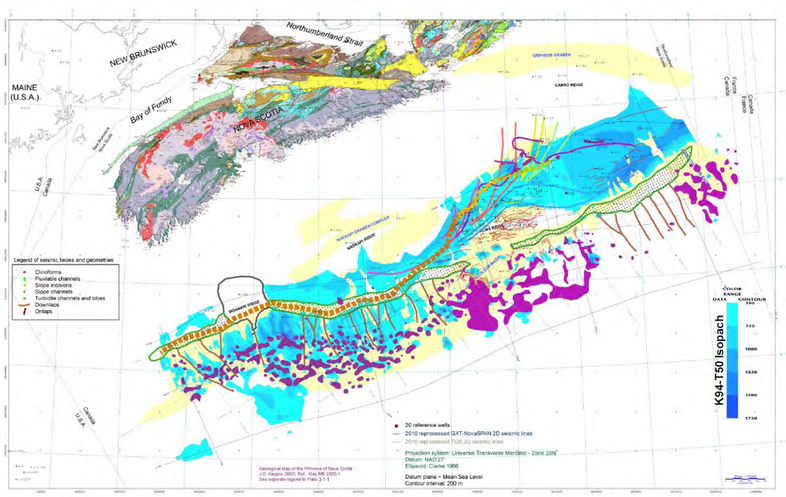

Figure 1: Schematic structural and stratigraphical framework of the unit K94 – T50

Structural and Stratigraphic Framework of the Scotian Margin: Summary from the 2011 PFA (OETR, 2011)

Thickness maps at left show depocenter evolution through time from the Lower Jurassic to the Eocene. To highlight differences along the margin, the threshold has been set at 1000 m: thicknesses above 1000 m appear in blue; thicknesses below 1000 m appear in yellow.

The margin appears split in two with thicker (early) deposits to the northeast representing the influence of the Sable Delta, which does not extend to the Shelburne Subbasin. Sediment distribution changes during the mid-Cretaceous through the Eocene. This different distribution highlights the increased influence of secondary distributary systems from the Meguma Terrane during the mid-Cretaceous and the formation of the Cree Member.

Gross sand distribution and gross sand to gross thickness ratios echo observations from the thickness maps. The Scotian Basin appears divided during the Late Jurassic to Early Cretaceoous, with very low sand content in the Shelburne Subbasin. It must be noted that the influence of the Shelburne Delta further south was not considered at the time of the 2011 study. Work done in 2015 has shown that a large delta system was feeding clastic sediments to the southwestern part of the Shelburne Subbasin (OERA, 2015).

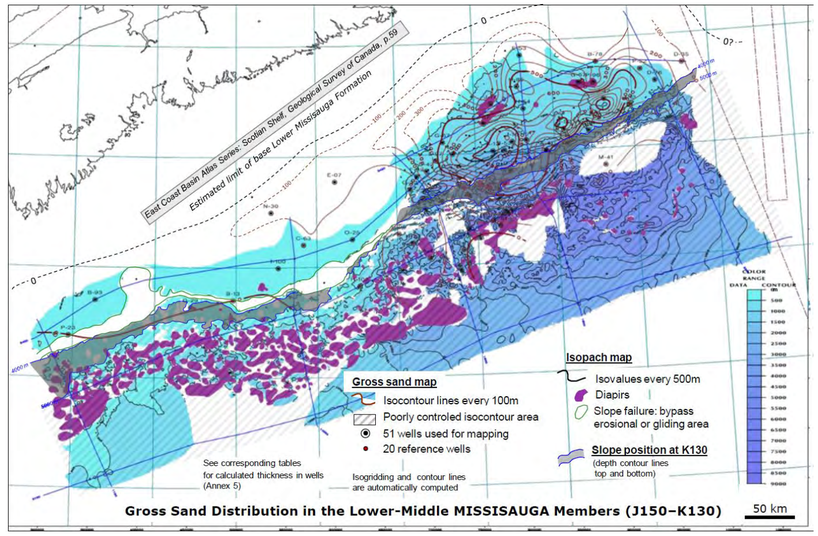

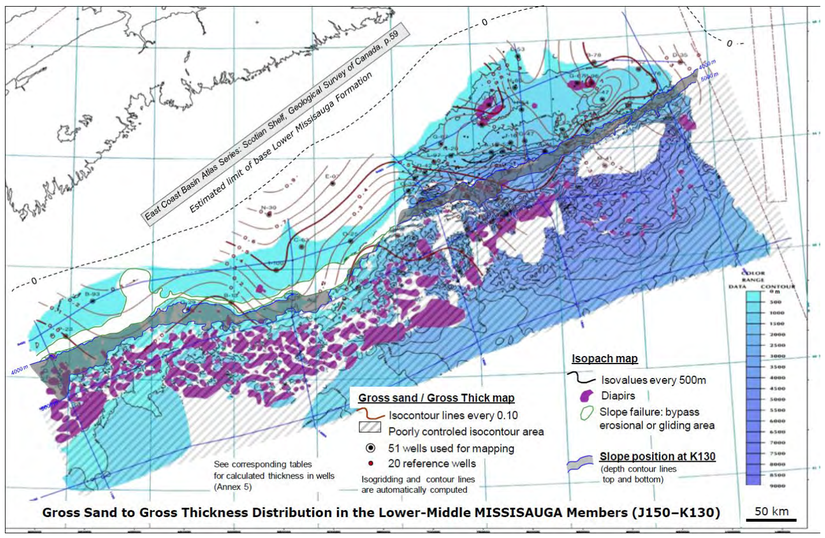

Summary

Successive thickness maps shown in PL. 1.1.5 are summarized on Figure 1.1.10. The difference in sedimentary supply controlled the margin architecture and related traps. The margin is clearly divided into two distinctive provinces:

- A northeastern province with a large clastic supply from the Sable Delta system resulting in more than 15 km of sediment. Traps are related to allochthonous salt (detachment, rollover, salt tongue, canopy, turtle-back, etc.).
- A southwestern province with less than 9 km of sediment interpreted as a relatively starved margin. Traps are related to diapirs and associated mini-basins.

As output from the 2011 PFA, a play concept map was created and updated in 2018 (Figure 1.1.11; OETR, 2011; OERA, 2015; Saint-Ange et al., 2018). The map summarizes the distribution of the different plays both geographically and through time. Plays are listed below from south to north:

- Shelburne Subbasin:
  - ✓ Mid-late Jurassic carbonate reefs
  - ✓ Mid Jurassic and Cretaceous delta and related turbidites
- Central Region (transition between Shelburne and Sable Subbasins; **Shell parcels area**):
  - ✓ Mid-late Jurassic carbonate reefs
  - ✓ Upper slope Cretaceous and Eocene turbidites
- Sable Subbasin:
  - ✓ Mid-late Jurassic carbonate reefs
  - ✓ Banquereau Synkinematic Wedge
  - ✓ Mid Jurassic and Cretaceous delta and related turbidites

Figure 1.1.10: Mesozoic sediment thickness map and salt related structures defining two major provinces *(from PFA 2011, (OETR, 2011))*

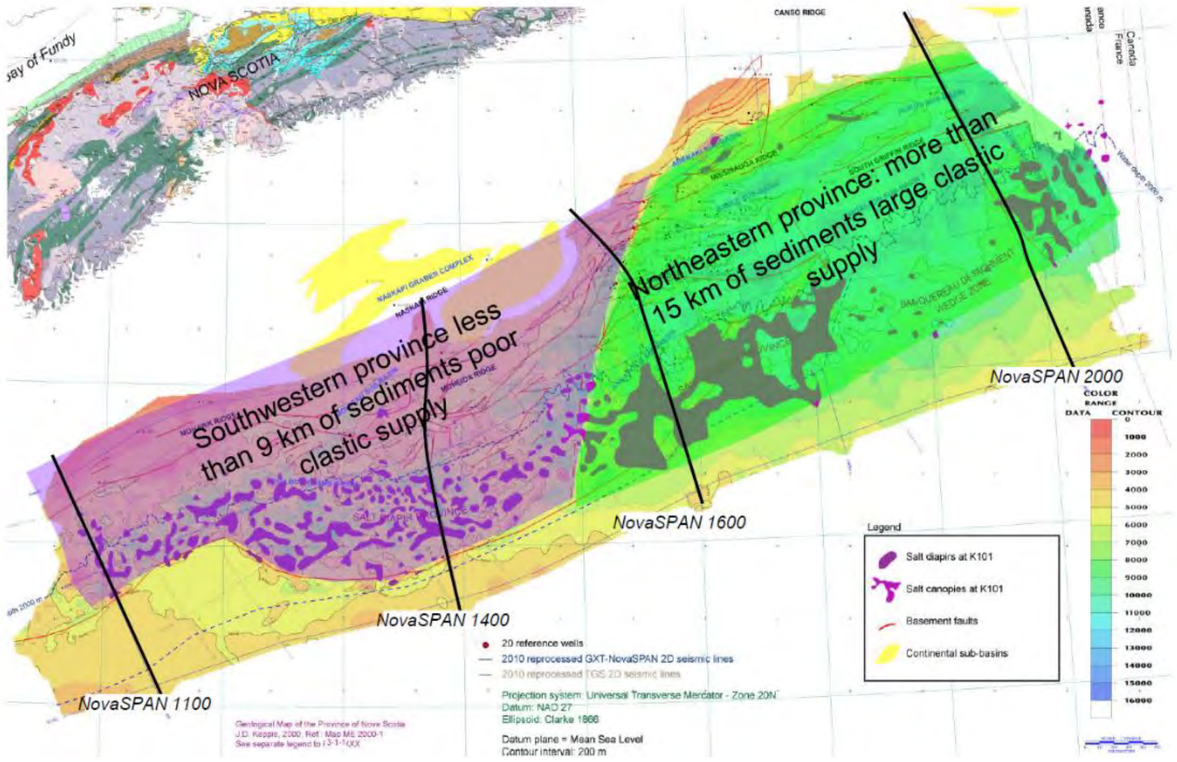

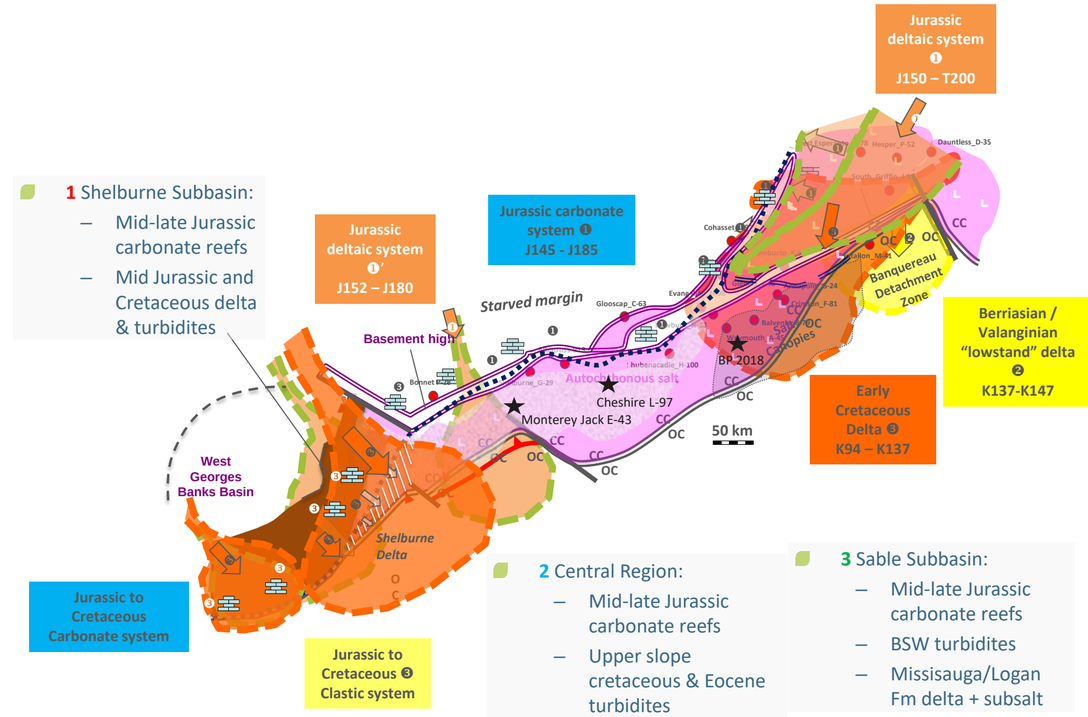

Figure 1.1.11: Play concept map by geography through time, updated 2018 (OETR 2011; OERA 2015; Saint-Ange et al 2018)

Validity of the Shell Geological Model with Respect to the Current State of Knowledge

Available information regarding the Shell geological model is limited at this time. It is possible Shell geologists considered the Sable Delta to be the only clastic source for more than half the margin. This is consistent with a simple net-to-gross interpolation between existing wells on the shelf. Similarly, canyons and channels are observed on seismic data in the Jurassic and Cretaceous intervals, which when correlated to the net-to-gross maps would naturally lead to the assumption of sandy reservoirs in deep water. So, why wasn't Shell's model confirmed by the wells?

Shell's geological model proved to be wrong because of several assumptions and/or misinterpretations, particularly for the Jurassic (Table 1.1.3). The existence and significance of the Abenaki Formation in the Shelburne Subbasin seems not to have been considered, or at least underestimated. Similarly, the restriction of the Sable Delta's influence to the Sable Subbasin and the existence of secondary Meguma Terrane sources were not considered. Misinterpretation of sedimentary facies (e.g., carbonate facies taken for clastic and source rock facies) may have led to a misinterpretation of seismic facies, thus misleading seismic characterization and AVO analysis.

Shell geological model for the Shelburne Subbasin	Literature and PFA 2011 geological model for Shelburne Subbasin	Well Results
Sable Delta sole source of clastics through the Mohican Graben	Multiple entry points. Sable Delta influence limited to the Sable Subbasin	
Clastic dominated margin	Starved margin	Low sedimentation rates; traces of sand; no reservoir
MicMac/Mohawk Mid-Late Jurassic sandstone in deep water	Abenaki Carbonate rim; limited clastic input into deep water. Predominance of carbonate and shaly facies	Predominance of shale and carbonate facies
Possible Tithonian SR	Possible Tithonian SR	No Tithonian SR

Table 1.1.3: Comparison of geological models between Shell, literature review + the 2011 PFA, and well results.

1.2 Stratigraphic Modelling Postmortem Analysis & Additional Plays

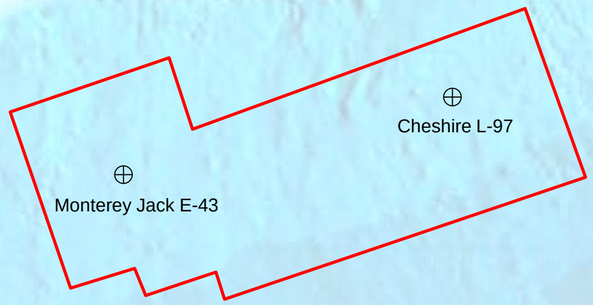

Shelburne Subbasin Postmortem Analysis

Stratigraphic Modelling Postmortem Analysis

A regional forward stratigraphic model was performed in 2010 using the IFP software DionisosFlow. The Area of Interest covered the entire deep water Offshore Nova Scotia margin.

The objectives of this model were:

- to dynamically test and validate the depositional and stratigraphic concepts that were initially proposed in the 2010 project.
- To provide Gross Depositional Environment maps that were used afterwards for petroleum systems modelling of the offshore Nova Scotia Margin.

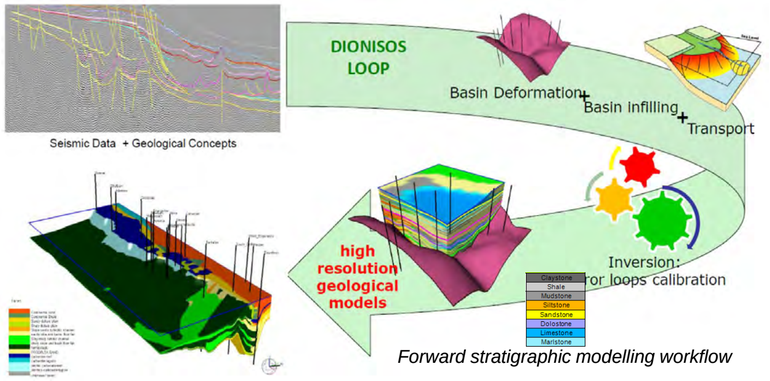

Forward stratigraphic modelling workflow

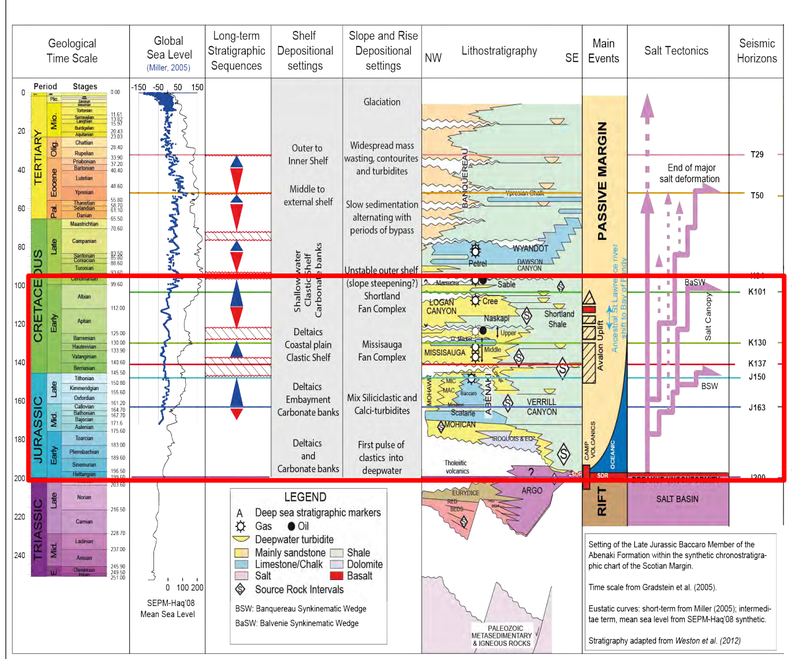

Setting of the Late Jurassic Baccaro Member of the Abenaki Formation within the synthetic chronostratigraphic chart of the Scotian Margin.

Time scale from Gradstein et al. (2005).

Eustatic curves: short-term from Miller (2005); intermediate term, mean sea level from SEPM-Haq'08 synthetic.

Stratigraphy adapted from *Weston et al. (2012)*

Review of DionisosFlow Model and Facies Update

CARBONATE

The two maps presented below present two facies dress-up designs for the same calibrated model. The initial 2011 model facies grouping did not distinguish between clastic shales and carbonate mudstones. Defining a higher facies resolution in 2018 highlights the simulated carbonate mud fraction.

Mudstone and clastic shale were initially grouped in a single "hemipelagic mud facies"

J160 MAP

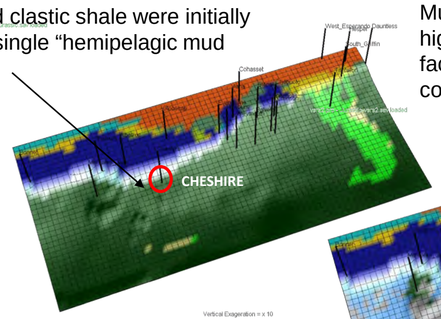

FINAL MODEL JURASSIC - INITIAL FACIES CUTOFF

Mudstone deposition was simulated but not highlighted in the facies geocube. One additional facies cutoff allows the display of such a lithological component

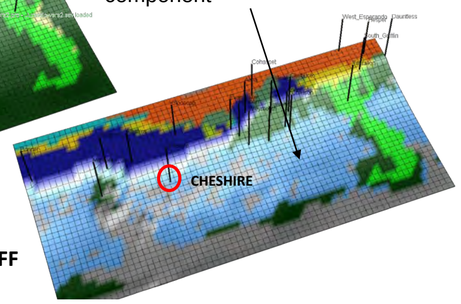

FINAL MODEL JURASSIC - ALTERNATIVE FACIES CUTOFF

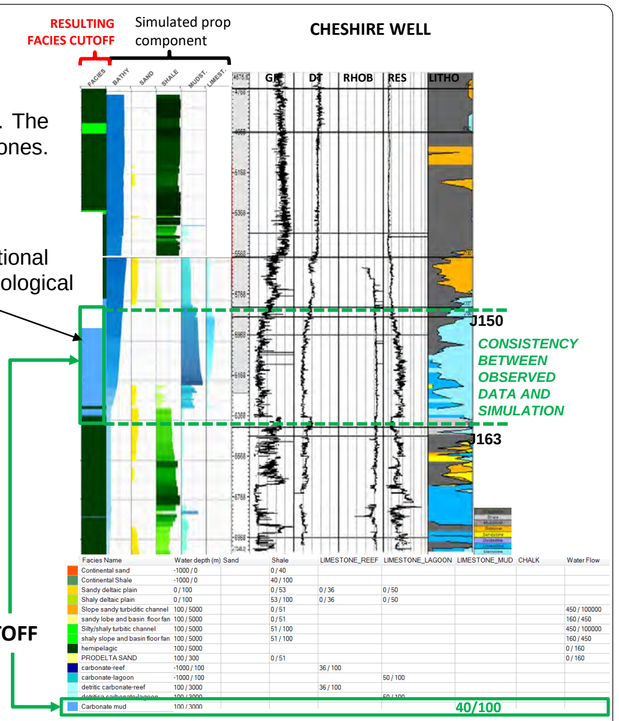

CLASTICS

Deep sandy deposits newly considered in revised facies cutoff

Deep sandy deposits facies range initially considered in initial facies cutoff

100 m³/s

K130-137 GROSS MAPS

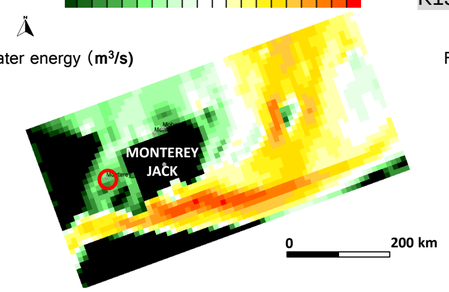

FINAL MODEL CRETACEOUS - SIMULATED WATER FLOW ENERGY

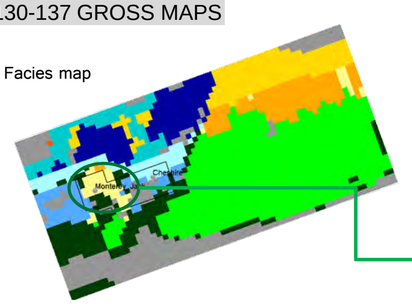

FINAL CRETACEOUS MODEL - ALTERNATIVE FACIES CUTOFF

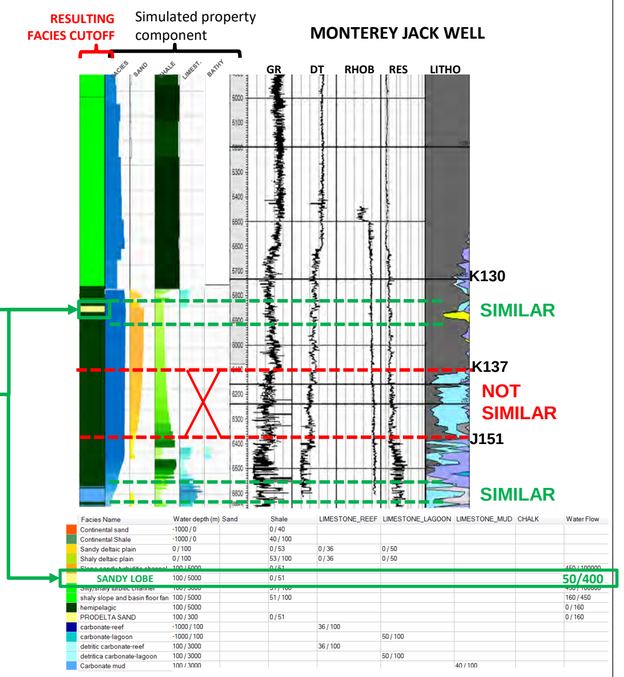

RESULTS OF REVIEW

- Simulated carbonate thickness and facies are consistent with the Cheshire well data for the Upper Jurassic.
- Cretaceous thickness and facies are also consistent with well data (especially the local Valanginian sandy interval predicted in Monterey Jack, and the overall shaly to silty interval).
- Partially missing carbonate in the Upper Jurassic model around Monterey Jack. This is mainly due to the poor constraint on paleobathymetry, which may have been overestimated in the Dionisos model in this region.

Cretaceous Play

Seismic Amplitude Anomalies:

RMS maps were produced for each horizon provided by NSDEM (Figures 1.2.1 & 1.2.2). Maps show strong, widespread anomalies for the Callovian (J163), anomalies that decrease through time. The strongest anomalies are observed during the Jurassic, particularly southeast of Monterey Jack E-43 (Figure 1.2.1a). During that time, most anomalies are within salt induced mini-basin (Figure 1.2.1). Using Shell well results these anomalies can be associated to changes in lithologies between shaly limestone, shale and marls. During the J163 – J150 interval, in no case do these anomalies correlate with sandstone or source rock presence, nor with evidence for hydrocarbon charged reservoirs.

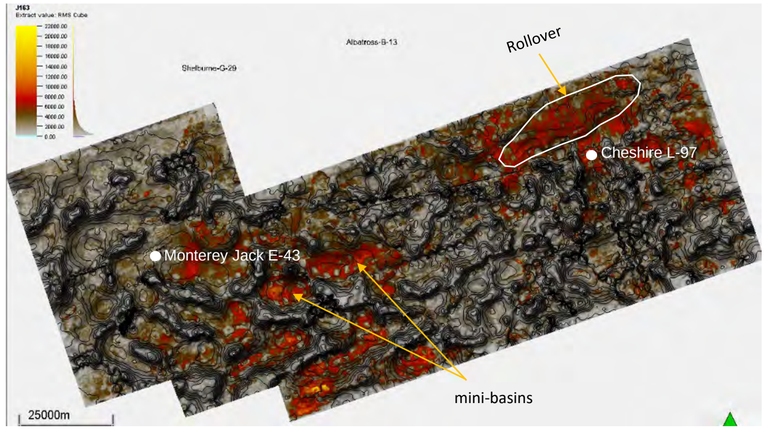

Figure 1.2.1 : RMS maps of the Jurassic interval. All horizons were provided by NSDEM.

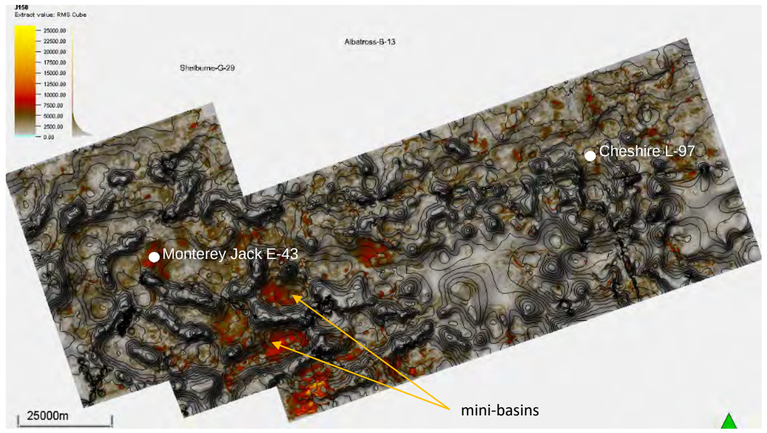

Figure 1.2.1a: RMS map of J163 Hz (Callovian). Both Cheshire L-97 and Monterey Jack E-43 are located near amplitude anomalies. These amplitudes are related to facies changes between carbonate and shale.

On the western part of the survey, amplitude anomalies are located within salt induced mini-basins, whereas on the northeastern side they are mostly located on a large rollover structure.

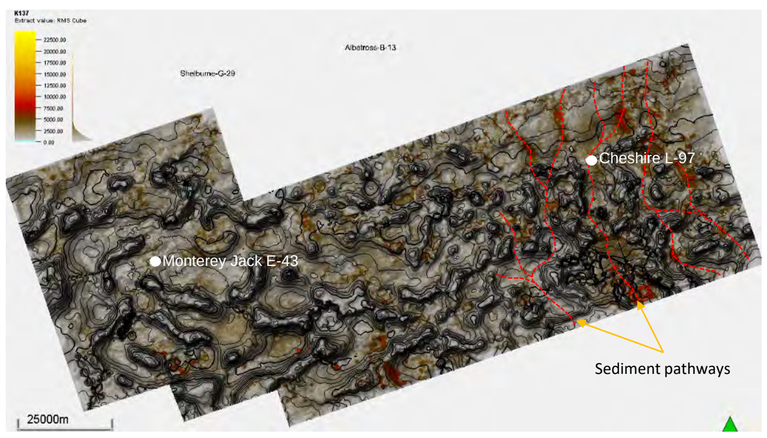

Figure 1.2.1b: RMS map of J150 Hz (Tithonian). For this interval, amplitude anomalies are only located in salt induced mini-basins southeast of Monterey Jack E-43.

Figure 1.2.1c: RMS map of K137 Hz (Valanginian).

Amplitude anomalies are very faint but tend to be associated with sediment pathways. No significant volume of clastic reservoir is expected since the Valenginian – Tithonian interval is a condensed stratigraphic section.

During the Cretaceous, amplitude anomalies are located in more restricted areas. They begin to define sediment pathways, mostly near Cheshire L-97 (Figures 1.1.12 to 1.1.14). An area with a high amplitude is noted south of Cheshire L-97. The signal is strong for the Hauterivian (K130) but faint in the Mid Cretaceous. The K101 interval is particularly poor in terms of seismic anomalies. Changes occur to the Albian, with higher amplitudes to the lower part of the seismic cube, particularly downslope from Cheshire L-97 (Figure 1.1.12c). Changes between low RMS value to high RMS values coincide with the transition from a by-pass area to a depositional area. It is notable that the few amplitude anomalies for the Cretaceous are located in the lowermost part of the seismic cube (Figures 1.1.12 a to c).

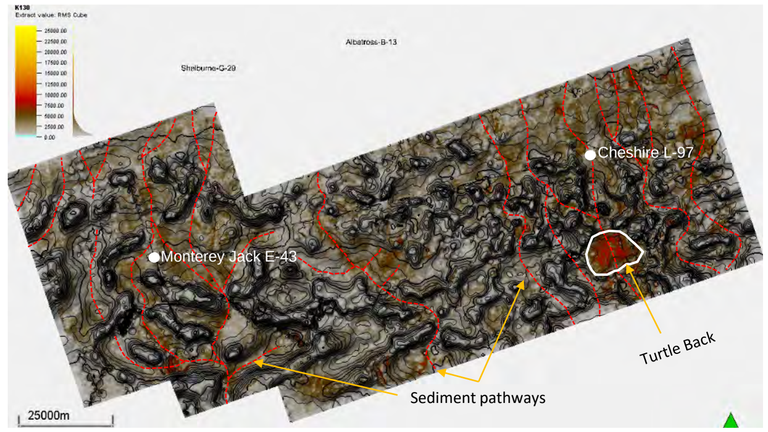

Figure 1.2.2 : RMS map of Cretaceous interval. All horizons were provided by NSDOE.

Figure 1.2.2a: RMS map of K130 Hz (Hauterivian). This interval was the primary target for both Cheshire L-97 and Monterey Jack E-43. RMS values are a bit stronger than K137 Hz but remains generally low. They allow identification of clear sediment pathways. South of Cheshire, a strong anomaly is observed. This anomaly is visible only at the K130 Hz and is tied to a turtle back structure (Figure 1.2.16b).

Seismic and well data suggest that both Cheshire L-97 and Monterey JackE-43 remain in the by-pass area during this geological period, although it is notable that sediment accumulation remains low (see thickness map K130-K137 in OETR, 2011).

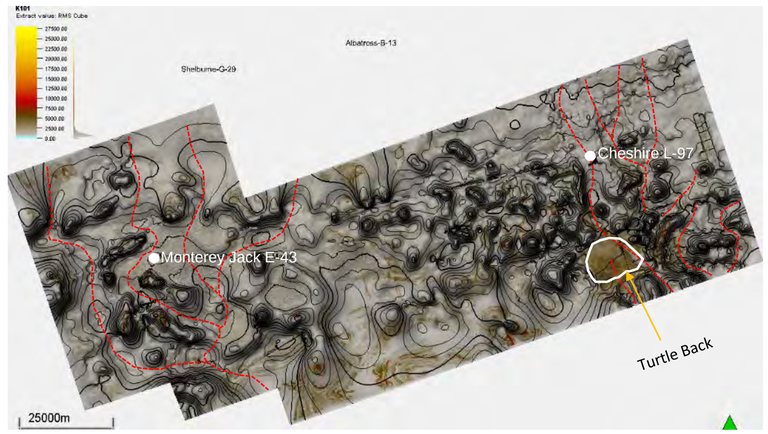

Figure 1.2.2b: RMS map of K101 Hz (Albian). RMS values are the lowest of all maps. A slight increase in RMS value is observed on the turtle back structure. At K101, wells indicate shale. The lack of changes in amplitude values suggest a widespread shaly lithology at that time.

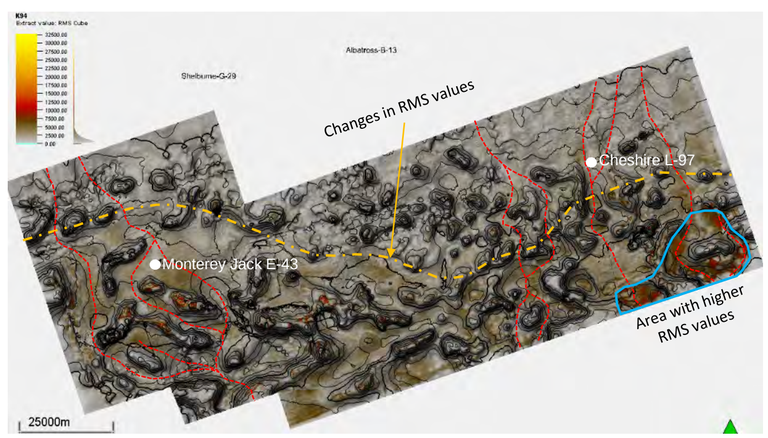

Figure 1.2.2c: RMS map at K94 (Cenomanian). The map appears divided in two, with an upper slope showing very low RMS values and a lower slope with increasing RMS values. Overall values remain low excepted on the lower right corner.

Evidences for Canyons, Gullies and Downslope Sediment Transfer

Evidence for sediment pathways and transfer into deep water is common across the Shell acreage (Figures 1.2.1 to 1.2.4). Canyons and gullies are widespread throughout the Cretaceous interval, but they cannot be directly linked to downslope sandstone presence and reservoir facies. Well correlation (PL. 1.1.4) shows that shale is the dominant lithology for the Cretaceous but this doesn't preclude the presence of sandstone reservoirs. For the Jurassic section, reservoirs are more difficult to pick due to the presence of the thick Abenaki carbonate facies (Figure 1.2.3). If they exist and depending on the specific Jurassic interval, they are more likely related to carbonate than clastic processes.

Seismic transects upslope from the Shell 3D cube show a fairly condensed Cretaceous section with small canyons, which together suggest a bypass area (Figure 1.2.3). Nonetheless, it's notable that the 2011 PFA thickness maps suggest sediment accumulation in this part of the margin remained low for the lower – mid Cretaceous (OETR, 2011). Significant accumulation is localized in salt induced-mini-basins (see thickness map K130-K137 in OETR, 2011). Figure 1.2.4a shows a dip section across a sediment pathway observed on the 3D seismic dataset. The transect shows a very condensed K130 – K137 section (Lower Cretaceous) which abruptly increases downslope within a salt induced mini-basin. For the Hauterivian – Albian interval, the transect shows sediment thickening until a salt wall and a thinner section past the salt (Figure 1.2.4a).

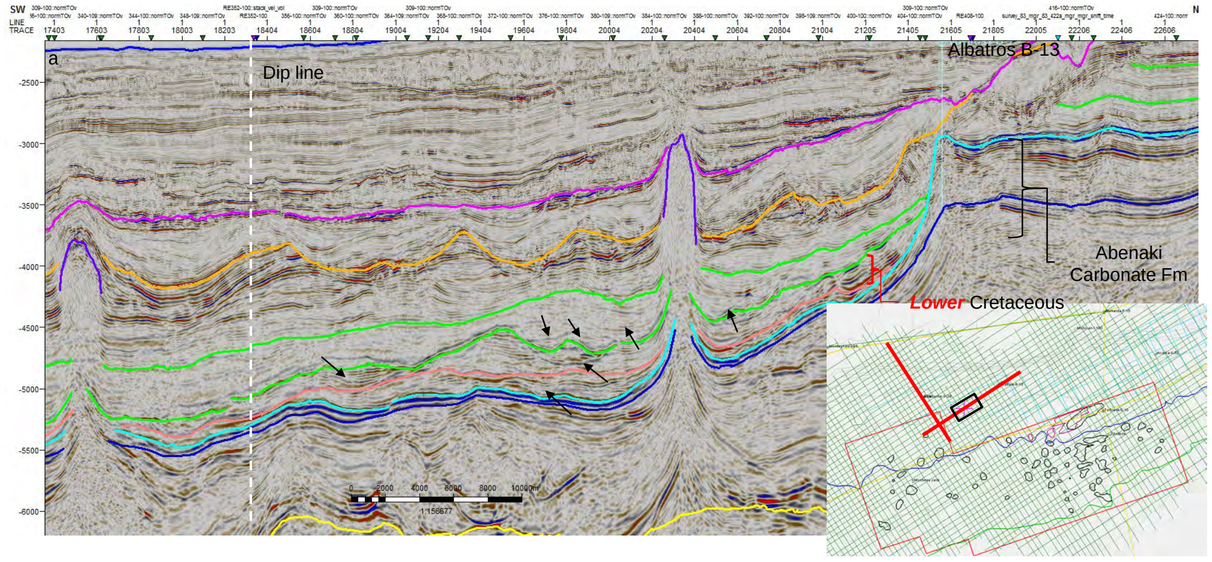

Figure 1.2.3 : Strike (a) and dip (b) 2D seismic transects in Shell acreage. Arrows indicates canyons and gullies. Note the condensed section for the Lower Cretaceous.

For the Albian – Cenomanian interval, sediment shows a thickening trend downslope of the section. This suggests that most of the area was bypassed by sediment during the Hauterivian and Cenomanian and stored downslope in mini-basins or far out onto the abyssal plain as turbidite fans. Observations for the Albian interval suggest that sediment can be trapped upslope on the back side of salt walls.

Correlation between Cheshire and the Hauterivian seismic interpretation shows a very high silt content in the bypass area (Figure 1.2.4a). For most of the transect up to the mini-basin, the acoustic facies is quite homogeneous suggesting widespread siltstones. In the salt induced min-basin, the acoustic facies abruptly changes with stronger impedances around the Hauterivian (K130). This mini-basin is located directly downstream from Cheshire L-97. The change in seismic facies may be related to changes in sediment facies. In contrast to the Jurassic interval where strong impedances correlate with carbonate facies, we infer here that the strong reflectivity may be correlated with sandstone facies. Silt deposited within the bypass area may represent the tail of turbidity currents, whereas sand is more likely to be ponded within downslope mini-basins due to changes in slope which would impact turbidity current velocity and dynamics. Additionally, the period around 130 Ma is clastic-dominated with widespread river systems across the shelf. This implies an increased likelihood of finding sand trapped within mini-basins downslope from a bypass area, although it cannot be excluded that the seismic facies may be related to shale or a higher concentration of siltstones.

These observations suggest that very fine scale mapping is required to localize Cretaceous depocenters as both Monterey Jack E-43 and Cheshire L-97 might still be within the bypass area. That would mean that sand would start accumulating in the lower part of the seismic data close to the 3000m WD curve and beyond.

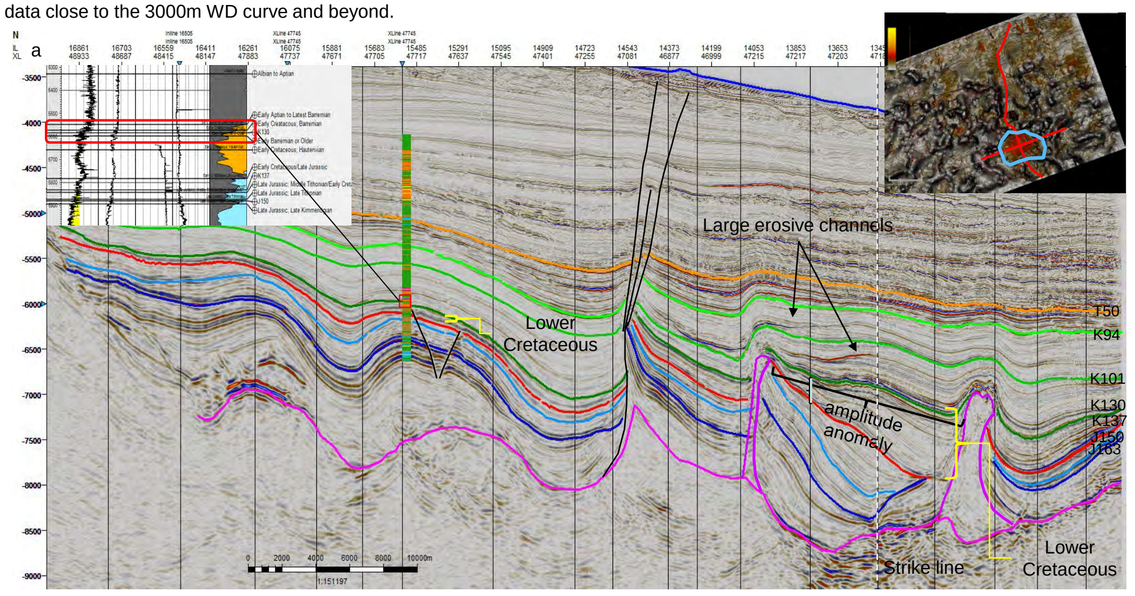

Figure 1.2.4 : Dip and strike transect from Shell's 3D seismic data. a) dip line along a large channel; b) strike line across a large turtle back structure downslope from Cheshire L-97. Note the large erosive channels during the Albian and Cenomanian.

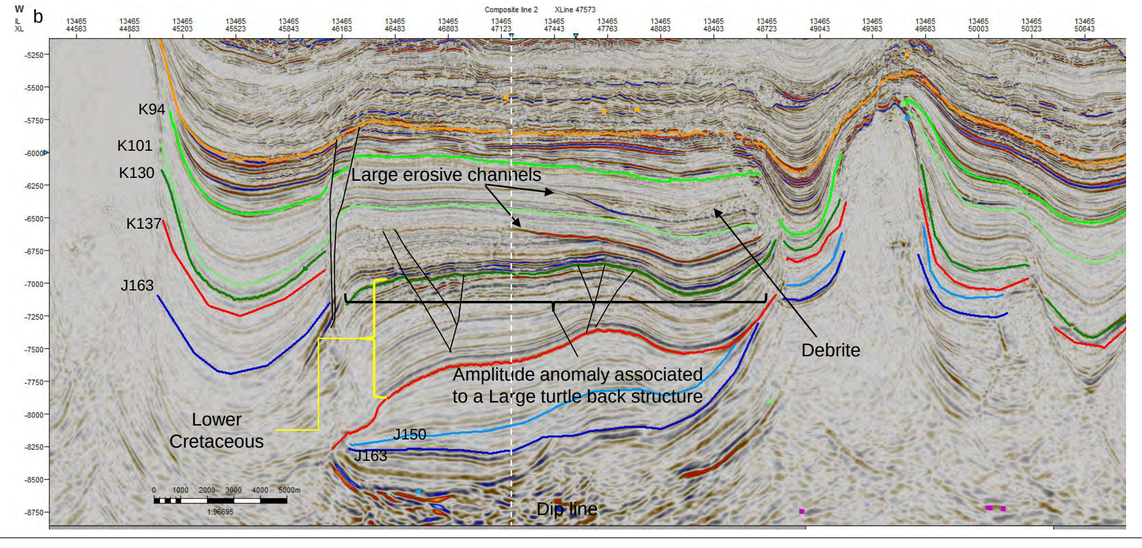

Tertiary and Related Traps

Thickness maps from late the Cretaceous to Eocene (see PL 1.1.5) show a thickening trend in the Shelburne Subbasin and a decrease in sediment accumulation in the Sable Subbasin. This is due to the developing Laurentian Fan. The Shelburne Subbasin transitions from a starved margin i\to a clastic dominated margin. At the time of the 2011 PFA, work focused on Jurassic and Cretaceous strata while the Tertiary and Lower Jurassic sections were not considered. In 2015, work published by the CNOSPB suggested that the Tertiary interval of the Shelburne Subbasin could hold upslope turbidite reservoirs (Deptuck et al., 2015), particularly during the Late Cretaceous - Early Eocene transition. In light of the new 3D seismic and well data, the early Tertiary play has become more substantial. A quick review of the 3D seismic data shows widespread amplitude anomalies associated with large stratigraphic traps within the Tertiary succession. The main traps observed for the Tertiary are:

- Upslope onlap and pinch-out turbidites
- Turbidite channel reservoirs
- Basin – floor sand lobes
- Fine grained drift and channelized sands complex

Note: pinch-out turbidites and basin floor fans are not observed within Shell's 3D datasets. They are observed on 2D lines and on the Barrington 3D data (pinch-out turbidites).

Stratigraphic traps in Tertiray play

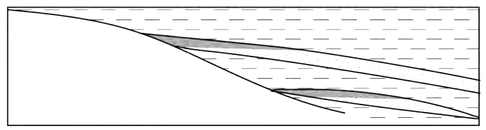

Onlap and pich out

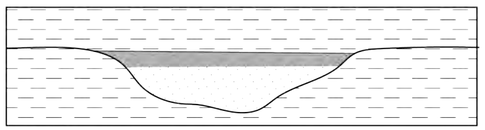

Valley/Channels

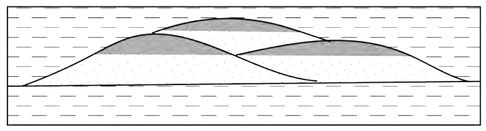

Basin-floor sand lobe

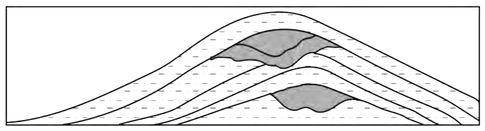

Fine grained drift and channelized sands complex

Pinch-out and Onlap Traps

Dip Transect (A) and RMS maps (B) through the Cayuga lead (from Deptuck et al., 2015). The transect shows a series of turbidite channel reservoirs contained within a pinch-out trap. The amplitude anomaly of Cayuga shallow is taken along the floor of erosive canyons. These features are related to the Montagnais bolide impact.

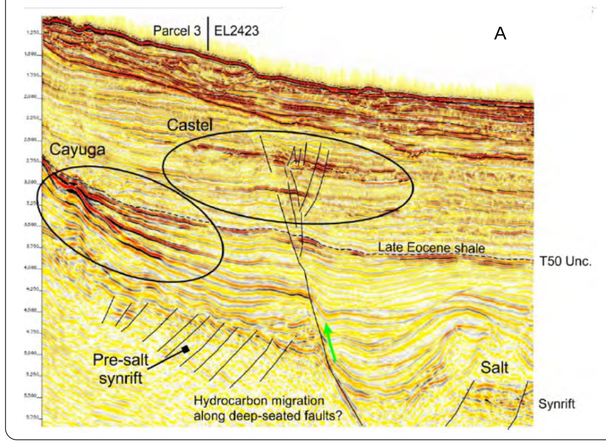

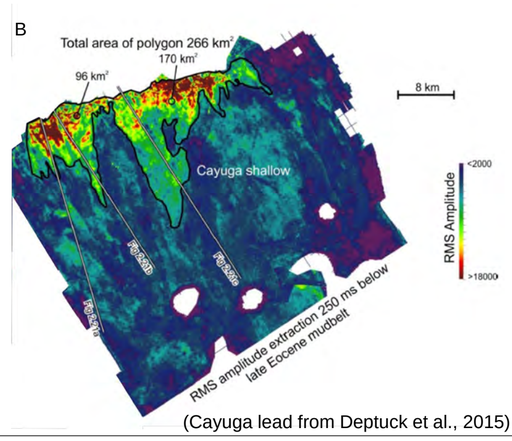

(Cayuga lead from Deptuck et al., 2015)

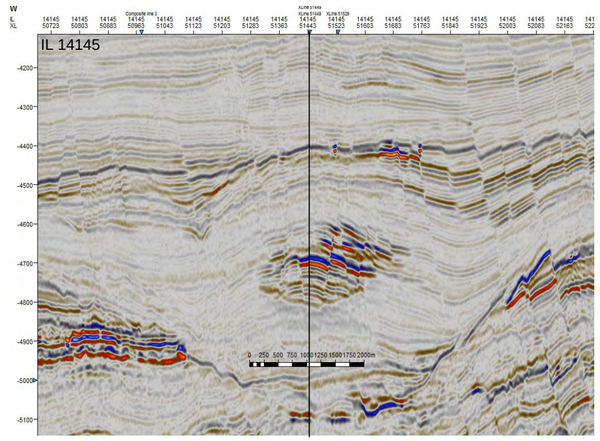

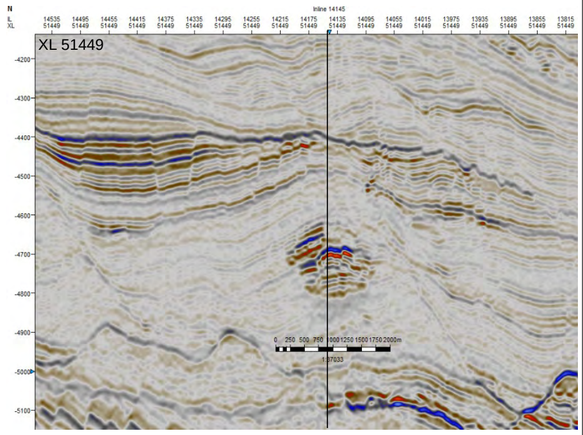

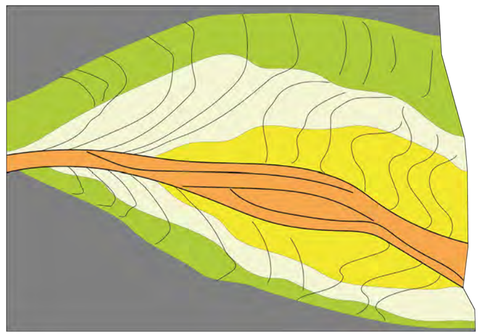

Fine grained drift and channelized sands complex

Inline and crossline sections showing an Eocene – Oligocene turbidite channel complex interbedded within fine grained drift. The channel complex is highlighted by the high amplitude anomaly.

Basin Floor Fan

Dip and strike sections showing the beginning of stacked channels, Tertiary valley and turbidite fans from Cretaceous to Eocene. In the Shell 3D dataset, these turbidite systems are barely covered in the southwestern-most part of the cube. They are well expressed southward and eastward of the 3D cube location.

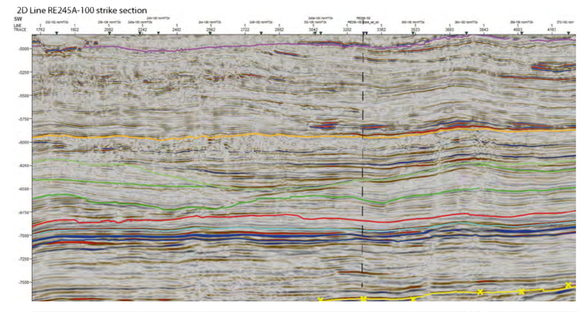

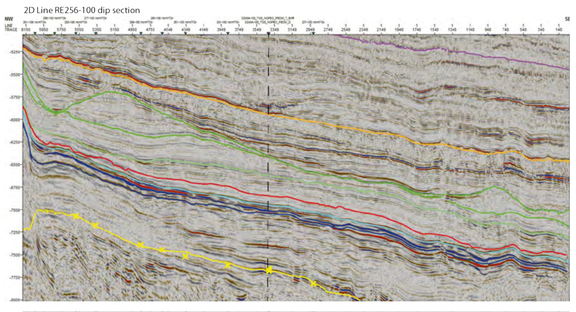

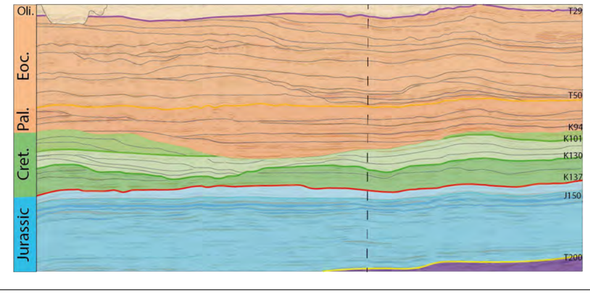

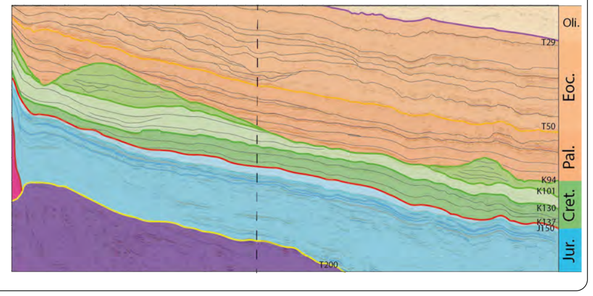

Lower Jurassic Play

Petroleum system and forward stratigraphic modelling performed in the 2011 PFA study (OETR, 2011) highlighted a potential play in the Jurassic series of the Scotia Basin (Figure 1.2.5). To date, this play has not been proven in the Shelburne Subbasin. However, there is room for an Early-Middle Jurassic play below the Late Jurassic rocks tested by Shell.

The Early to Middle series of the Scotian Basin were drilled decades ago by a few exploration wells. On the shelf of the Shelburne Subbasin four wells reached rocks older than the Base Callovian MFS marker (Bonnet-B-13, Moheida P-15, Mohican I-100 and Glooscap C-43). These rocks consist primarily of sandstones and dolostones referred to as the Mohican and Iroquois facies in previous work (e.g., MacLean and Wade, 1993; Weston et al., 2012). Lateral equivalents of the Mohican/Iroquois facies are still unknown in the Scotian Slope but could bear potential reservoirs close to the active Jurassic kitchen.

Here we report regional geological evidence suggesting that the presence of potential carbonate reservoirs is probable along the proximal part of the Scotian Slope. This analysis relies on integrating the recent Shell well results with older wells drilled in the Middle Jurassic series of the Scotian Shelf.

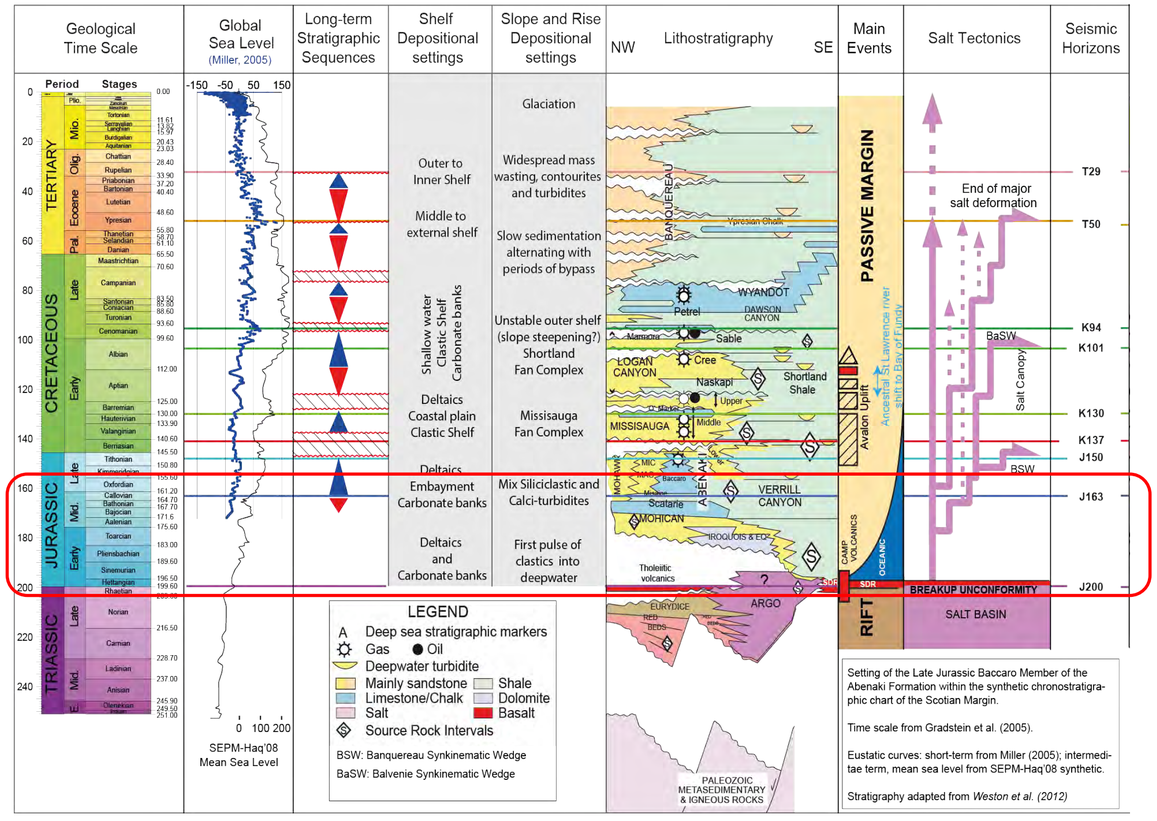

Figure 1.2.5: Detailed stratigraphic chart of the Scotian Basin highlighting a poorly constrained geological interval in the 2011 PFA (OETR, 2011).

The Middle Jurassic Iroquois and Mohican Facies on the Scotian Shelf:

Mohican I-100 and Glooscap C-63 were drilled to Late Triassic salt (Argo Formation) and dated by biostratigraphic methods (Weston et al., 2012). These two wells, which entirely penetrated the Mohican and Iroquois facies, provide a unique picture of the Jurassic series (Figure 1.2.6). The uppermost part of the Mohican facies was dated as Callovian to Late Bathonian (Weston et al., 2012).

The lower part of the Mohican and the Iroquois facies were assigned a Middle to indeterminate Jurassic age as no biostratigraphic markers were found. The actual presence of Early Jurassic was not biostratigraphically determined either due to the lack of fossils or to the presence of a time gap associated with a major uniformity visible on regional 2D seismic lines.

The overall depositional environments interpreted at Glooscap C-43 showed that both the Iroquois and Mohican facies were associated with non-marine depositional conditions (OETR, 2011; Weston et al, 2012). The biostratigraphically-tied correlation of the pre-Callovian/Late Triassic interval between Glooscap C-43 and Mohican I-100 implies some lateral facies changes between the Mohican and the Iroquois facies. It is suggested that "Mohican" arid flood-plain deposits passed seawards to "Iroquois" sabkha deposits (see analysis of conventional core of Mohican I-100 in Weston et al., 2012).

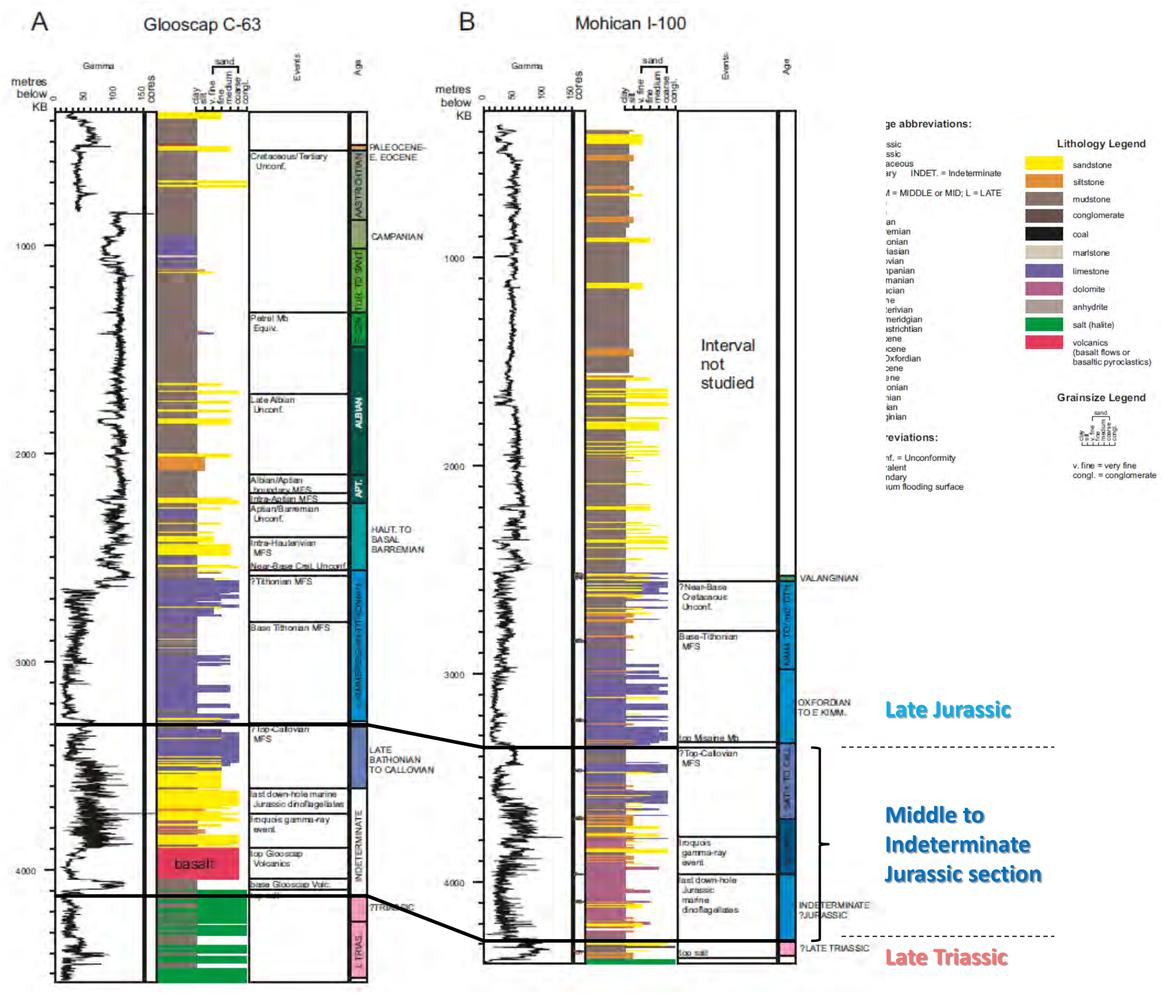

Figure 1.2.6: Summary plots for Glooscap C-63 (A) and Mohican I-100 (B) wells. Adapted from Weston et al. (2012).

Correlation of Monterey Jack E-43 and Cheshire-L-97 Wells with Older Scotian Shelf Wells

The recent Shell Monterey Jack E-43 and Cheshire-L-97 exploratory wells drilled on the Scotian Slope penetrated sediments of Middle Jurassic age. For Cheshire L-97 new biostratigraphic analysis indicates a Bajocian age for sediments close to the total depth of the well. This sedimentary succession allows a regional correlation to be established between the Scotian Shelf and the Scotia Slope. The typical lithofacies of the Middle Jurassic section of Monterey Jack E-43 and Cheshire-L-97 were claystones, marls, mud-supported carbonates, dolostones, with subordinate siltstones and sandstones (in Cheshire L-97).

The paleoenvironmental interpretations of Monterey Jack E-43 and Cheshire-L-97 indicate that shallow marine conditions prevailed throughout the Middle Jurassic despite the outboard position of the two wells (Figure 1.2.7). Although it remains to be confirmed, the presence of ooids in cuttings samples of the Middle Jurassic interval was mentioned in Shell's end of well reports (Martell et al., 2016; Van Noort et al., 2017). Their presence would be compatible with other shallow-water proxies identified in the two wells.

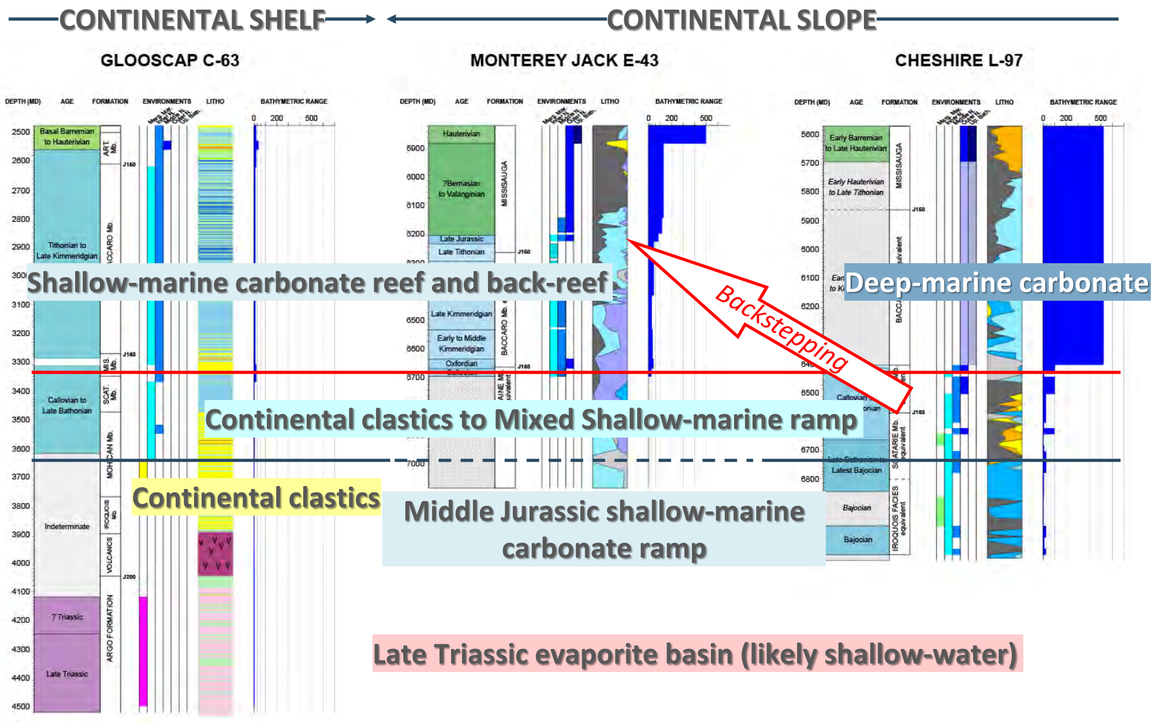

Figure 1.2.7: Correlation panel across the Shelburne Subbasin illustrating the shallow-marine conditions prevailing across the Scotia Slope during the Middle Jurassic.

Towards a Middle Jurassic Carbonate Ramp System for the Shelburne Subbasin:

One of the major results of the Monterey Jack E-43 and Cheshire-L-97 biostratigraphic analysis was the realization that shallow marine conditions lasted until at least Late Jurassic in the Shelburne Subbasin (Figure 1.2.3).

The more careful way of reconciliating paleoenvironmental interpretations at wells across the Shelburne Subbasin is to consider the existence of a ramp system extending from the Scotian Shelf down to the Scotian Slope (Figure 1.2.8). The Mohican facies represents the proximal, fluvial-dominated part of a shallow ramp. Seaward the clastics passed laterally into intertidal dolostones (innermost ramp) and then to more open marine carbonate and/or clastic deposits. The shallow-marine ramp extended at least as far as 50 km beyond the edge of the Scotian Shelf.

The rimmed platform profile with a pronounced slope was developed as late as Late Jurassic at the time when the Baccaro reef developed on the structurally-controlled edge of the Scotia Shelf. The Late Jurassic shallow water depths interpreted at Monterey Jack even tend to suggest that the slope generated by the Baccaro reef was gentler than initially thought in PFA 2011. Such consideration may have implications for the extent and type of reservoirs that could be expected in the Jurassic section of Shelburne Subbasin.

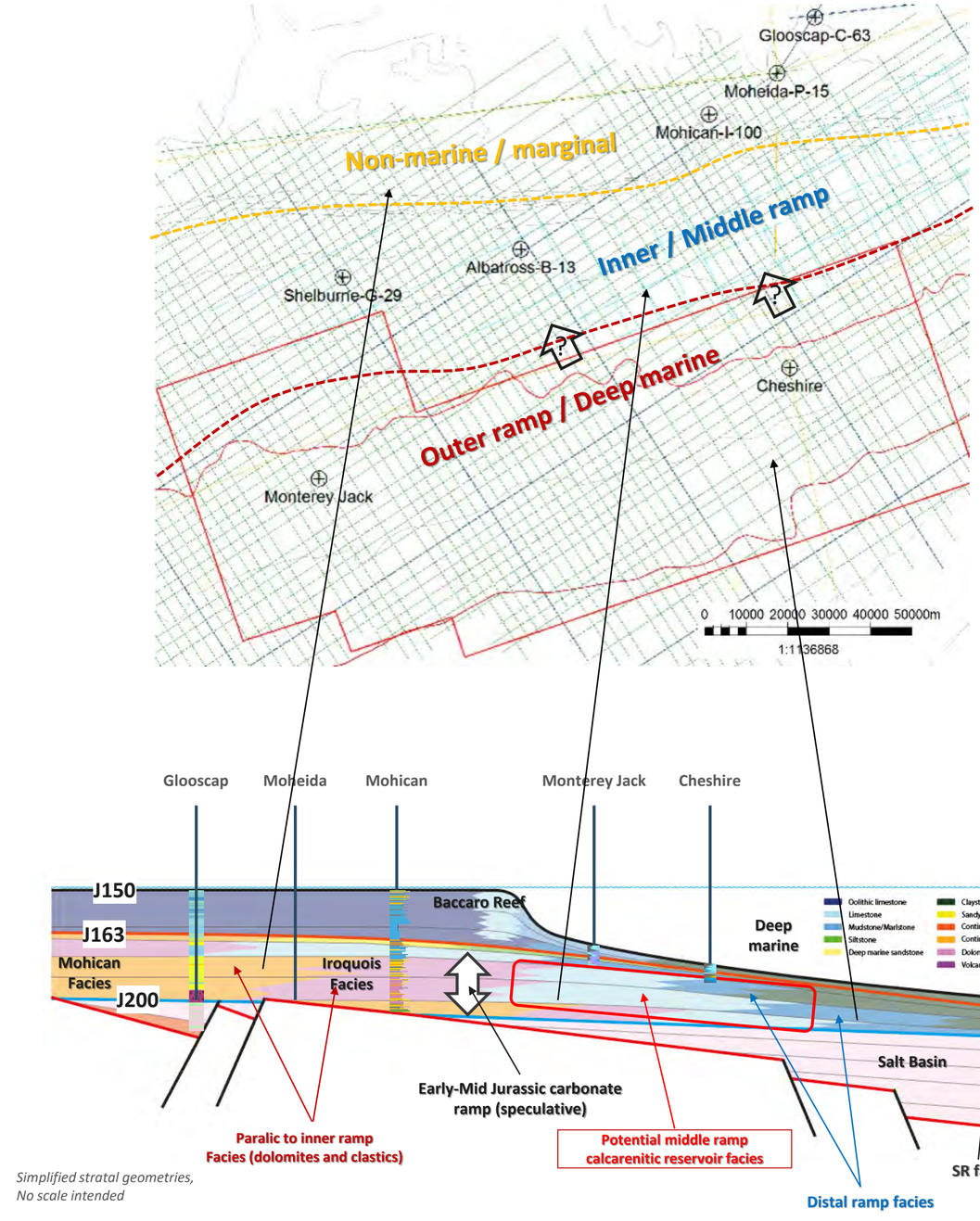

Figure 1.2.8: Geological sketch illustrating the concept of Middle to Early Jurassic carbonate ramp

Analogy to the Early-Middle Jurassic Amellago Carbonate Ramp System, High-Atlas, Morocco:

Carbonate ramp systems are widespread throughout the geological record. The closest ancient analogue to the Iroquois/Mohican system we found was the Early-Middle Jurassic Amellago carbonate ramp, exposed in the High Atlas of Morocco (Pierre et al., 2010). Sedimentary facies, age and dimensions of this system are similar to the carbonate ramp postulated in the Shelburne Subbasin (Figure 1.2.9).

The Amellago outcrop of the southern High Atlas shows the detailed depositional and stratigraphic relationships of an ooid-dominated ramp system that is almost completely exposed along a dip profile (37 km long and 1000 m thick) in the Lower to Middle Jurassic (Early Toarcian to Early Bajocian). The carbonate ramp system is subdivided into an inner ramp dominated by micritic limestones, dolostone and marls, a middle ramp dominated by oobioclastic calcarenites, and an outer ramp dominated by marls interbedded with beds of oobioclastic limestones.

The Amellago carbonate system appears to share some similarities with Middle Jurassic deposits of the Shelburne Subbasin. The Iroquois dolostones interpreted by Weston et al. (2012) as sabkha deposits are equivalent to the inter- to supratidal deposits of Amellago's inner carbonate ramp. Shelfal marls and carbonates with possible scattered ooids documented in Shell's wells are compatible with the outer ramp setting documented in the Moroccan analogue. The middle ramp oobioclastic carbonates of the Amellago ramp system were not identified in the Shelburne Subbasin. However, if the analogy is correct such calcarenitic facies belt should be expected on the proximal part of the Shelburne Subbasin.

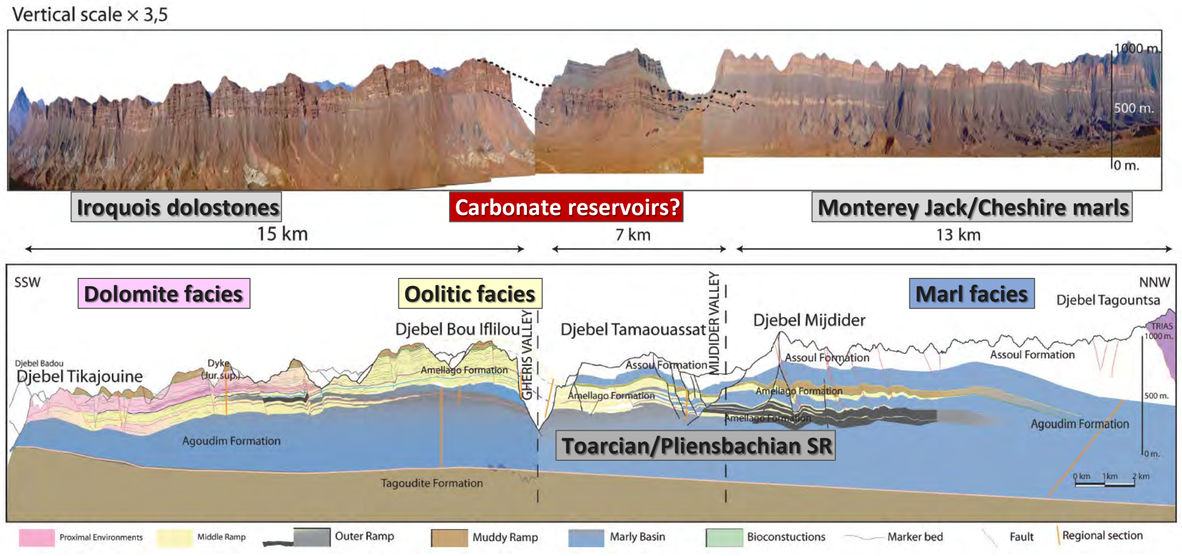

Figure 1.2.9: Analogy between the Toarcian-Bajocian Amellago carbonate ramp, High Atlas, Morocco and the Middle Jurassic facies documented in the Shelburne Subbasin.

Analogy to the Albian Carbonate Ramp Systems of South Atlantic Basins, offshore Brazil and Angola

A distinctive feature of the Shelburne Subbasin is that Jurassic rocks rest conformably on thick Late Triassic salt (according to seismic geometries). This stratigraphic configuration is similar to the post-salt sedimentary record of South Atlantic basins (e.g., Angola and Brazil), in which the thick Aptian salt sequence is conformably overlain by an Albian age shallow marine carbonate ramp system (Guarujá and Macaé Formations of the Santos and Campos Basins, and Pinda Group of Kwanza Basin; Figure 1.2.10). South Atlantic basins show that the transition from salt to marine sedimentation develops through gradual deepening of the depositional system, resulting in the establishment of a ramp system. A comparable evolution could be postulated for the Early to Middle Jurassic of the Scotian Slope, implying the deposition of shallow-marine carbonates during the Early Jurassic.

Another point of comparison between the Mohican/Iroquois facies and the Pinda Group is the high proportion of marginal marine siliciclastics landwards of shallow-marine carbonates and dolostones. In both cases, the amount of siliciclastics varies along strike, reflecting the influence of local terrestrial supply (see Plate 1.1.3).

A striking characteristic of oil-prolific Albian carbonate reservoirs found in South Atlantic basins is the porosity-enhancing dissolution of carbonate grains coupled with massive dolomitization. In the Pinda Group, massive dolomitization occurred preferentially in the inner to middle ramp carbonate facies and appears to be related to pervasive mixing zone dolomitization and fabric-selective carbonate dissolution (Eichenseer et al., 1999). Assuming that calcarenite facies are actually present in the Shelburne Subbasin, porosity enhancement through dolomitization/dissolution is not yet proved. However, considering the burial depth of potential carbonate reservoir units, porosity enhancment through dolomitization/dissolution is certainly a necessary condition for these reservoirs to be attractive.

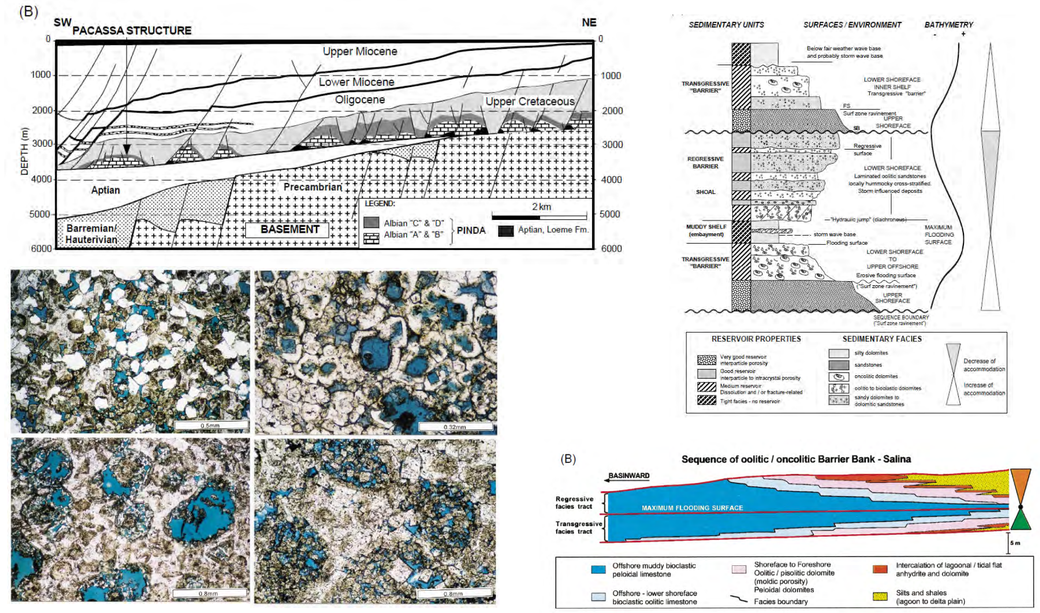

Eichenseer et al. (1999)

Figure 1.2.10: The South Atlantic Albian carbonate play: a possible analogue of the Early-Middle Jurassic speculative play in the Shelburne Subbasin.

Conclusions

The Early to Middle Jurassic series recorded in the Shelburne Subbasin are still poorly known. Although the recent Shell exploratory wells failed to prove the Late Jurassic turbidite play concept and did not reach strata older than Bajocian, the wells provided invaluable insights in the geological understanding of the undrilled Early to Middle Jurassic rocks of the Scotian Slope.

Paleobathymetry estimates conducted on Jurassic sediments from the Monterey Jack and Cheshire wells indicate that prior to Late Jurassic the Scotia Slope was shallower than previously assumed in 2011. The presence of shelfal carbonates as old as Bajocian and the occurrence of Late Triassic salt underneath them imply that a carbonate ramp system likely developed across the Shelburne Subbasin throughout the Early to Middle Jurassic interval. By analogy to the nearly contemporaneous Amellago carbonate ramp from the Morocco conjugate margin, a calcarenite facies belt is assumed to be present in the proximal part of the Shelburne Subbasin, north of Shell's exploratory wells.

Calcarenitic ramp facies can be prolific HC reservoirs especially when their porosity is enhanced through dolomitization/dissolution processes. This is the case with the Albian carbonate ramp facies of South Atlantic (Angola and Brazil), where calcarenite reservoir potential was acquired through intense fabric-selective dolomitization/dissolution of carbonate grains. If calcarenite facies are present along the Scotian Slope, they must certainly meet this diagenetic condition to be prolific reservoirs at such a burial depth.

Way Forward

- Update the sedimentological model of the Mohican/Iroquois facies by reviewing conventional cores and cuttings from Scotian Shelf wells (Moheida P-15, Mohican I-100, Glooscap C-43 and Bonnet P-23).
- Integrate Monterey Jack E-43 and Cheshire L-97 into the sedimentological model and produce a robust regional depositional system.
- Perform a detailed seismic stratigraphic analysis of regional 2D lines and 3D seismic cubes at the Shelburne Subbasin scale and integrate this framework within the sedimentological model into a sequence stratigraphic scheme.
- Build a high-resolution forward stratigraphic model to test the conceptual sedimentological and sequence stratigraphic schemes.

1.3 Postmortem Structural Analysis of Shelburne Subbasin

Shelburne Subbasin Postmortem Analysis

PFA 2011 Versus Shell Shelburne Subbasin Data

The newly acquired 3D seismic data (approximately 50 -100 km wide x 200 km long) covers part of the deep offshore domain of the Southwestern Scotian Margin (Figure 1.3.1). It spans the dip GXT 1400 and strike GXT 5300 reference lines. The dataset is located just east of the Barrington 3D survey and overlaps part of the Torbrook 3D seismic block. The Cheshire well is located on the 1400 reference line (several kilometers south of the Torbrook well located at the 1400-5300 line intersection) while the Monterrey Jack well is very close to the 5300 reference line.

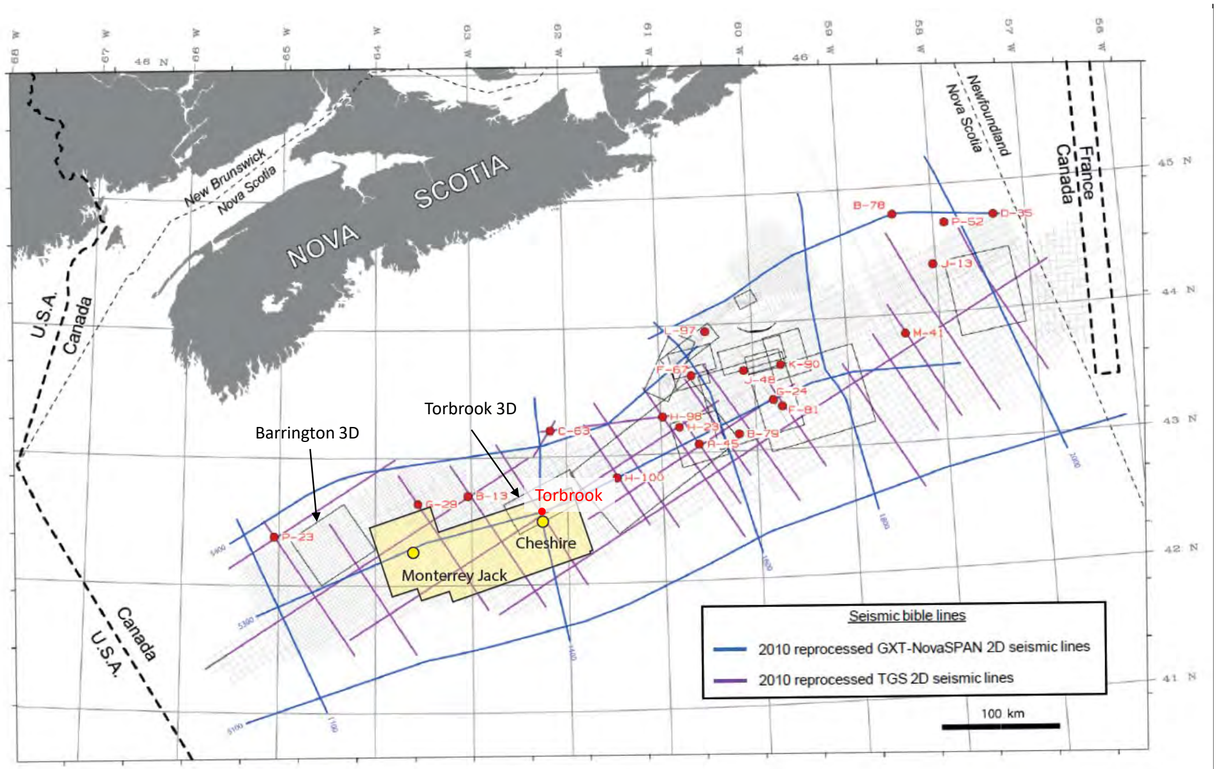

Figure 1.3.1: Location of the 3D Shelburne seismic data (yellow polygon) with the Monterrey Jack E-43 and Cheshire L-97 exploration wells shown as yellow circles. Red dots are reference wells analyzed during the PFA 2011 project. In grey are 2D seismic lines. Dark rectangles: 3D seismic surveys available for the PFA 2011 project.

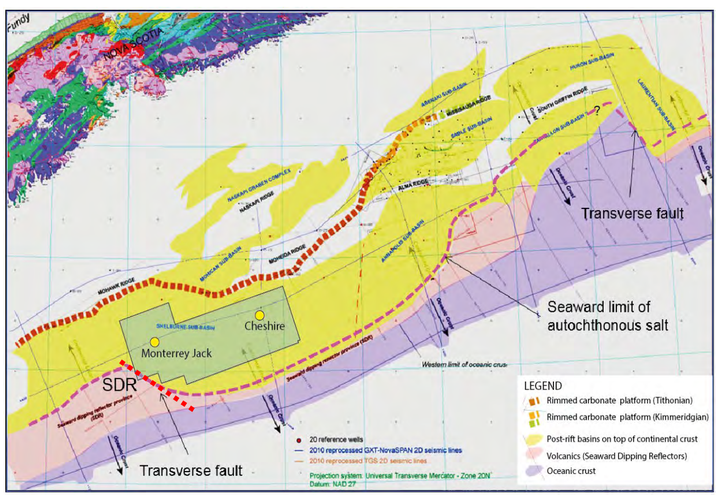

Figure 1.3.2: Main tectonic domains of the Nova Scotia margin as defined in the PFA (OETR 2011) showing the location of the 3D Shell seismic survey (green polygon).

The Shell 3D survey was acquired on stretched continental crust of the Scotian passive margin (yellow color in Figure 1.3.2). It is located SW of the main shelf break (a rimmed carbonate platform) that appears to have been in the same location since the Jurassic. It is bounded to the SW by a major NW-SE transverse fault separating the salt basin from the volcanic province, the latter characterized by Seaward Dipping Reflectors (SDRs). This major fault affecting the continental crust may have acted as a transform fault during the first breakup event.

Only very limited part of the survey could have imaged this transform boundary (see Figures 1.3.14 and 1.3.15).

It's notable that the shape of the rimmed carbonate platform mimics the salt basin boundary (seaward limit of the autochthonous salt) suggesting the salt basin strongly controlled the structural and sedimentary evolution of the margin.

The 3D survey is essentially located in the salt basin.

Offshore Nova Scotia's Main Structural Provinces as Defined in PFA 2011

Four main structural provinces have been defined on the basis of salt tectonic styles along the deep offshore domain of the Nova Scotia margin.

- The Laurentian province in the northeast is characterized by a mix of subvertical diapirs and canopies.
- The Banquereau Synkinematic Wedge (BSW) province characterized by a major gravity gliding allochthonous wedge mainly active during the Jurassic - Early Cretaceous. This wedge is detached on top of a large, early created salt tongue. Late vertical diapirs stake the northeast and southwest boundaries of this wedge.
- The Canopy province characterized by large allochthonous salt tongues (canopies) fed by one or several deep salt stems that may be of allochthonous or autochthonous origin. These canopies can be completely disconnected from their feeding zones, the stems corresponding to steeply dipping weld zones.
- The Diapir province characterized by numerous salt diapirs, mainly developed vertically, mostly circular in shape with local salt tongues of reduced extent compared to structures in the Canopy province.

The block acquired by Shell in 2012 and explored by their two deep wells covers the northeastern part of the Diapir Province.

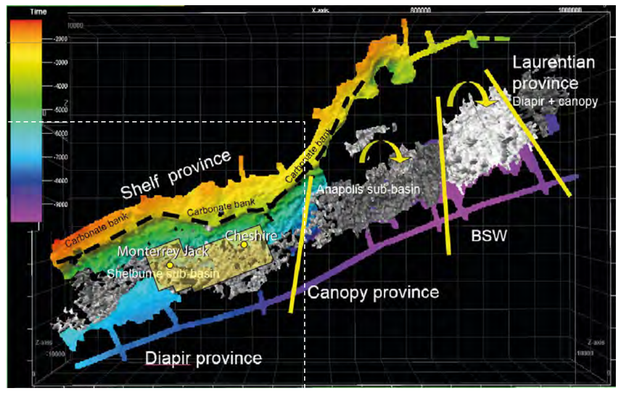

Figure 1.3.3: 3D view of the TWT structural map of the base of Mesozoic sediments and allochthonous salt (grey map) showing the main structural provinces recognized in the 2011 PFA study. The 3D Shell seismic survey corresponds to the yellow polygon. Thick yellow lines indicate boundaries of the structural provinces. Arrows indicate main salt movements from the slope to the basin. White dotted line indicates the northern and eastern limits of Figure 1.3.4. BSW: Banquereau Synkinematic Wedge.

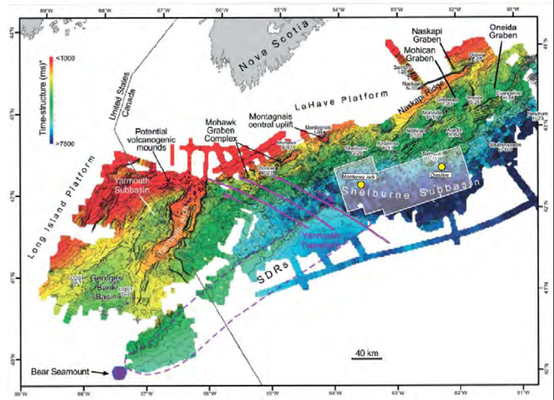

Figure 1.3.4: TWT structural map of the top of crystalline-volcanic basement and oceanic crust (from Deptuck et al. 2015) showing the main NW-SE transverse (transform) fault zone (violet lines) bounding the salt basin to the SW.

Plate Tectonic Reconstruction

The Scotian offshore domain is a typical passive margin developed during the central Atlantic opening. A rifting phase during the Triassic-Early Jurassic led to the deposition of a thick evaporitic sequence and basaltic volcanism (the CAMP volcanic event). Plate reconstruction using magnetic anomalies of the conjugate Canadian and Moroccan margins indicates breakup occurred after 190 Ma (Figure 1.3.5 and 1.3.6; Sibuet et al., 2011). East Coast Magnetic Anomaly – ECMA -- and West African Coast Magnetic Anomaly – WACMA – and Blake Spur Magnetic Anomaly -- BSMA and African equivalent anomaly .

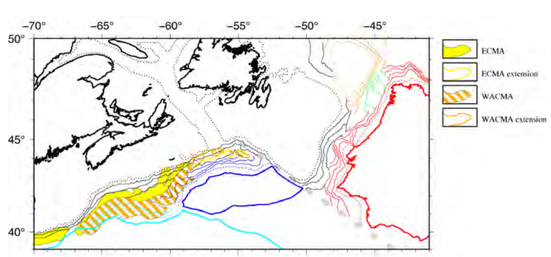

Figure 1.3.5: Kinematic reconstruction at chron ECMA - East Coast Magnetic Anomaly (Sinemurian/Pliensbachian limit, 190 Ma). (From Sibuet et al. 2011)

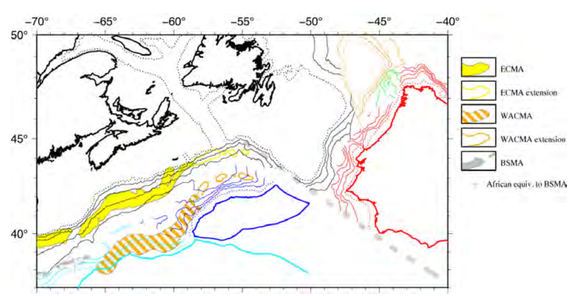

Figure 1.3.6: Kinematic reconstruction at chron BSMA - Blake Spur Magnetic Anomaly (Middle Bajocian, 170 Ma). (From Sibuet et al. 2011)

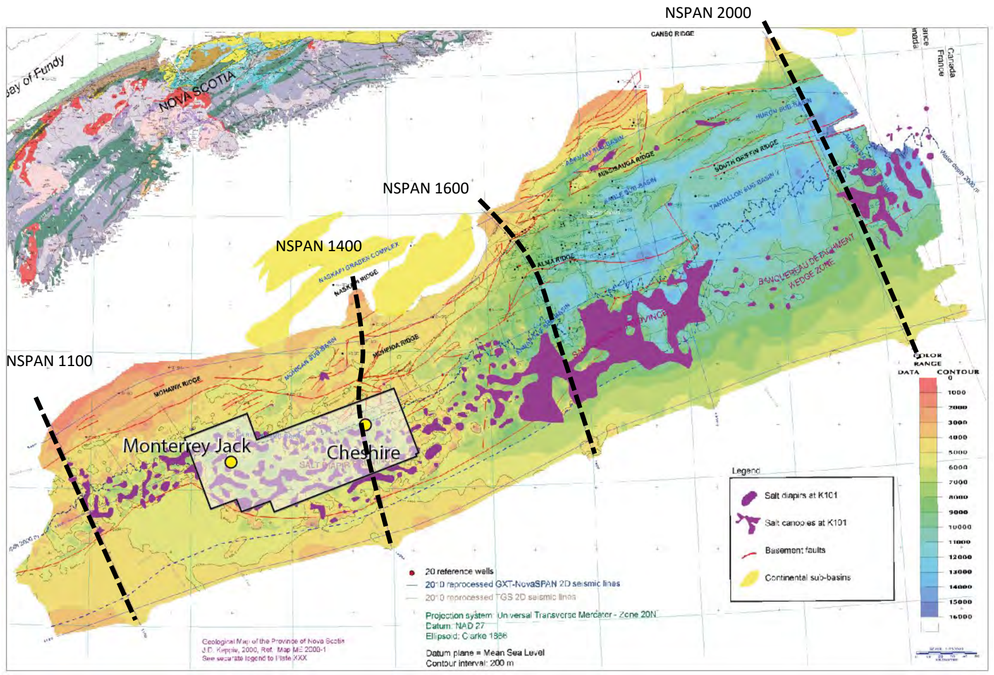

Figure 1.3.7: Mesozoic sediment total thickness (T200 to Seabed)

Nova Scotia Margin Architecture

The total post Triassic sediment thickness map (Figure 1.3.7) clearly shows two main provinces:

1) the northeastern province: a 7 to 15 km thick sedimentary sequence with major deposition during the Jurassic and Lower Cretaceous (section Novaspan 2000 and Novaspan 1600; Figure 1.3.8).

2) The southwestern province: total post Triassic sediment thickness ranges from 3 and 7 km with approximately the same volume of sediments deposited during the Jurassic/Cretaceous as during the Tertiary. Average preserved sediment accumulation is less than 0.2 m/ky which corresponds to starved conditions or bypass zone.

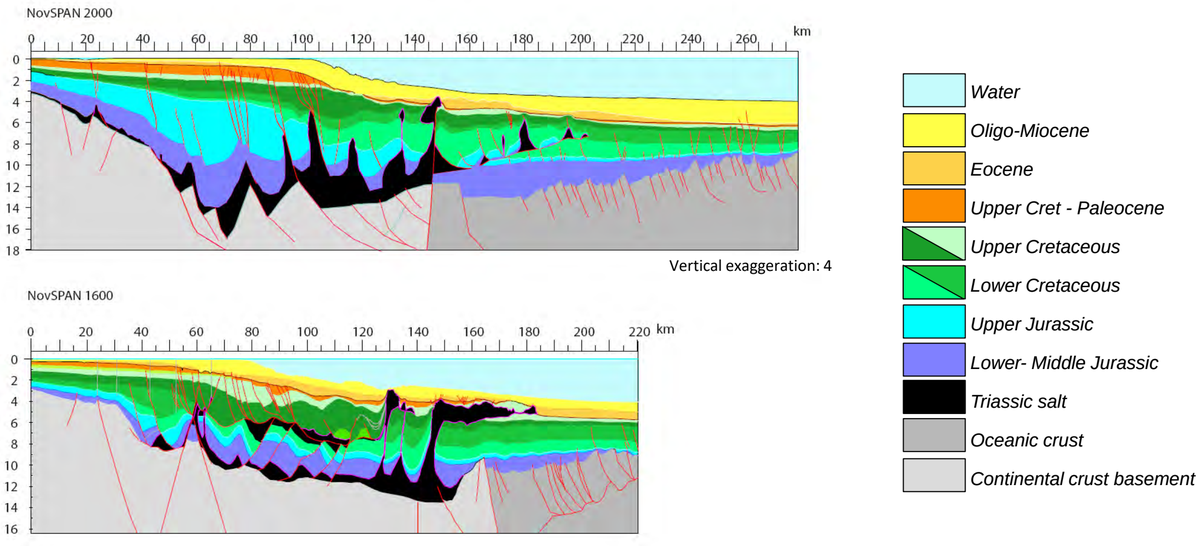

Figure 1.3.8: Interpreted depth converted geological cross-section from the NovaSPAN2000 and NovaSPAN 1600 seismic sections

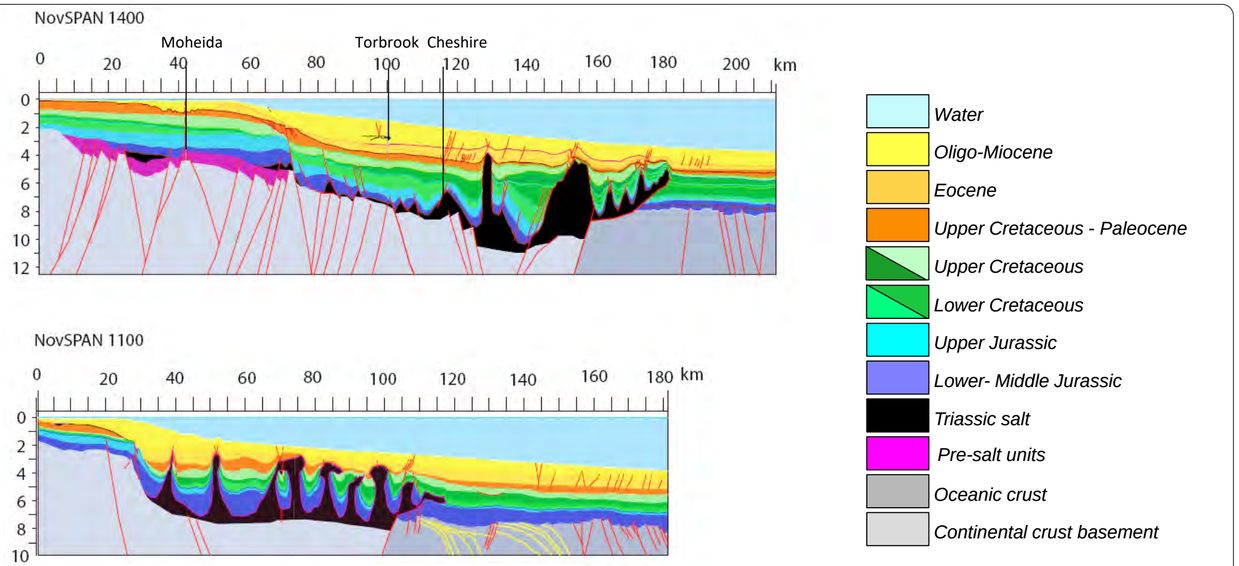

Figure 1.3.9: Interpreted depth converted geological cross-section from NovaSPAN1400 and NovaSPAN 1100.

The Shelburne Subbasin is located in the southwestern (starved) province. It developed below the La Have platform an has been rimmed by a carbonate reef since the Mid Jurassic.

The geometry of the Subbasin is controlled by basement faults and synrift salt distribution (Figure 1.3.4). To the northwest, salt onlaps the basement platform slope; here salt thickness is highly reduced (salt pinch out) and salt was likely never deposited in several parts of this slope (e.g., see Novaspan 1400 Fig. 1.3.10 and Deptuck et al. 2015 Fig. 2.7). Southeast of the slope, salt thickness increases abruptly along basement normal faults (down to the SE). Toward the abyssal plain, the salt basin terminates abruptly along a down to the NW fault scarp bounding SDRs volcanics(?) or oceanic crust. The width of the salt basin in the Shelburne Subbasin is 60 to 80 km. The original salt thickness between the two major bounding faults is estimated to be 2 to 4 km. Because of the relatively low sediment supply, diapirs do not show large allochthonous structures (salt tongues and canopies) such as those found in the northeastern province. Salt tectonics is characterized by more symmetrical salt walls or columnar subvertical diapirs except in the distal zone where salt tongues overhang oceanic crust (Novaspan 1400 in Figure 1.3.9).

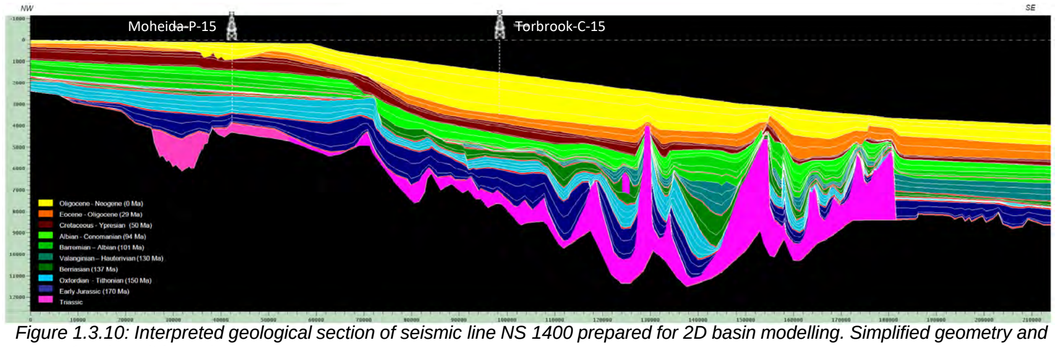

Figure 1.3.10: Interpreted geological section of seismic line NS 1400 prepared for 2D basin modelling. Simplified geometry and ages of main unit boundaries.

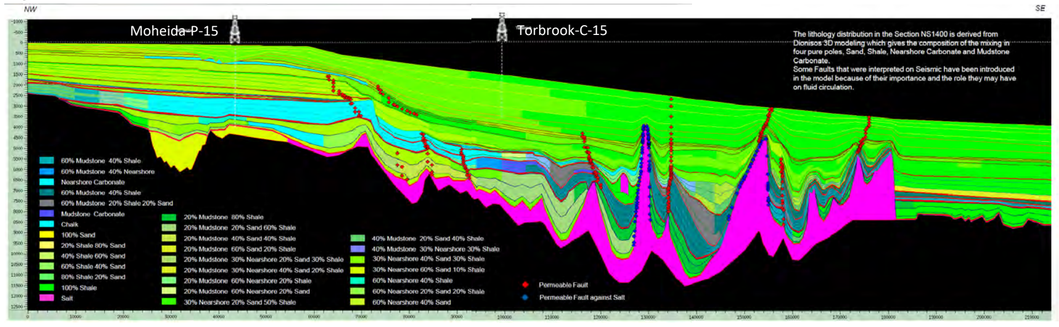

Figure 1.3.11: Interpreted geological section of seismic line NS 1400 prepared for 2D basin modelling. Lithology and fault zones at Present Day.

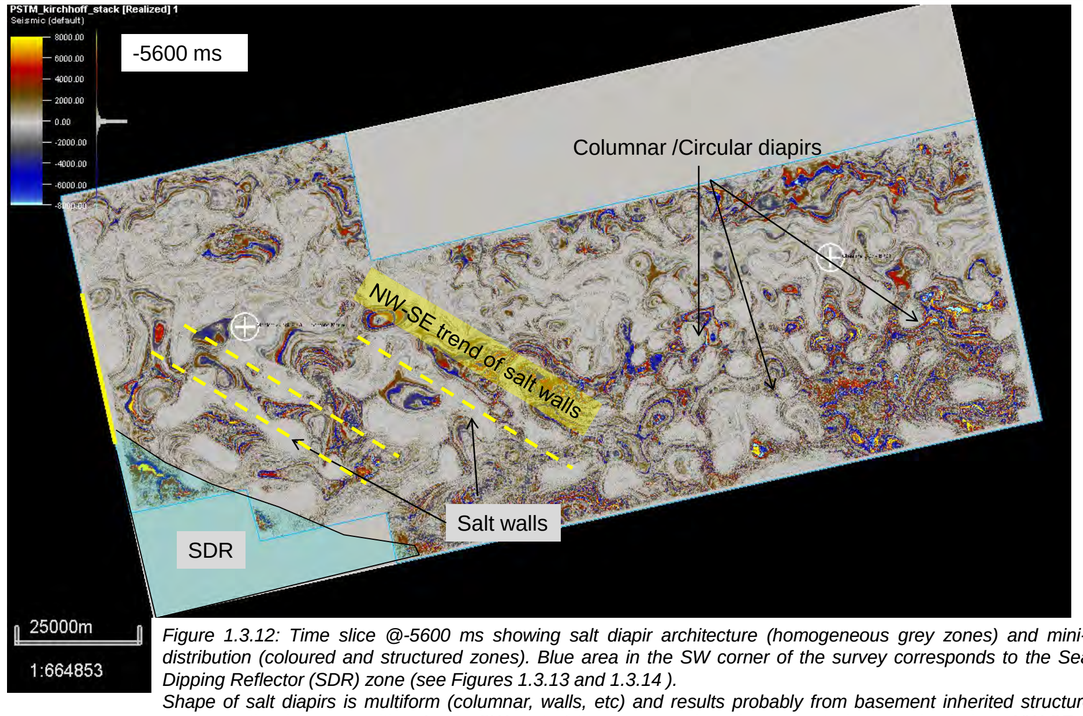

Figure 1.3.12: Time slice @-5600 ms showing salt diapir architecture (homogeneous grey zones) and mini-basin distribution (coloured and structured zones). Blue area in the SW corner of the survey corresponds to the Seaward Dipping Reflector (SDR) zone (see Figures 1.3.13 and 1.3.14).
Shape of salt diapirs is multiform (columnar, walls, etc) and results probably from basement inherited structure and sedimentation heterogeneities. In the SW part of the survey, salt walls appear to be organized along NW-SE trends corresponding to the major transform boundary described by Deptuck et al., 2015 (Figure 1.3.4)

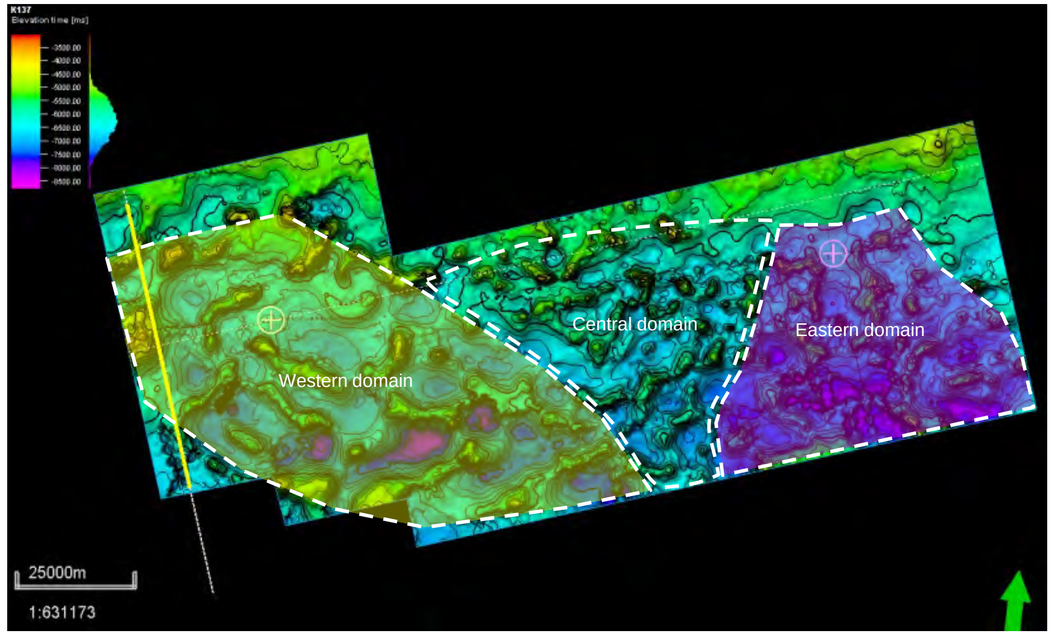

Figure 1.3.13: Structural map of the K137 horizon (NSDEM seismic interpretation grid) showing main diapirs and mini-basin distribution. 3 domains can be recognized:
1) The western domain with large NW-SE elongated deep mini-basins
2) The central domain with small and shallow mini-basins
3) The eastern domain with deep NS and EW mini-basins
The NW-SE trends In the western domain may be explained by faulted basement influencing diapir orientation suggesting deep seated control. In the eastern domain NS diapir trends appear to be directly related to sediment supply perpendicular to the slope producing NS elongated basins.

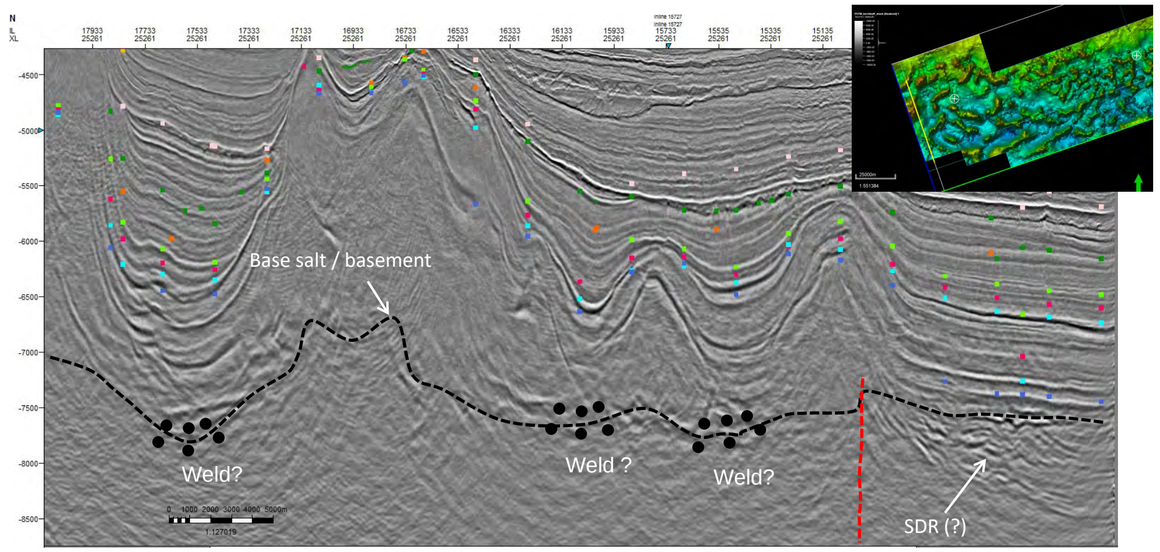

Figure 1.3.14: Xline 25261 showing the SW boundary of the salt basin with a possible transverse NW-SE fault separating the basement of the salt basin with Seaward Dipping Reflectors. The base of the mini-basins may correspond to weld zones where salt has been totally removed by sediment loading and pushed into the diapirs.

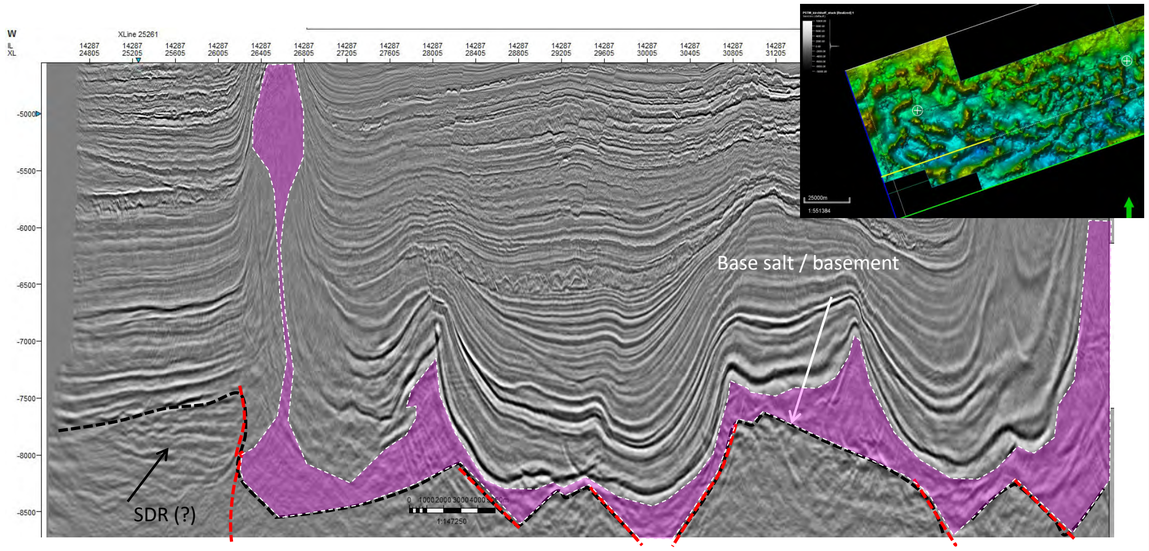

Figure 1.3.15: InLine 14287 showing the SW boundary of the salt basin with a possible transverse NW-SE fault separating the basement of the salt basin with Seaward Dipping Reflectors. This line suggests that diapirs are partly controlled by basement faults that may be related to the major "transform" faults bounding the salt basin (Deptuck et al., 2015)

Shelburne Subbasin Postmortem Analysis

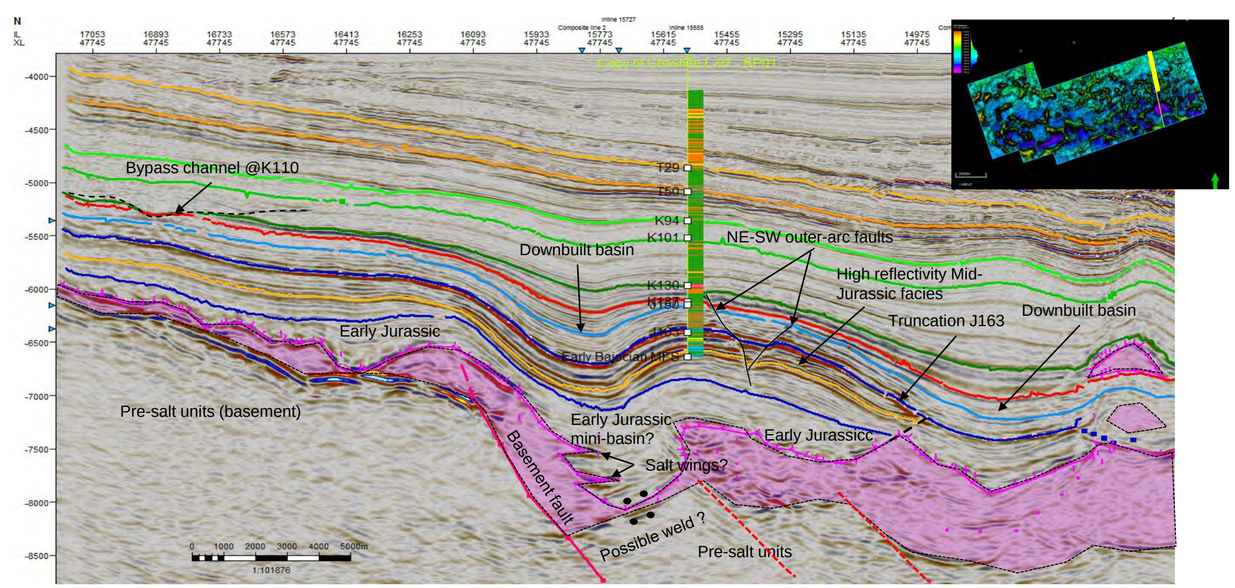

Figure 1.3.16: Interpreted Xline 47745 crossing through the of the Cheshire structure. Interpreted horizons were calibrated on well data. Additional horizons (dark blue and orange colour) have been picked in the Early Jurassic units.

At the level of the Jurassic and Cretaceous units, the Cheshire structure is an **"extensional anticline"** developed just SE of a major basement fault bounding the salt basin. It is bounded to the NW and the SE by two basins developed by salt withdrawal. **It mimics a turtle structure** but is not really an inverted early formed mini-basin between two diapirs (see below) and because a salt diapir is still present below the anticline. Moreover as shown by the structural map (Figure 1.3.19) no real 4D closure exists. However, it could have been the location of clastic deposits in the Mid and Early Jurassic since very early salt movements created Early Jurassic mini-basins between diapirs that may have reached the sea bottom. Unfortunately, high reflectivity mid Jurassic facies correspond to silt and carbonates with no porosity.

In the XLine, maximum closure is at the Jurassic level with a 7.5 km long structure and a potential closure height of 400 ms (TWT). At the Early Cretaceous level, the closed structure is only 5 km long and 200 ms (TWT) height. Structural closure disappears completely in the Tertiary.
In the IN-line, the structure appears as a V shaped mini-basin bounded by two major salt walls. Width of the basin is 20 km at the T50 level but only 5 km at the Early Jurassic level. Salt walls are almost perpendicular (NNW-SSE oriented) to the slope direction. A very small (2.5 km wide X 100 msTWT height) closed structure exists at the level of the K130 but was not the one drilled by the Cheshire well. For all other horizons, closure is against salt walls.

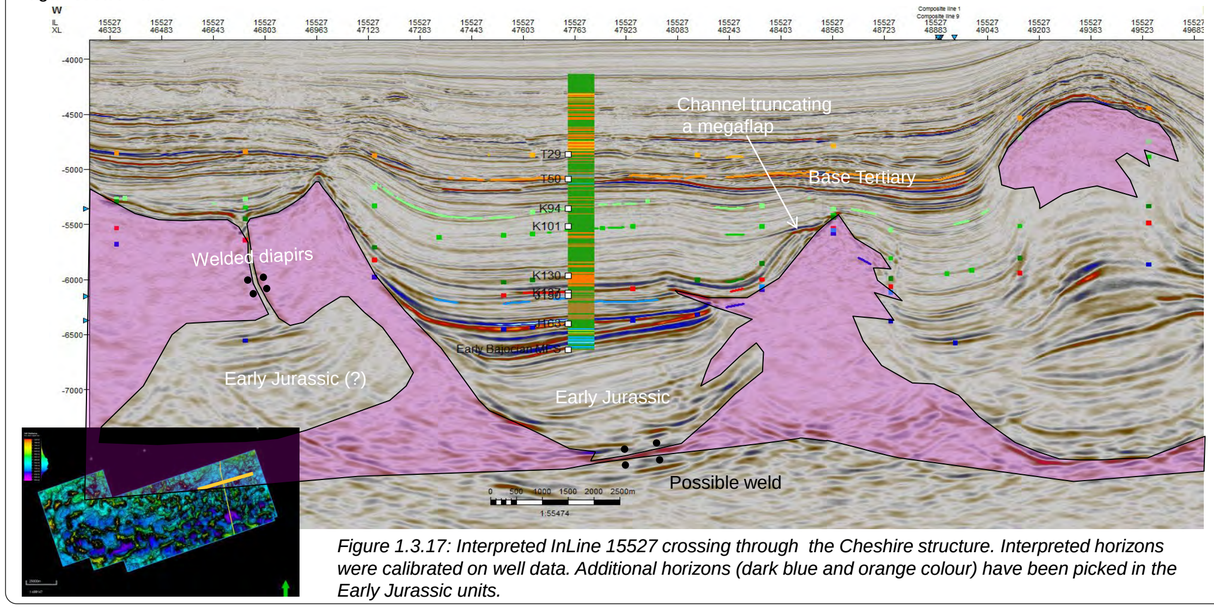

Figure 1.3.17: Interpreted InLine 15527 crossing through the Cheshire structure. Interpreted horizons were calibrated on well data. Additional horizons (dark blue and orange colour) have been picked in the Early Jurassic units.

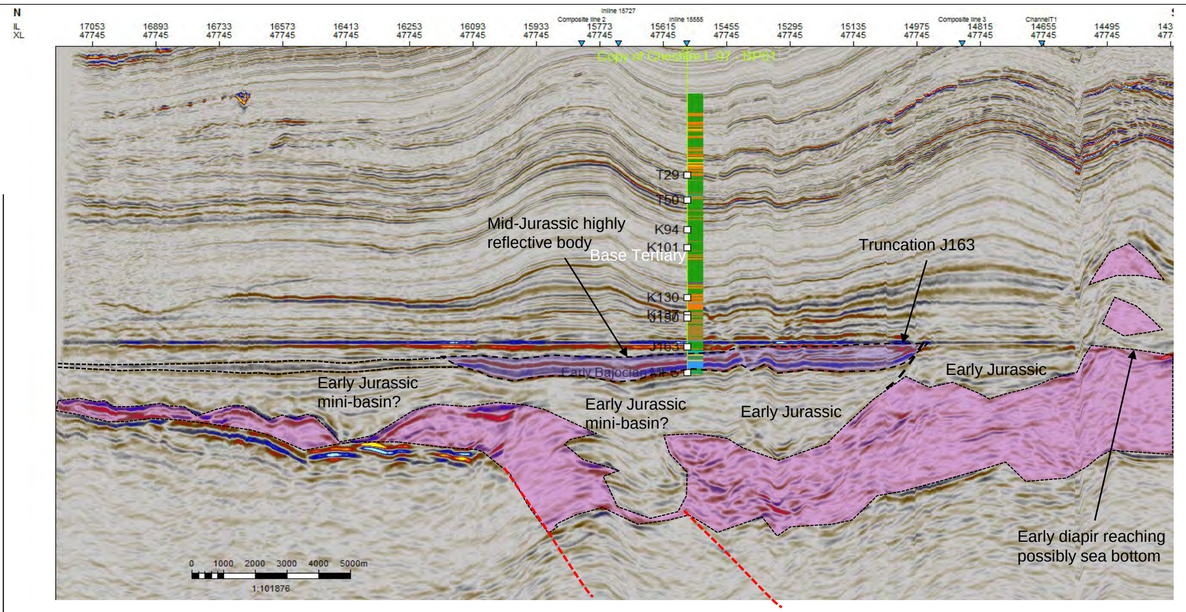

Figure 1.3.18: Flattening of the XLine 47745 crossing through the Cheshire structure. This flattening shows clear salt related structure during the Early Jurassic.

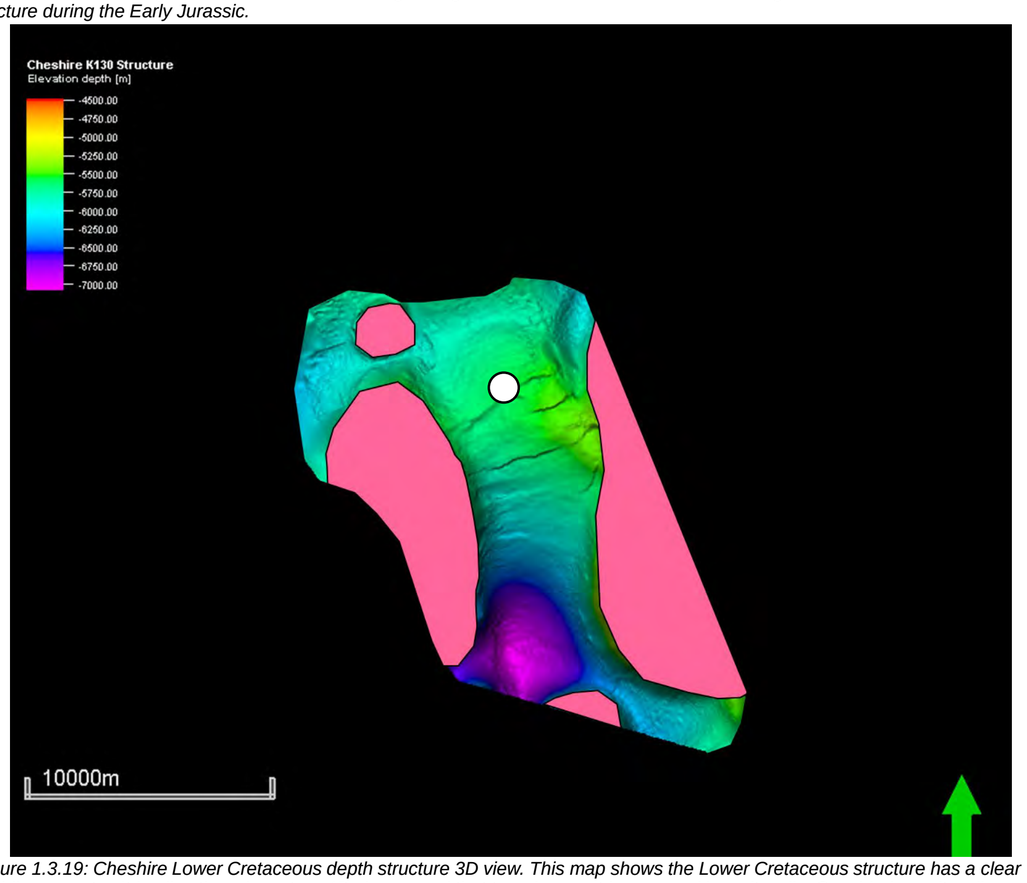

Figure 1.3.19: Cheshire Lower Cretaceous depth structure 3D view. This map shows the Lower Cretaceous structure has a clear saddle geometry. It implies there is no true 4D closure and that trapping must be ensured by salt walls. Considering salt wall as potential seals, the trap at the Lower Cretaceous level has an estimated areal extent of 55 km2 and 800 meters of relief.

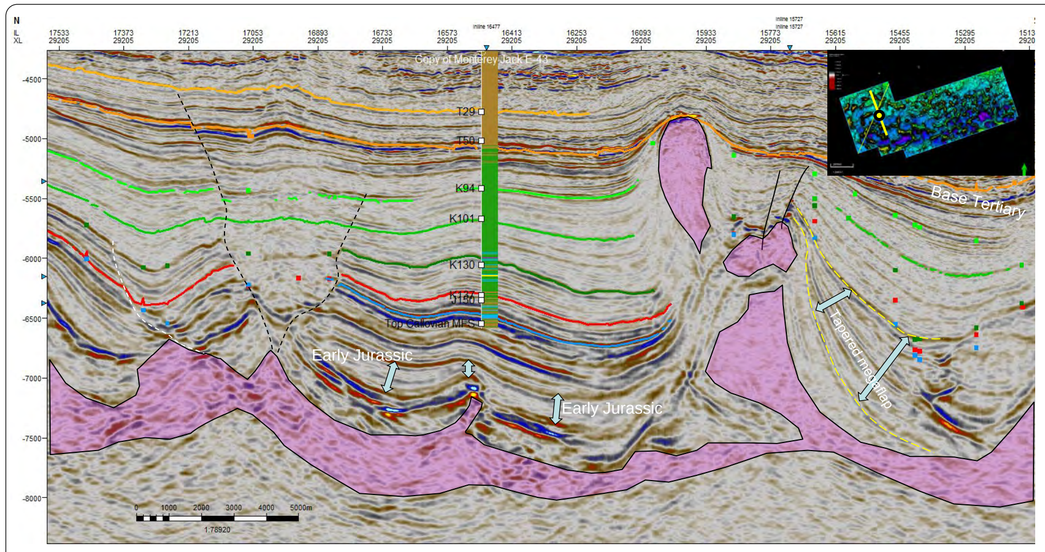

Figure 1.3.20: Interpreted Xline 29205 crossing through the Monterrey Jack structure. Interpreted horizons were calibrated on well data.

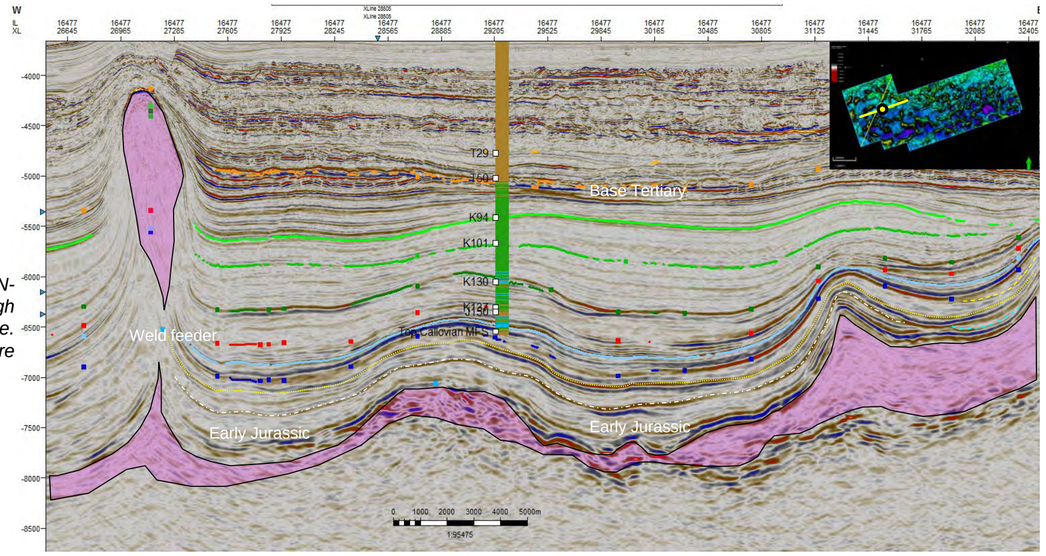

Figure 1.3.22: Interpreted IN-line 16477 crossing through the Monterrey Jack structure. Interpreted horizons were calibrated on well data.

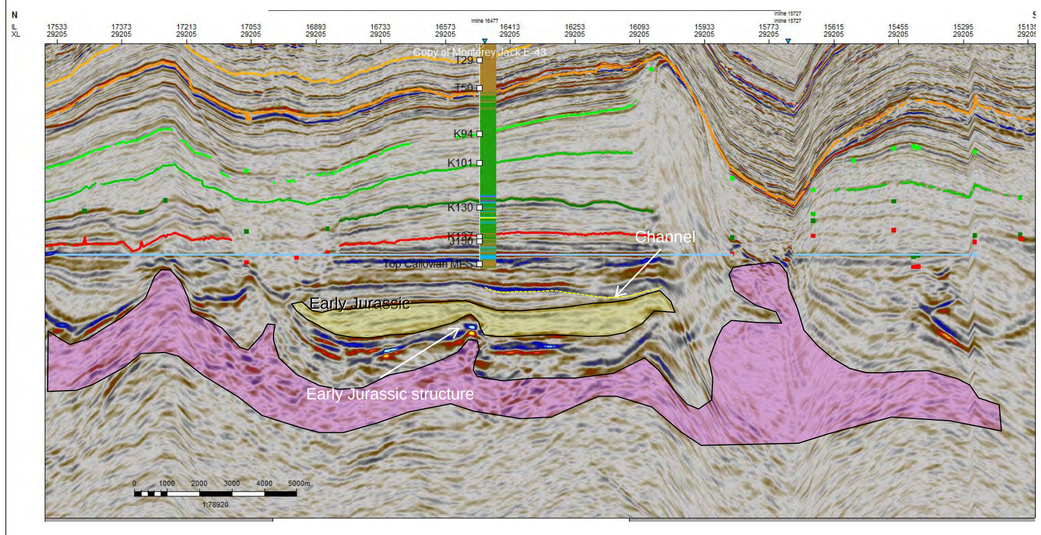

Figure 1.3.21: Flattening @ J150 of the XLine 29205 crossing through the Monterrey Jack structure. It shows that the Monterrey Jack structure is superimposed on an Early Jurassic salt structure controlling sedimentation of Early Jurassic series (yellow underline series)

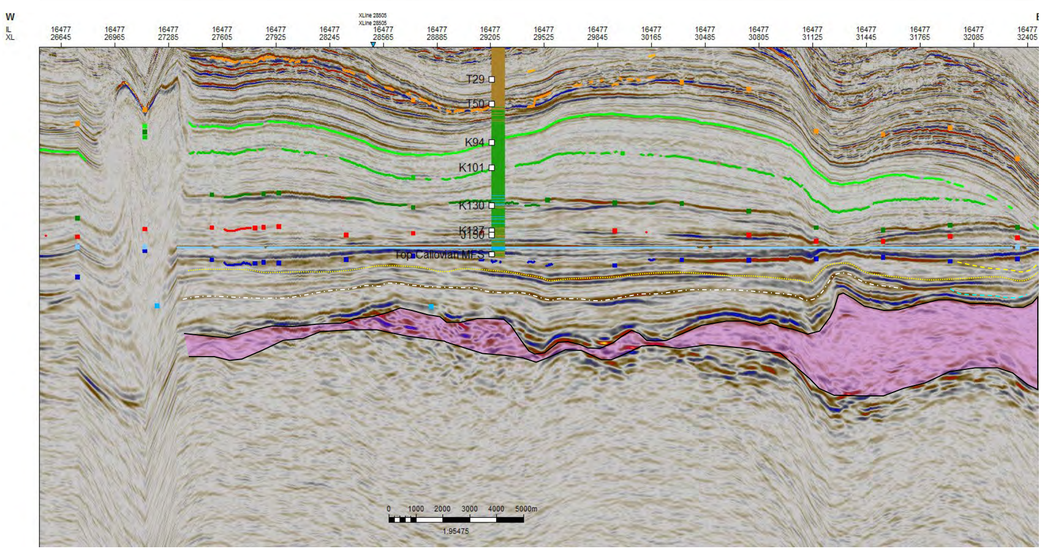

Figure. 1.3.23: Flattening @ J150 of the IN-line 16477 crossing through the Monterrey Jack structure. Interpreted horizons were calibrated on well data

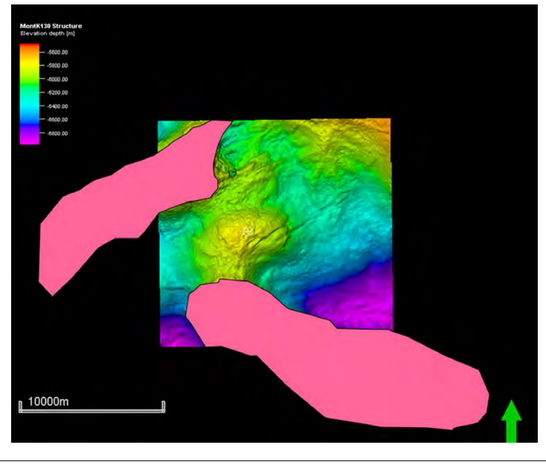

Figure 1.3.24: Depth structural map of the Monterey Jack structure at K130

Monterey Jack Structure

Monterey Jack is a **drape structure on top of a diapir**. The formation mechanism appears to be related to the relative collapse by salt withdrawal around an early asymmetrical salt dome. It results in a drape structure with 4 way dip closure for all the horizons from Early-Jurassic to Late Cretaceous (Figure 1.3.16 and 1.3.18). The structure is unconformably covered by Tertiary sediments and is not expressed in the more recent deposits. Locally the top of the structure may have been partially eroded by base Tertiary channelling systems (Figure 1.3.18). Flattened sections (Figure 1.3.17 and 1.3.19) suggest the structural high was initially formed during the Early Jurassic and continued to grow until the end of the Cretaceous. Relatively isopachous Jurassic and Cretaceous series on top of the structure indicate a very slow growth of the structure.

Contrary to the Cheshire structure, Monterey Jack has 4 way dip closure (Figure1.3.20). However the closed structure is no more than 12 km^2 (approximately 4 X 3 km; Figure 1.3.24) for a vertical relief of 125 m. Diapirs to the NW and to the S are potential seals, which could result in a much larger closed structure at an estimated 22 km^2.

Structural Traps

As in most of worldwide salt basins (e.g., Gulf of Mexico, North Sea, conjugate West African and Brazilian margins, etc. see for instance Hudec and Jackson, 2007) numerous structural traps can be observed in the Shelburne Subbasin. These structural traps have been successfully drilled in most of the salt provinces (i.e Pilcher et al. 2011; Weimer et al. 2017; Bourollec et al; 2017). Due to the viscous mechanical properties and almost constant specific weight of salt during burial, halokinetic structures have very special geometries since salt behaves as a fluid during basin evolution.

Halokinetic traps have been described in great detail using high definition seismic imaging and their genesis is now rather well understood even if their 3D geometrical evolution remains often difficult to reconstruct (Hudec and Jackson, 2017).

Most of the classical diapir-related traps in the Shelburne Subbasin can be recognized and constitute potential plays (Figures 1.3. 7 and 1.3.9). However, because the Shelburne Subbasin is located in a relatively starved part of the Scotian Margin, no large canopies nor large allochthonous sedimentary wedges are observed.

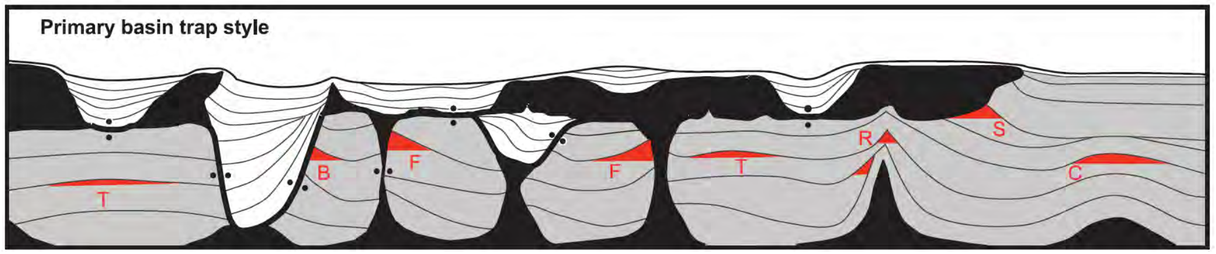

Figure 1.3.25: Schematic salt geometry highlighting primary basin trap types: turtle structure (T), bucket weld (B), salt feeder (F), salt ridge (R), base-of-salt truncation (S), and salt cored fold (C) from Pilcher et al. 2011

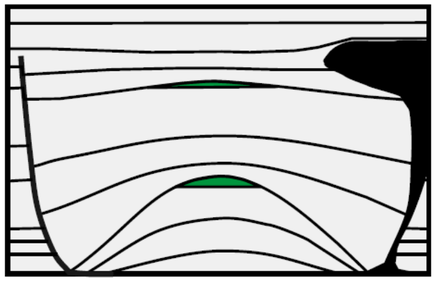

1a - Extensional anticlinal trap

Blind Faith (MC 696), bowl/sheet, 15.3 to 13.05 Ma, Fig. 54.
Gunflint (MC 948), bowl, 15.3 to 13.05 Ma, Fig. 89.
Kodiak (MC 771), possibly bowl, 15.3 to 13.05 Ma, Fig. 88.
Marmalard (MC 300), sheet, 15.3 to 13.05 Ma, Fig 33.
Niedermeyer (MC 253), sheet, 14.35 Ma to 13.05 Ma, Fig. 32.
Thunder Horse (MC 778), trough, 15.3 to 14.35 Ma, Fig. 77.

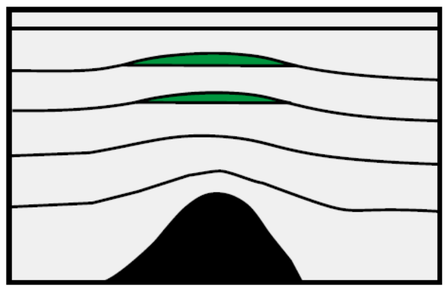

1b - Compactional drape trap

Atlas (LL 50), sheet, 13.05 to 10.75 Ma, Fig. 19.
Atlas NW (LL 5), sheet,10.75 to 9.0 Ma, Fig. 18.
Cheyenne (LL 399), sheet, 10.75 to 9.0 Ma, Fig. 20.
Jubilee (AT 349), sheet,10.75 to 9.0 Ma, Fig. 8.
San Jacinto (DC 618), sheet, 13.05 to 10.75 Ma, Fig. 15.
Vortex (AT 261), sheet, 13.05 to 10.75 Ma, Fig. 7.

Figure 1.3.26: Schematic cross-sections showing two types of four-way closure traps in the Gulf of Mexico province (from Bouroullec et al, 2017). 1a) Extensional anticlinal trap is generally described as "turtle structure" and results from the removal of salt below an initial mini-basin inducing an inversion of this initial syncline geometry. 1b) Drape fold anticline produced by combination of compaction and peripheral salt removal.
Example of Gulf of Mexico oil fields are indicated for each style with reservoir types and age; figure number refers to AAPG datashare 81 attached to the oilfield atlas (Weimer et al, 2017)

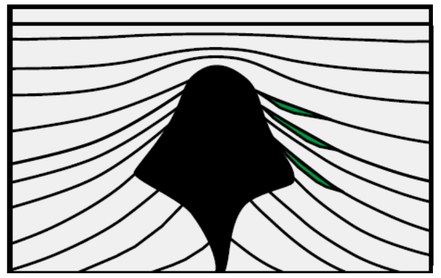

2a - Suprasalt trap against salt flank

Appaloosa (MC 460), wedge, 4.1 to 3.6 Ma, Fig. 41.
Dantzler (MC 782), wedge, 7.45 to 6.2 Ma, Fig. 78.
Devil's Tower (MC 773), wedge, 6.2 to 4.1 Ma, Fig. 75.
Europa (MC 935), wedge/trough, 6.2 to 4.1 Ma, Fig. 83.
Gladden (MC 800), sheet, 4.1 to 3.6 Ma, Fig. 79.
Goose (MC 751), trough, 4.1 to 3.6 Ma, Fig. 64.
Matterhorn (MC 243), wedge, 5.4 to 4.1 Ma, Fig. 26.
Merganser (AT 37), sheet, 15.3 to 13.05 Ma, Fig. 5.
Valley Forge (MC 707), wedge, 4.1 to 3.6 Ma, Fig. 59.
Who Dat (MC 503), wedge, 9.0 to 4.1 Ma, Fig. 43.

2b - Subsalt trap against base salt

Crosby (MC 899), wedge, 9.0 to 7.45 Ma, Fig. 82.
Deimos (MC 806), wedge, 11.4 to 9.0 Ma, Fig. 68.
King (MC 764), wedge/sheet, 9.0 to 5.4 Ma, Fig. 70.
Mars (MC 807), wedge/sheet, 9.0 to 5.4 Ma, Fig. 69.
Mirage (MC 941), wedge, 9.0 to 7.45 Ma, Fig. 84.
Morgus (MC 942), wedge, 9.0 to 7.45 Ma, Fig. 85.
Power Nap (MC 987), wedge, 18.3 to 15.4 Ma, (No Figure)
Princess (MC 765), wedge/sheet, 9.0 to 5.4 Ma, Fig. 71.
Telemark (AT 63), wedge, 18.3 to 15.3 Ma, Fig. 86.
Thunder Hawk (MC 734), wedge, 14.35 to 13.05 Ma, Fig. 87.
Thunder Horse North (MC 776), wedge, 14.35 to 13.05 Ma, Fig. 76.
Tubular Bells (MC 725), bowl, 15.3 to 13.05 Ma, Fig. 62.
Ursa (MC 809), wedge/sheet, 9.0 to 5.4 Ma, Fig. 72.
Vito (MC 984), wedge, 18.3 to 15.4 Ma, Fig 90.
West Boreas (MC 762), wedge/sheet, 9.0 to 5.4 Ma, Fig. 67.

Figure 1.3.27: Schematic cross-sections showing two types of traps against salt in the Gulf of Mexico (from Bouroullec et al, 2017). 2a) Suprasalt: the flank of the diapir and the reservoir have the same dip direction 2b: Infra salt (or subsalt): reservoirs and salt flanks or feeders (or weld feeders) are dipping in the opposite direction.
Examples of Gulf of Mexico oil fields are indicated for each style with reservoir types and age; figure number refers to AAPG datashare 81 attached to the oilfield atlas (Weimer et al, 2017)

- Fault-bounded trap

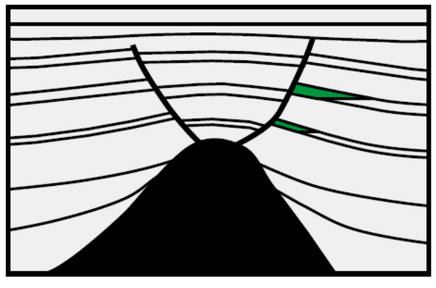

Aconcagua (MC 305), wedge, 10.75 to 9.0 Ma, Fig. 34.
Anduin (MC 755), wedge, 6.2 to 5.4 Ma, Fig. 66.
Anduin West (MC 754), wedge, 6.2 to 5.4 Ma, Fig. 65.
Appomattox (MC 392), trough, 163 to 160 Ma, Fig. 37.
Ariel (MC 429), trough, 7.45 to 6.2 Ma, Fig. 39.
Bass Lite (AT 426), sheet, 0.6 to 0.5 Ma, Fig. 9.
Biddy Ball (MC 705), trough, 1.3 to 1.1 Ma, Fig. 58.
Big Bend (MC 698), wedge, 15.3 to 13.05 Ma, Fig. 56.
Coulomb (MC 657), sheet, 13.05 to 12.2 Ma, Fig. 55.
East Antsey (MC 607), wedge, 10.75 to 9.0 Ma, Fig. 53.
Gomez (MC 711), trough/wedge, 4.1 to 1.3 Ma, Fig. 60.
Herschel (MC 520), trough, 13.05 to 10.75 Ma, Fig. 46.
Horn Mountain (MC 127), wedge, 10.75 to 9.0 Ma, Fig. 23.
King (MC 84), wedge, 10.75 to 9.0 Ma, Fig. 22.
Mandy (MC 199), sheet, 4.1 to 3.6 Ma, Fig. 25.
Mars (MC 807), wedge, 5.4 to 4.1 Ma, Fig. 69.
MC 161 (MC 161), sheet, 4.1 to 3.6 Ma, Fig. 24.
MC 837 (MC 837), sheet, 1.3 to 1.1 Ma, Fig. 80.
Medusa (MC 582), wedge, 6.2 to 3.6 Ma, Fig. 50.
Medusa North (MC 538), wedge, 5.4 to 4.1 Ma, Fig. 49.
Otis (MC 79): sheet, 13.05 to 10.75 Ma, Fig. 21.
Pluto (MC 718), wedge, 9.0 to 7.45 Ma, Fig. 61.
Q (MC 961), sheet, 15.3 to 13.05 Ma, Fig. 6.
Rydberg (MC 525), sheet, 163 to 160 Ma, Fig. 48.
Santa Cruz/Santiago (MC 519/563), sheet, 15.3 to 13.05 Ma, Fig. 45.
Spiderman (DC 621), sheet, 13.05 to 10.75 Ma, Fig. 16.
Triton (MC 772), wedge, 6.2 to 4.1 Ma, Fig. 74.
Vicksburg (DC 353), trough, 163 to 160 Ma, Fig. 14.

Figure 1.3.28: Schematic cross-sections showing fault related traps in the Gulf of Mexico (from Bouroullec et al, 2017). This kind of trap is the most common in producing fields of the Gulf of Mexico.
Example of Gulf of Mexico oil fields are indicated for each style with reservoir types and age; figure number refers to AAPG datashare 81 attached to the oilfield atlas (Weimer et al, 2017)

Turtle back (also called “turtle structure” or “extensional anticline” or “inverted structure”)

A turtle structure is a present day anticline with a four-way dip closure. Because the present day apex of the structure was previously a basin surrounded by diapirs or domes, the basin could have been the locus of clastic deposits.

During the salt migration from the bottom of the mini-basin toward the peripheral growing diapirs, previous sedimentary wedges of the basin collapse while the thick central accumulation remains in a higher position due to thickness differences between the centre and the border of the mini-basin.

This structure is characterized by the associated development of new mini-basins surrounding the turtle anticline and by extensional faults (outer-arc normal faults) at the crest of the turtle back. These faults (as all the outer-arc extensional faults) have a maximum vertical throw at the crest of the structure; the vertical throw disappears at depth where the faults die out.

In the Shelburne 3D survey, few (if any) turtle structures with four-way dip closure could be identified in a first quick overview. As described in plate 1.3.4, the Cheshire structure is not really a “turtle” even if in XLines it mimics this geometry.

The structure shown in Figures 1.3.21 and 1.3.22 developed in a similar way with inversion of initial half mini-basin and the creation of rim synclines. However the only way to characterize such structures is 3D mapping of the various horizons.

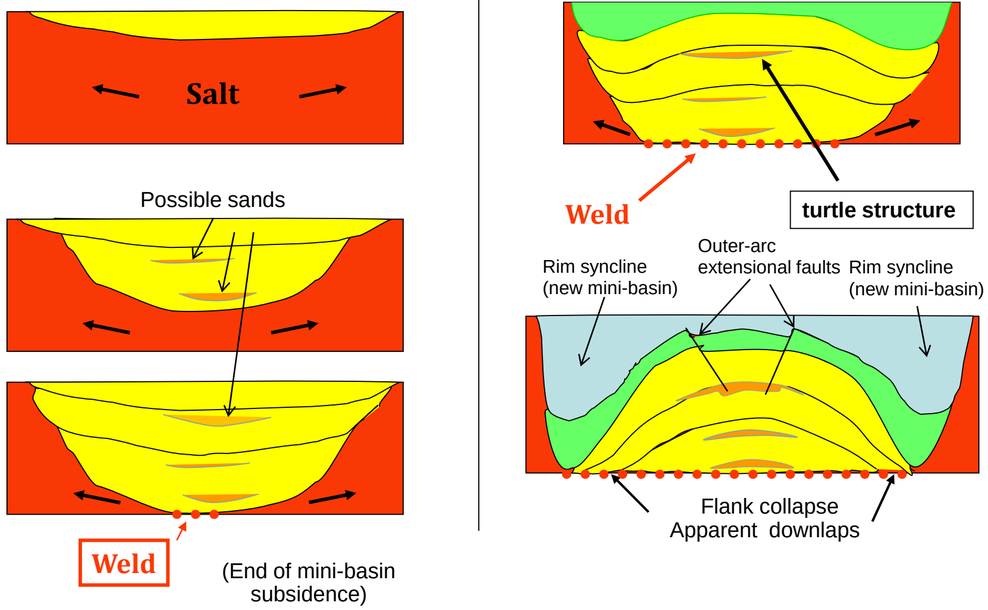

Figure 1.3.29: Schematic cross-section of the theoretical evolution and formation of a turtle structure (modified from Letouzey, 1990). Because the initial syncline geometry of the mini-basin becomes an anticline during salt movement, “turtle structures” are also called “inverted structures”.

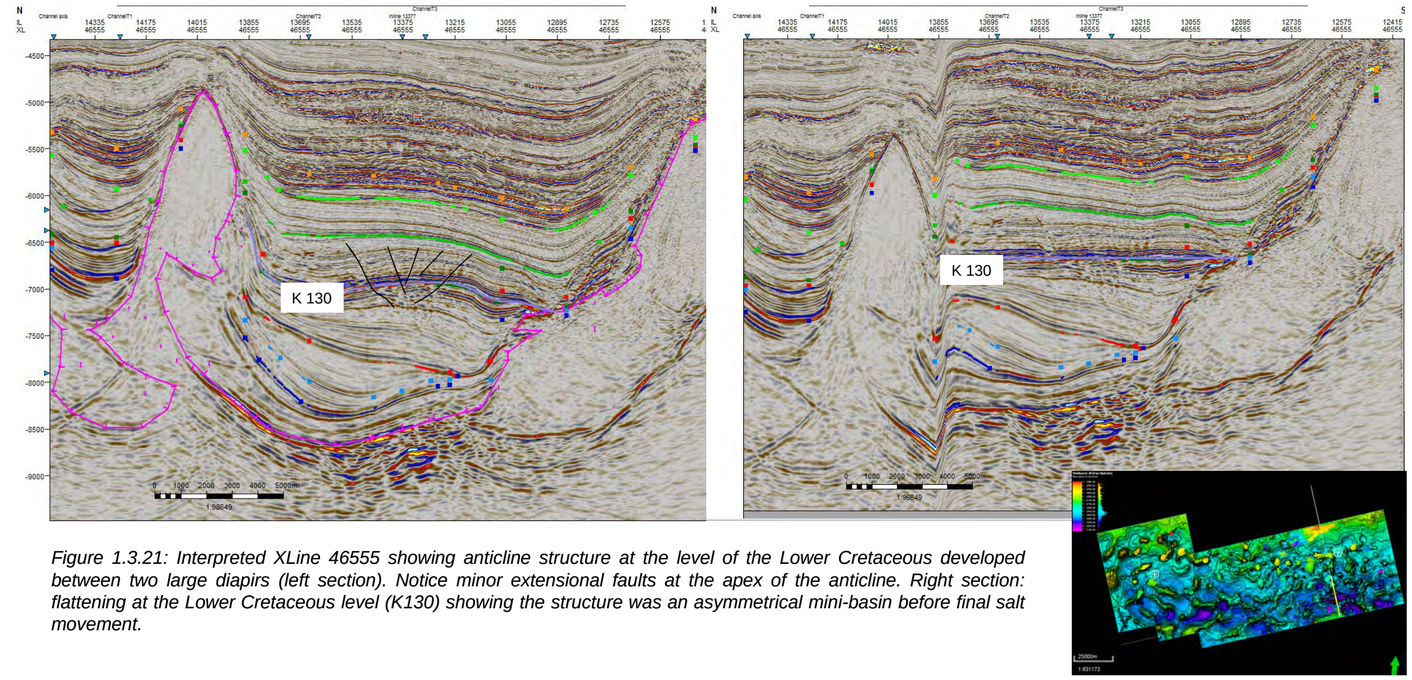

Figure 1.3.21: Interpreted XLine 46555 showing anticline structure at the level of the Lower Cretaceous developed between two large diapirs (left section). Notice minor extensional faults at the apex of the anticline. Right section: flattening at the Lower Cretaceous level (K130) showing the structure was an asymmetrical mini-basin before final salt movement.

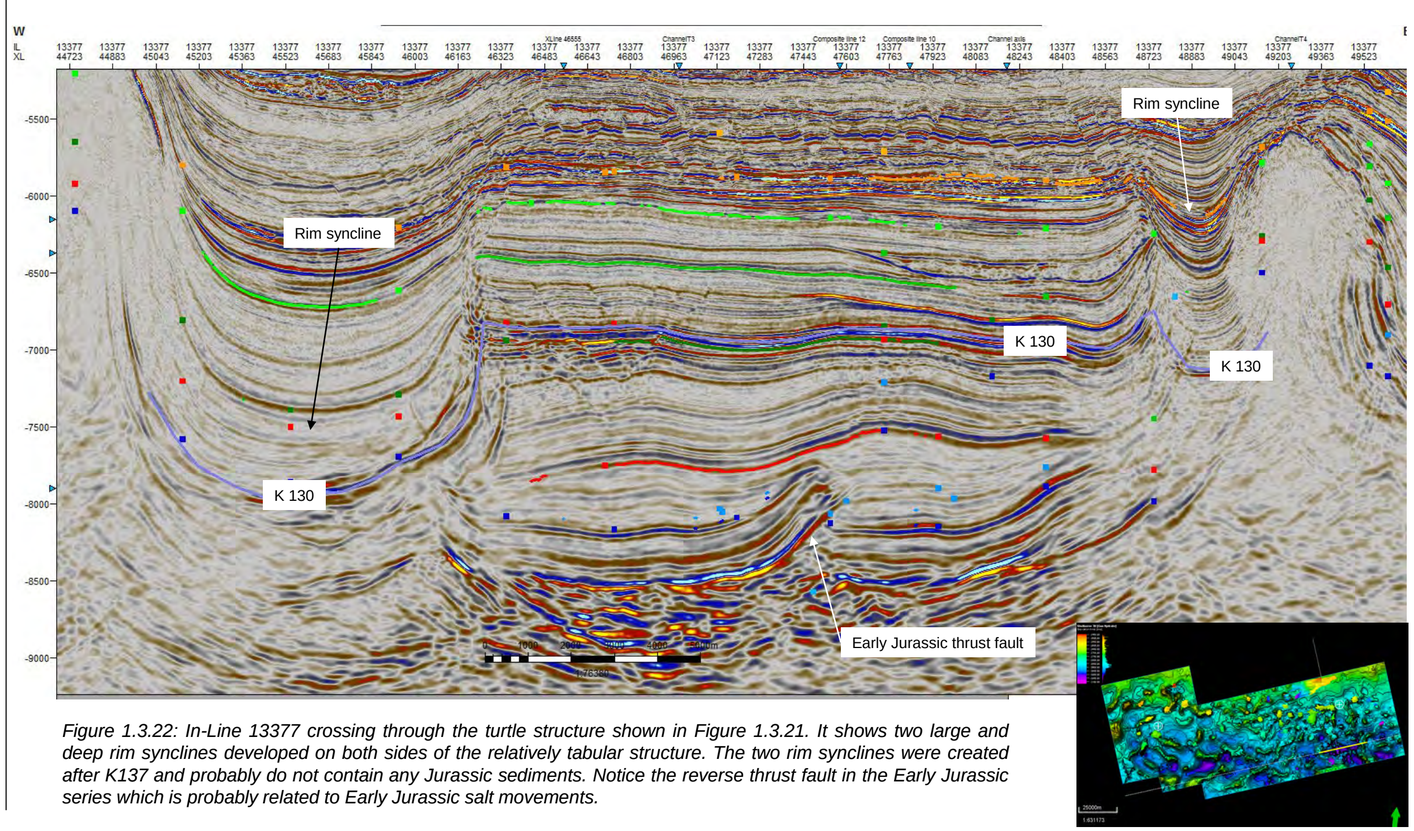

Figure 1.3.22: In-Line 13377 crossing through the turtle structure shown in Figure 1.3.21. It shows two large and deep rim synclines developed on both sides of the relatively tabular structure. The two rim synclines were created after K137 and probably do not contain any Jurassic sediments. Notice the reverse thrust fault in the Early Jurassic series which is probably related to Early Jurassic salt movements.

Shelburne Subbasin Postmortem Analysis

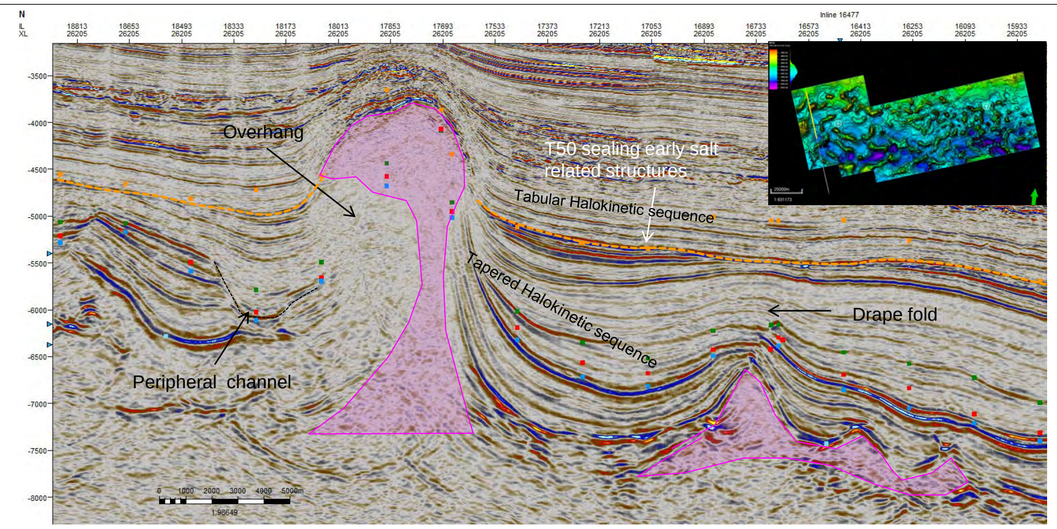

Figure 1.3.22: XLine 26205 showing two main salt structures: 1) drape faulted structure in the Jurassic and Cretaceous series sealed by the Tertiary 2) asymmetric diapir with possible overhang in its north flank and large tapered megaflap in its southern flank. This large diapir was active during Tertiary. Tapered halokinetic sequences prevailed during the Jurassic and Cretaceous while tabular halokinetic sequences seems to be the rule for Tertiary units.

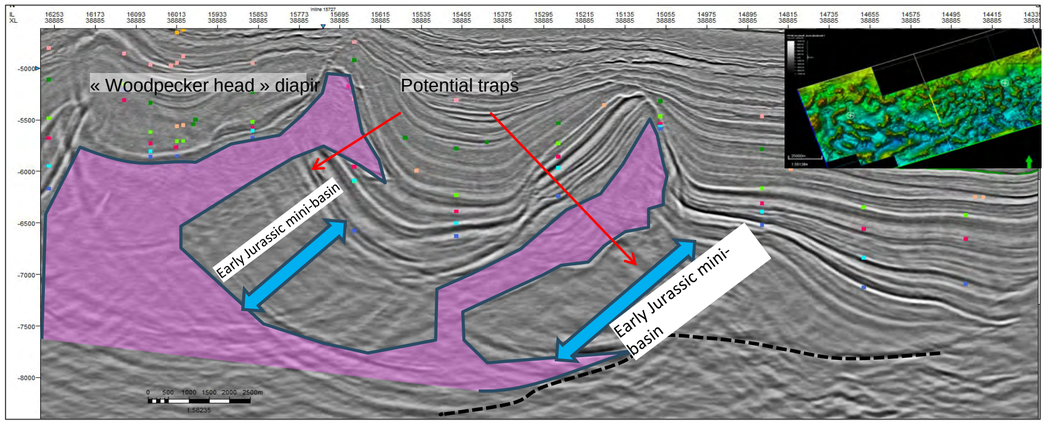

Figure 1.3.23: Seismic XLines 38885 and 28505 showing various diapir structures with potential subsalt and suprasalt traps. Notice the high variability in the Early Jurassic thicknesses indicating early salt tectonics.

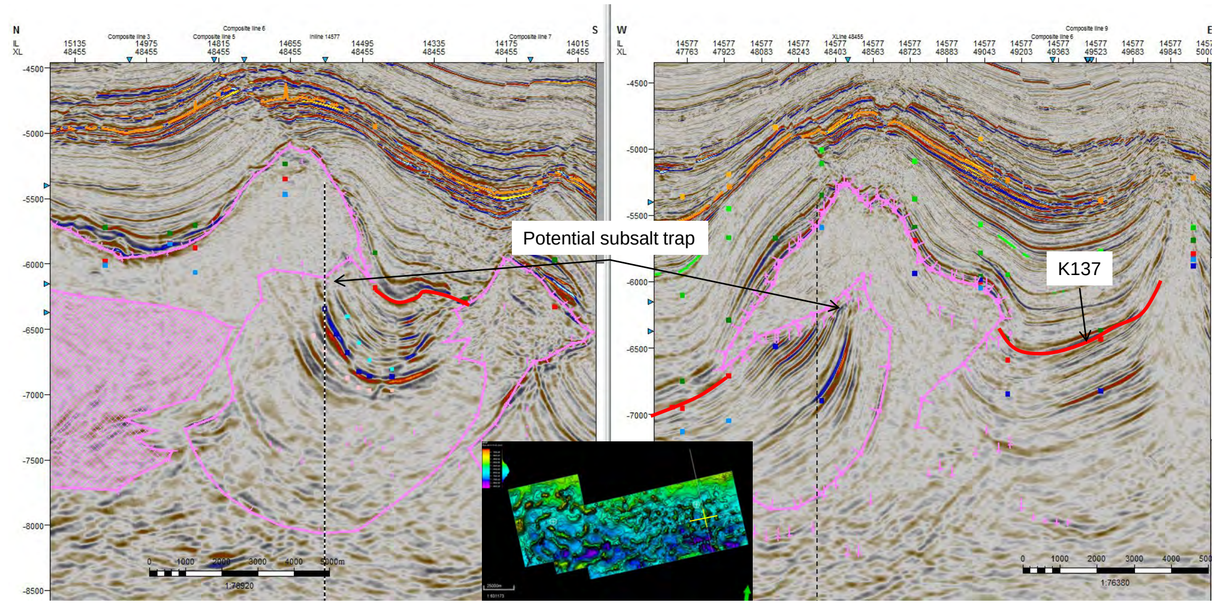

Figure 1.3.24: Seismic XLine 48455 and In-Line 14577 crossing through a potential subsalt trap (vertical dotted line indicates the intersection of the lines). Structural closure appears efficient in both the dip and strike lines but should be better constrained by 3D seismic interpretation. The overhang seems to develop by the salt tongue flowing on the sea bottom between K150 and K137 (red horizon). Potential reservoirs should be found in the Jurassic series.

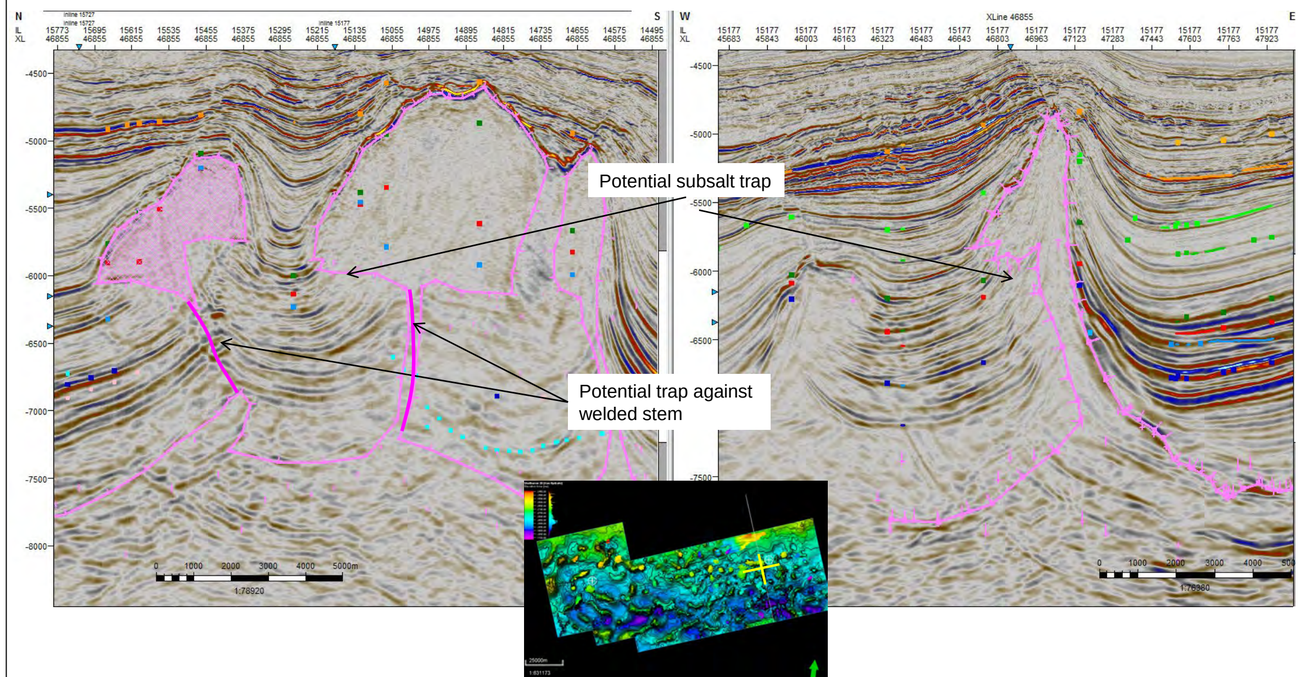

Figure 1.3.25: Seismic XLine 46855 and In-Line 15177 crossing through a potential subsalt trap (vertical dotted line indicates the intersection of the lines). Structural closure appears efficient in both the dip and strike lines but should be better constrained by 3D seismic interpretation. The overhang seems to develop by salt tongue flowing on the sea bottom between K150 and K137 (red horizon). Potential reservoirs should be found in the Jurassic series.

Fault Traps

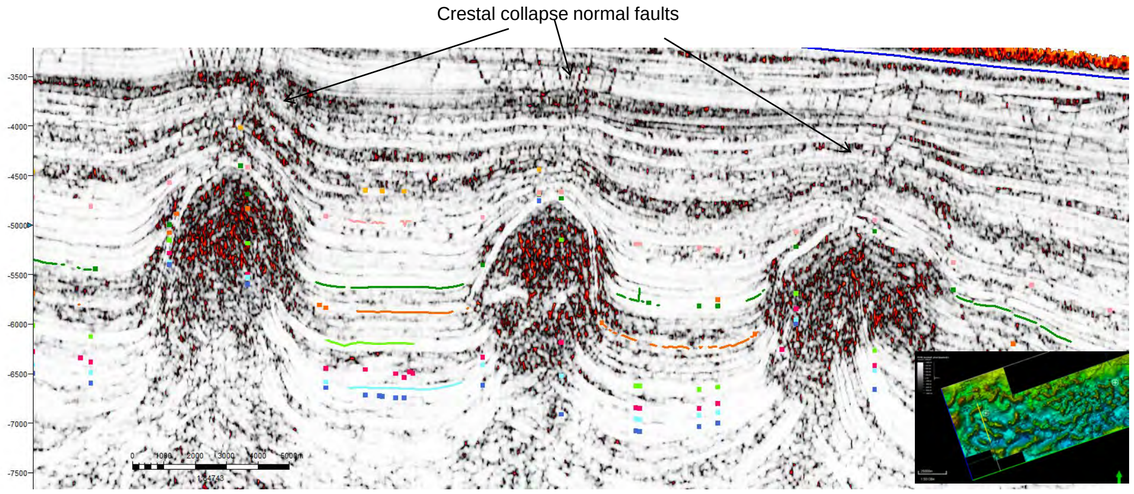

Figure 1.3.26: Seismic Xline 28505 with variance attribute highlighting 3 diapirs topped by numerous normal faults developed during the sinking of the sediments in the salt. These normal faults constitute one of the most numerous producing targets in the Gulf of Mexico where clastic sediment supply is very important. These faults act as transverse barriers (and potential traps) when coated by shale or when juxtaposing a reservoir with a sealing rock, but also constitute longitudinal / vertical conduits inducing HC leakage.

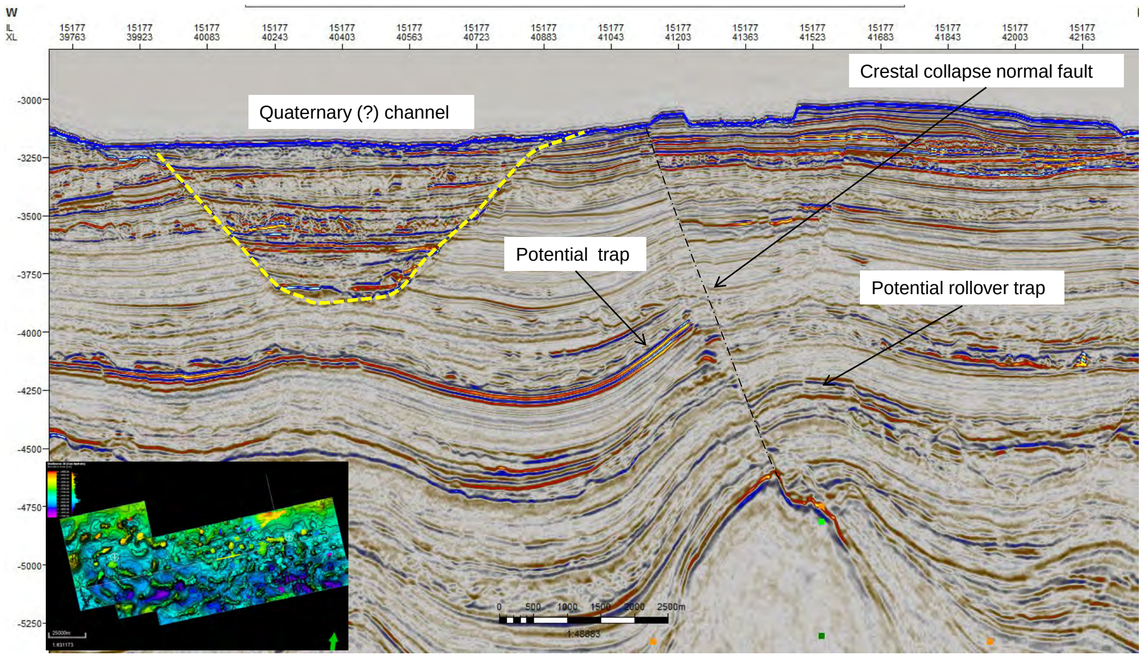

Figure 1.3.27: Seismic InLine 15177 highlighting a normal fault rooted in the apex of a diapir. This fault is active at present and cuts through the whole sedimentary sequence reaching the sea floor. Entrapment generally occurs in the footwall of the normal faults but hanging wall structures, like rollovers, also constitute potential targets
Notice the huge (more than 5 km wide) V shaped channel of possible Quaternary age, infilled by sediments with heterogeneous seismic facies.

Conclusions and Recommendations

Structural Trap Types

The structural trap types of the two recently drilled wells are:

1) Monterey Jack:

Drape fold on an early salt high (diapir possibly controlled by a basement fault). It corresponds to a 12 km^2 4-way dip closure at the K130 level.

2) Cheshire:

Saddle like structure (without 4-way dip closure) at the level of the K130. The trap mimics a “turtle structure” in the N-S direction (XLine) but is a syncline confined between two salt walls in the E-W direction (InLines). Unless salt walls constitute efficient seals, the Cheshire structure is not closed at the level of the Lower Cretaceous.

Most of the classically described and producing traps in salt basins can be found in the Shelburne area and can be identified on the present 3D seismic data. However salt diapirs in the Shelburne Subbasin have a relatively chaotic distribution with varied geometries and orientations. In the southwestern part of the survey, NW-SE salt walls may have been induced by basement transform faults.

Overhang, lateral wings and high angle megaflaps with both tapered and tabular halokinetic sequences exist in several parts of the 3D survey. Subsalts traps seem to be relatively numerous but need to be investigated with detailed mapping of the salt diapirs to define closed traps.

Despite the presence of traps, the main issue remains the definition of potential reservoirs in the different units.

Early Salt Tectonics and the Early Jurassic Petroleum System

Most of the analysed data indicate that salt tectonics began very early, probably during Early Jurassic times with salt diapirs and salt tongues reaching the sea bottom. This implies the Early Jurassic deposits were already partly controlled by salt diapirs. Mini-basins were already active and constituted separated ponded basins progressively sinking in the salt “fluid”. This means that deposition and distribution of Early Jurassic sediments were not continuous and ubiquitous because salt highs and ridges already existed. This implies that the assumption made in PFA 2011 of a simple, ubiquitous early Jurassic source rock distributed everywhere as a continuous unit coincident with the primary salt basin, is unlikely. A more likely scenario is that any Early Jurassic source is distributed in a series of discrete mini-basins. To better understand the distribution of potential Early Jurassic source rocks and possible reservoirs, the following recommendations are made:

1) Interpret complementary horizons in the Early Jurassic units (between J163 and top salt).
2) Interpret the top salt in detail. A refined picking of the top salt, every 25 or 10 lines, is needed to define salt-related traps, given all the structural variations.
3) Build isopach maps of the Early Jurassic units and superimpose them on the structural maps to better define inverted early mini-basins that can constitute potential targets either for source rocks or for reservoirs. True isopachs are necessary (not only vertical projections) since diapir flanks may be very steep.
4) Focus on connected and long-lasting mini-basins since hydrocarbon maturation and migration will remain an issue if the only source rock is Early Jurassic.

1.4 Basin Modelling Postmortem Analysis

Shelburne Subbasin Postmortem Analysis

PFA 2011 TemisSuite™ Model and Adaptation in OpenFlow™

The TemisSuite™ 3D model built in 2011 was loaded on the new OpenFlow™ 2018 platform without modification. An alternative TemisSuite™ 2D section of the Line 1400 has also been reloaded. No new simulations have been performed except for confirming the stability of the legacy model on the new platform. Only minor modifications were made to the workflow to compute drainage area maps.

The legacy 3D model characteristics are:

- Pressure, maturity, expulsion modelling
- Prospect evaluation from map-based simulations (Petpot™ model converted to TCA ™ model for the review)
- Maximum mesh resolution = 1000*1000m (maps built from 2D seismic)

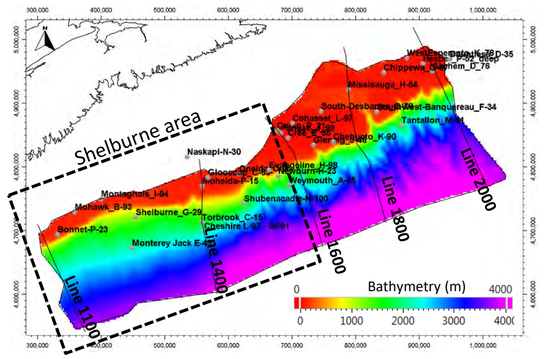

2011 PFA Petroleum System Hypothesis

The petroleum system hypothesis modeled in 2011 considered 5 plays fed by 5 potential source rock layers. The reservoirs and source rocks considered are described in the next table. The new wells revealed that several elements of the petroleum system are missing in the deep Shelburne area, in particular Cretaceous and Upper Jurassic source rocks, however the basin model has not been modified at this stage.

PETROLEUM SYSTEM ELEMENTS	STRATIGRAPHIC AGE	RESERVOIRS		SOURCE-ROCKS	NEW WELL DATA INPUT (Cheshire L-97 and Monterey Jack E-43)
		Lithostratigraphic equivalent	Seismic marker	Kerogen type	
RSR	Albian-Cenomanian	Logan	K112-K94		Absence of significant reservoir confirmed in the area
SR	Aptian			III	Potential source rock potential not confirmed
SR	Valanginian			III	Potential source rock potential not confirmed
RSR	Hauterivian-Barremian	Upper Mississauga	K130-K123		Absence of significant reservoir confirmed in the area
RSR	Berriasian-Hauterivian	Middle Mississauga	J150-K130		Absence of significant reservoir confirmed in the area
SR	Tithonian			II-III	Potential source rock potential not confirmed
RSR	Oxfordian-Tithonian	Baccaro/MicMac	J163-J150		Limited potential calcaneritic reservoirs (rather Monterey Jack)
SR	Callovian	Misaine		II-III	Potential source rock potential not confirmed (shale in Cheshire)
RSR	Early_Middle-Jurassic	Scatarie	J200-J163		**Potential calcaneritic reservoirs** (Lower Jurassic not reached)
SR	Pliensbachian			II	Not reached = **Possible Candidate SRs in Early Jurassic** (including Pliensbachian)

Calibration of PFA 2011 Model vs New Wells (Cheshire L-97 & Monterey Jack E-43)

The new well data (Cheshire L-97 and Monterey Jack E-43) werecompared with PFA 2011 3D model results to test the predictivity of the model. Temperatures and pressures are available for Cheshire L-97 only, while vitrinite was sampled in both wells.

Simulated data presented below display a good fit with observed data in both wells indicating an excellent predictivity of the PFA 2011 3D model (i.e., at a given depth the pressure, temperature and maturity level for the Mesozoic and Cenozoic is very sound and confirmed by the wells). It implies that the subsidence history and lithospheric model (coupled to the sedimentary model for computing the basal heat flow) used in 2011 were very accurate.

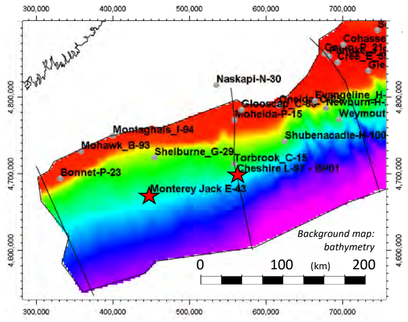

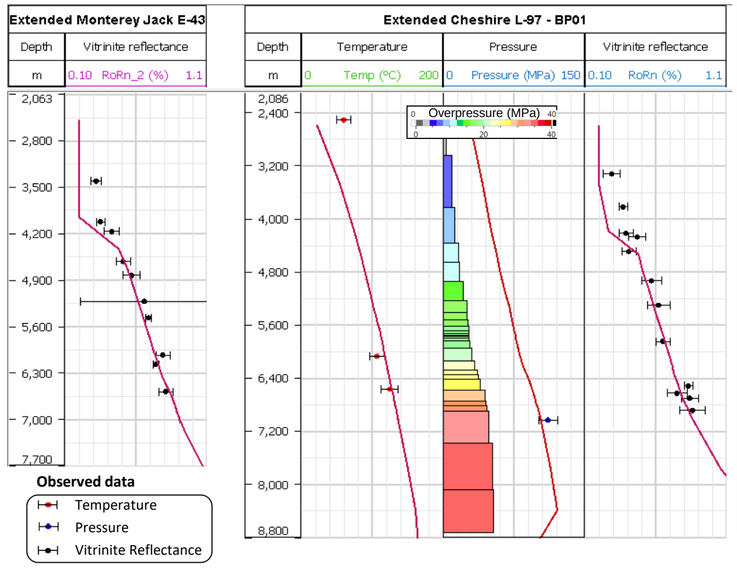

Maturity data confirms the Middle Jurassic is within the Oil Window in both wells (up to 0.9%VR0).

The relatively high overpressure, remarkably predicted by the model and confirmed by the Cheshire well test, strongly supports a very low estimate of overall permeability in the Lower Cretaceous and Jurassic layers. The hypothesis in the legacy model is that there is no regional carrier bed in the deep basin, although isolated reservoir may exist.

Map-based Simulation Hypothesis (PFA-2011 Petpot™ model)

The map-based simulation Petpot™ built in 2011 (advanced Ray Tracing module implemented in the TemisSuite source rock and structural 3D model) aimed at identifying drainage areas and closed traps through geological time, and at assessing in-place hydrocarbons at basin scale. The main hypotheses were: (1) relatively low resolution structural maps built with 2D seismic lines available in 2011 in the Shelburne Subbasin; (2) minimum 10m thick reservoir layer even if the sedimentary study did not forecast the presence of reservoir rocks; (3) hydrocarbon charge computed by TemisSuite This model remains reasonable after the drilling; (4) only four-way closure traps, no possible trapping against salt diapirs (sediment / salt body interface considered permeable based on observations of the new wells).

Significant salt tectonics in the deep basin defines a restricted drainage area (<100km² for Cheshire L-97 & <200km² for Monterey Jack E-43) leading mostly to vertical migration and limited lateral connection between small drainage areas. Closed traps have relatively small surfaces (often <10 km²). It is worth mentioning that the absence of a large trap at Cheshire and Monterey Jack is explained by the conservative hypotheses used in PFA 2011, in particular the focus on 4-way dip closures. According to this model the largest accumulations may hold 50 to 150 Mboe (optimistic scenario).

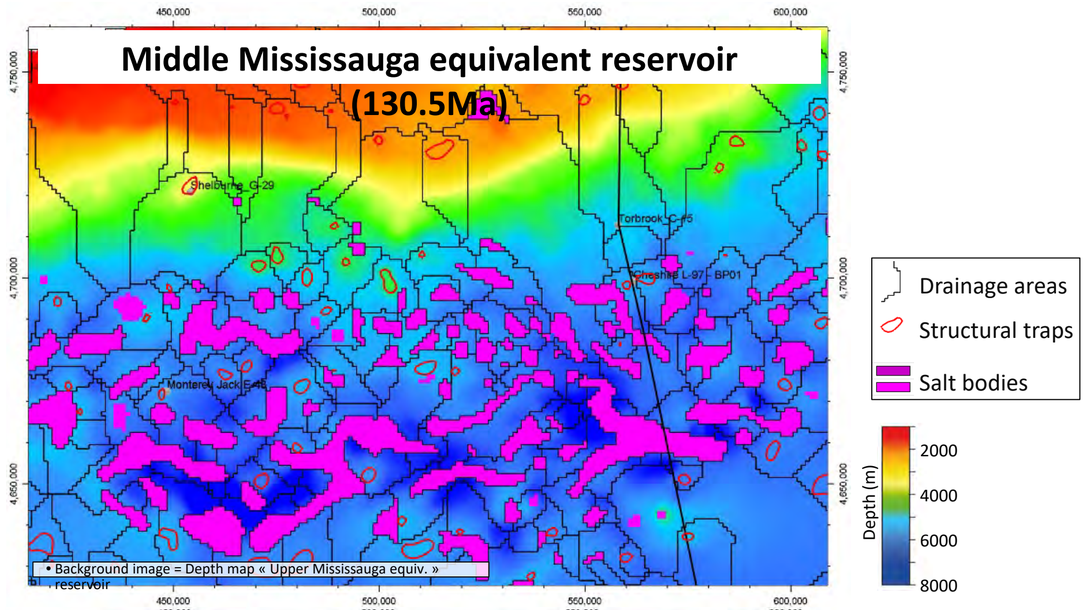

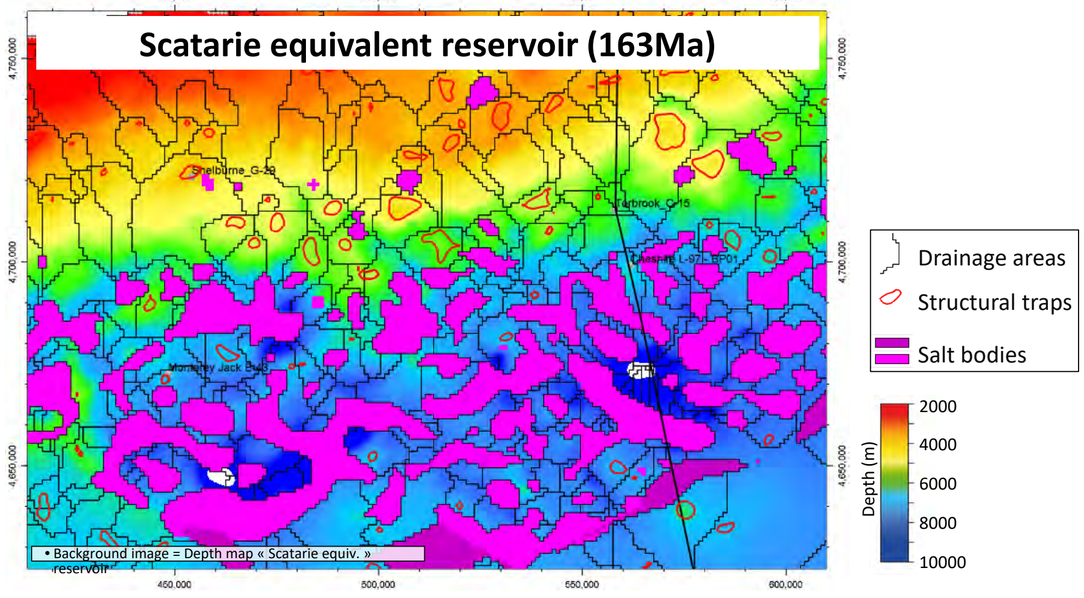

Shelburne Subbasin Postmortem Analysis

Thermal Maturity of Potential Lower Jurassic Source Rock

There is apparently no significant source rock potential in Cretaceous and Upper-Middle Jurassic intervals, at least in the drilled areas. The remaining candidate source rocks are expected in undrilled Lower Jurassic units (Pliensbachian according to Moroccan and Portuguese analogs, possibly Toarcian). The “Pliensbachian” SR in the legacy model represents this possibility; it is the deeper layer of the model just above the Triassic salt. This source rock has a limited extension in the model (deposited in local depressions after the rifting?).

3D modelling indicates that in the Shelburne Subbasin only deep source rocks of Jurassic age would have locally reached the oil window (VR0 >0.6%). The potential Pliensbachian SR is the only one with a relatively high maturity level (VR0 > 1%) in most of the salt mini-basins, where the gas window can be reached. The dry gas window (VR0> 1.8-2%) is never reached. This model is consistent with the observations from seabed seep samples collected by NSDEM (see next Plate).

At present day in the vicinity of Cheshire L-97 and Monterey Jack E-43, the maturity level of a potential Pliensbachian source rock would be close to 1.2-1.4% (wet gas window). A Toarcian / Middle Jurassic source rock would be in the oil/condensate window.

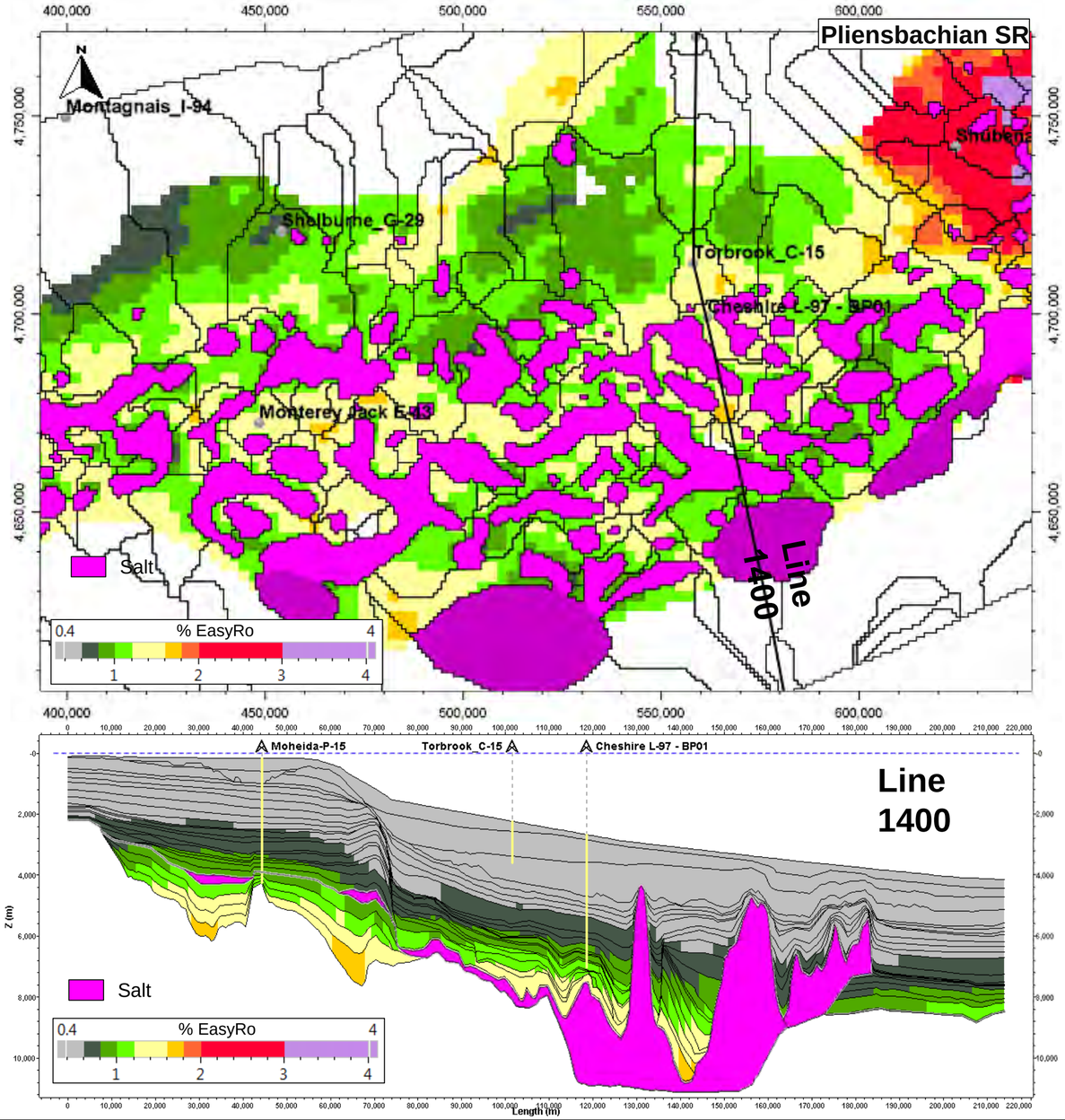

Transformation Ratio

Computed transformation ratios suggests that the contribution of a Toarcian / Middle Jurassic source rock (represented by the “Callovian SR” in the 3D model) would be limited to the deepest mini-basins in the Shelburne area. In contrast, potential Pliensbachian SR could fully contribute to an efficient petroleum system everywhere (TR > 70% in general). In the PFA 2011 its hydrocarbon generation potential was assumed to be greater than 1000kg$_{generated\text{-}HC}$/m^2 (~7 Mbble$_{generated\text{-}HC}$/km²).

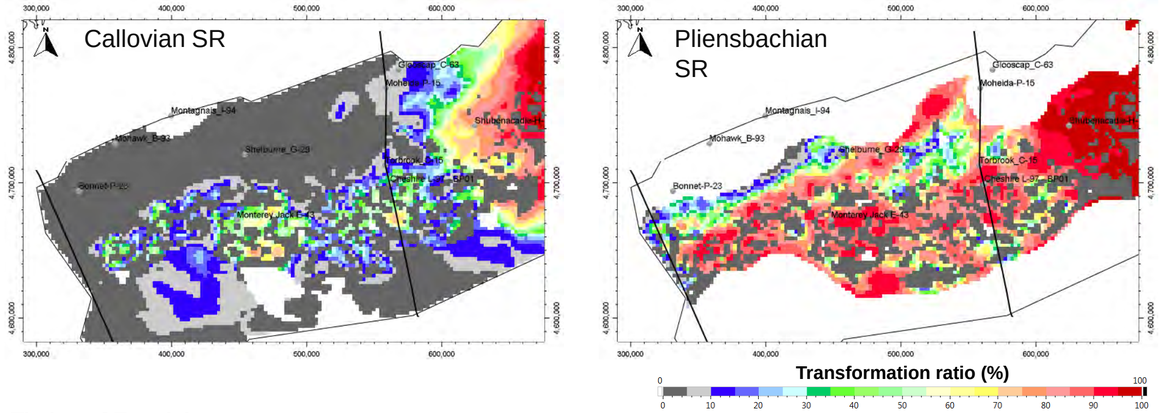

Timing of Expulsion

Extractions of transformation ratio through time at Cheshire (L-97) and Monterey Jack (E-43) locations indicate that a potential Lower Jurassic petroleum systems would be active at present-day. The onset of the oil expulsion begins at 90 to 120 Ma (earlier in Cheshire), but the hydrocarbon generation and expulsion drastically increases after the Eocene (~50 Ma). The Neogene burial stimulates hydrocarbon generation and expulsion at present day. The expulsion of gas has started to replace the expulsion of oil in the Cheshire and Monterey Jack areas since 20 Ma.

This hydrocarbon expulsion timing has several consequences on the play assessment: (1) the major expulsion phase post dates the last period of major salt deformation and the potential structuration of salt tectonic-related traps (good timing); (2) however a slower halokinesis is still active around some diapirs, which may locally enhance a progressive vertical migration of hydrocarbons; (3) shallow Cretaceous and Tertiary plays can be efficiently sourced from a deep Jurassic source rock.

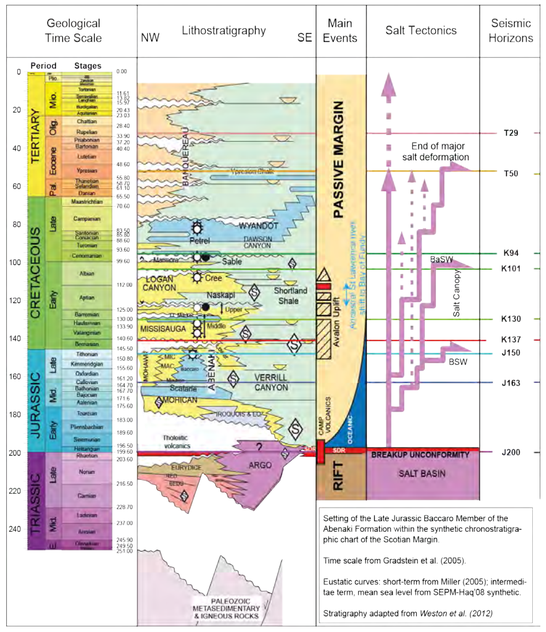

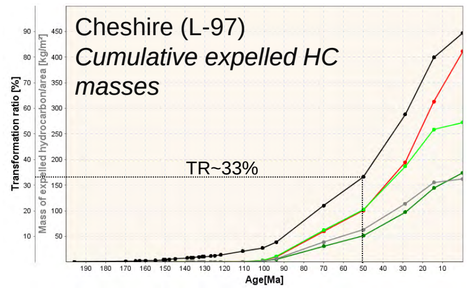

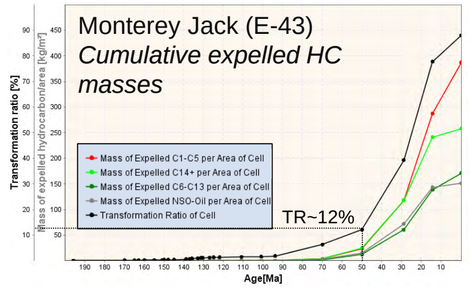

Shelburne Subbasin Postmortem Analysis

Postmortem Petroleum System Evaluation

Lack of hydrocarbon accumulation in the recently drilled wells may result from:

- A risk of **reservoir presence** and carrier beds in Cretaceous and Upper Jurassic units. Generated HCs could not concentrate in large reservoirs. Only pervasive HC accumulations in close vicinity to SR layers may be expected. This is a possible explanation of the diffuse gas observed on mudlogs (i.e., a reported small amount of in-situ generated biogenic and/or thermogenic gas in low-TOC shale intervals).
- A risk of **active source rock presence.** There is as yet no direct evidence for the existence of a prolific source rock in the deep Shelburne Subbasin (the potential Pliensbachian source rock was not drilled).
- A risk of **charge efficiency** (in addition to the risk on source rocks) due to small drainage areas and structure size, very poor lateral connection of drainage areas (i.e., isolated mini-basins between salt bodies), mostly vertical migration possibly along salt diapirs (drainage <100 km^2 for Cheshire & <200 km^2 for Monterey Jack). Observed high pressure (predicted in the model) confirms the lack of efficient lateral connection at large scale. Under these conditions a very rich source rock would be required to charge large traps.

Throughout the deep Shelburne Subbasin these risks were recognized in the PFA 2011 (OETR, 2011), in particular the risk of reservoir presence and the charge risk due to the structure of migration paths / drainage areas. The CCRS map of the targeted Upper Jurassic indicated a high risk everywhere in the deep basin. The ranking in terms of hydrocarbon resources was rather pessimistic; only small and isolated hydrocarbon accumulations were expected according to the TemisSuite 3D model (OETR, 2011).

New Evidence for Active Thermogenic Source Rock in the Shelburne Area

Several elements still favor an active petroleum system in the Shelburne Subbasin:

- Recent geochemical analyses (APT, 2018) confirm that no prolific oil/gas-prone source-rocks were detected in wells through the drilled section (Upper Jurassic to present). However, the presence of a thermogenic (isotopes, fluid inclusions) gas flare in a carbonate layer (Scatarie Mbr.) near the TD of Monterey Jack E-43 suggests the presence of an active source rock in the Early-Middle Jurassic (not penetrated).
- Recent DHI and gas hydrate mapping performed on seismic data by Beicip Franlab indicates a consistent fit between DHI location and the area of maximum maturity (potential Pliensbachian SR within the gas window, VR0>1.2%). This correlation strongly supports the existence of at least one active petroleum system. Hydrocarbons (rather condensate and gas at present day) generated in potential Early Jurassic source rocks would migrate vertically up to Cenozoic sediments and would often accumulate on top of the salt diapirs.
- Several hydrocarbon seeps have been identified in the area of interest in seabed surveys conducted by NSDEM (2015, 2016 & 2018). Thermogenic gas is quite common in the seeps in the Shelburne area, which is compatible with the maturity level of a potential Lower Jurassic source rock.

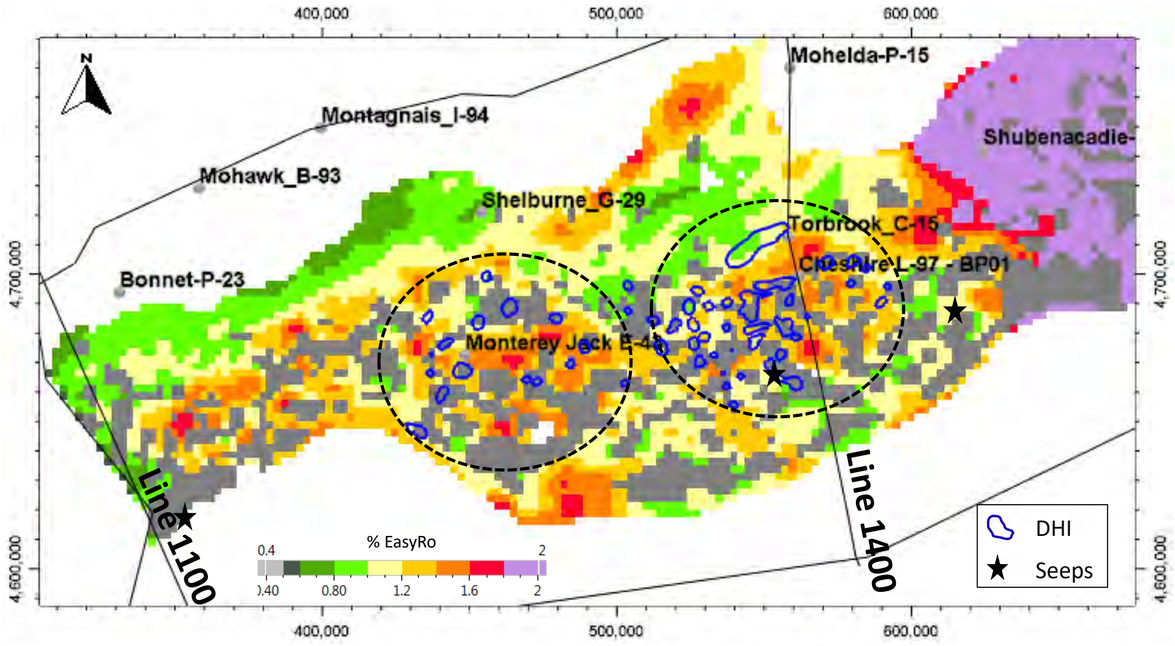

Even if the maturity model is predictive, the exact depth (and so the maturity) of the potential Lower Jurassic source rock(s) is uncertain. It can be expected that in new plays of the deep salt basin, the presence of condensates / humid gas is more likely than the presence of dry thermogenic gas or black oils.

New Considerations for Reservoir Presence and New Hypotheses on Petroleum Systems

Despite the high risk of certain petroleum system elements identified in the 2011 PFA, the potential of several plays should be re-evaluated based on new 3D seismic and well data:

- There is a potential **Tertiary and Lower Cretaceous clastic turbidites play** south of Cheshire and Monterey Jack (which is still on the slope of the sedimentary system). The Tertiary Play was not evaluated in the 2011 PFA.
- There are potential reservoirs in more proximal parts of the **Lower-Middle Jurassic carbonate ramp play** (shallow marine carbonates; See PL. 1.2.6). The geometry of this early ramp formed just after the salt deposition was poorly represented in 2011.

Both conceptual plays have been tested in a TemisSuite 2D section simulated in 2011 (line 1400, intersecting the well Cheshire). Reminder: Upper Jurassic and Lower Cretaceous layers are generating hydrocarbons in this legacy model.

- At Cheshire the model only predicts pervasive hydrocarbon accumulations in Upper Jurassic and Lower Cretaceous stratigraphic units (low hydrocarbon saturation despite the activation of several source rocks, no significant hydrocarbon accumulation, only hydrocarbon shows expected).
- However, hydrocarbon accumulations are observed in the Lower/Middle Jurassic carbonate ramp, particularly in its proximal parts where better reservoirs could be expected in accordance with the new concepts.
- There is also a possible charge of Lower Cretaceous turbidites south of Cheshire in the mini-basin where anomalies have been detected on the 3D seismic (see PL.1.1.6).
- Note the presence of migration paths up to the surface along some diapirs, which could explain the local occurrence of DHIs and seeps.

The effectiveness of traps (with reservoir rocks) under allochthonous salt bodies also has not so far been tested.

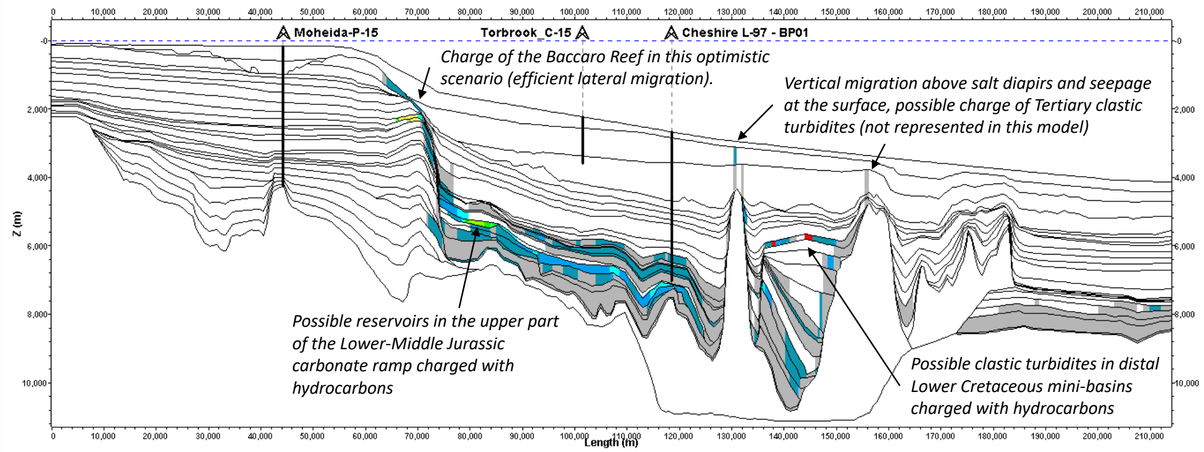

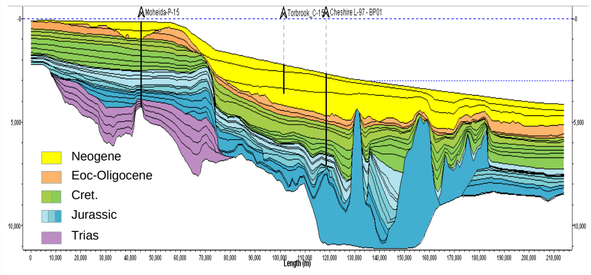

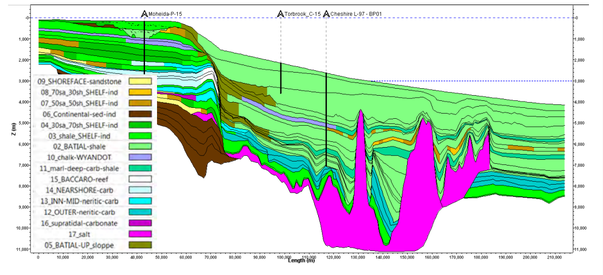

Petroleum systems modelling way forward

New 3D basin modeling is recommended to evaluate promising new plays:

- New concepts of facies distribution (Lower-Middle Jurassic carbonate ramp, Lower Cretaceous and Tertiary turbidites in distal mini-basins) should be implemented in the TemisFlow 3D model. These new targets are less **deep** and **potentially lower risk**.
- New structural maps from the 3D seismic give the opportunity to build a **high-resolution model of migration paths and traps**.
- An alternative scenario with less leakage at the sediment-salt interface can be tested (larger traps and drainages expected).
- **An updated hypothesis on source rocks distribution will be necessary.**

REFERENCES

APT Applied Petroleum Technology AS. 2018. Forensic geochemical study of deepwater Shell wells Cheshire L-97 and Montery Jack E-43. Final Report APT18-5346. 43 p.

APT Applied Petroleum Technology AS. 2019. Geochemistry Data Report for 2018 Scotian Slope Coring Program. Report APT-18-5348. 308 p.https://oera.ca/research/piston-coring-geochemistry-program

Bouroullec, R., Weimer, P., & Serrano, O. 2017. Petroleum geology of the Mississippi Canyon, Atwater Valley, western DeSoto Canyon, and western Lloyd Ridge protraction areas, northern deep-water Gulf of Mexico: Traps, reservoirs, and tectono-stratigraphic evolution. AAPG Bulletin, 101(7), 1073-1108.

Chavez, I., Piper, D.J.W., Pe-Piper, G. 2018. Correlation of the Aptian Naskapi Member of the Scotian Basin and its regional implications, Canadian Journal of Earth Sciences, 2018, 55:514-535, https://doi.org/10.1139/cjes-2017-020

Deptuck. M.E, Brown, D. E., Altheim. B. 2015. Call for Bids NS15-1 – Exploration history, geologic setting, and exploration potential: Western and Central regions, CNSOPB Geoscience Open File Report, 2015-001MF, 49 p.

Deptuck. M.E, Altheim. B. 2019. Rift basins of the central LaHavePlatform, offshore Nova Scotia, CNSOPB Geoscience Open File Report, 2018-001MF, 54 p.

Deptuck, M. and Campbell, D.C. (2012). Widespread erosion and mass failure from the 51Ma Montagnais marine bolide impact off southwestern Nova Scotia, Canada, Can. J. Earth Sci., 49, p.1567 – 1594.

Eichenseer H.Th., Walgenwitz F.R., Biondi P.J. 1999. Stratigraphic control on facies and diagenesis of dolomitized oolitic siliciclastic ramp sequences (Pinda Group, Albian, Offshore Angola). AAPG Bulletin, v. 83, p. 1729-1758.

Fensome, R. and Williams, G., 2001. The Last Billion Years, a geological history of the Maritime Provinces of Canada, AGS special publication, 15, 206p.

Hudec, M.R., and Jackson, M.P.A. 2007. Terra infirma: Understanding salt tectonics. Earth-Science Reviews 82 (2007) 1-28. 28 p.

Kidson, A.G., Brown, D.E., Smith B.M. and Altheim, B. (2005). The Upper Jurassic Abenaki Formation Offshore Nova Scotia: A Seismic and Geologic Perspective. Canada-Nova Scotia Offshore Petroleum Board, Halifax, 165p.

Letouzey, J. 1990. Salt related structures. IFP internal report.

Martell, B., Sosa, J., Payne, J. 2016. Cheshire L-97/L-97A End of Well Report, Nova Scotia – Shelburne Basin, Shell Canada Energy, EP201611202835, 178p.

OERA: Offshore Energy Research Association. 2015. South West Nova Scotia Expansion: Georges Bank and Shelburne Subbasin Study. Nova Scotia Department of Energy Report.
https://oera.ca/research/sw-nova-scotia-expansion-atlas-2015

OETR: Offshore Energy Technical Research Association. 2011. Play Fairway Analysis Atlas - Offshore Nova Scotia. Nova Scotia Department of Energy Report, NSDOE Records Storage File No. 88-11-0004-01, 347p.
https://oera.ca/research/play-fairway-analysis-atlas

Pilcher, R. S., Kilsdonk, B., Trude, J. 2011. Primary basins and their boundaries in the deep-water northern Gulf of Mexico: Origin, trap types, and petroleum system implications. AAPG bulletin, 95(2), 219-240.

Nagle, J., Pe-Piper, G., Piper, D.J.W., Saint-Ange, F. 2019. Predictive modelling of sandstone reservoir distribution in the SW Scotian Basin, AGS 45th Colloquium.

MacLean B.C. and Wade J.A. 1993. Seismic markers and stratigraphic picks in the Scotian Basin wells. East Coast Basin Atlas series, Energy, Mines and Resources Canada, 276 pp.

Pierre A., Durlet C., Razin P., Chellai E.H. 2010. Spatial and temporal distribution of ooids along a Jurassic carbonate ramp: Amellago outcrop transect, High-Atlas, Morocco. *From*: Van Buchem F., Gerdes F., Esteban M. (Eds) *Mesozoic and Cenozoic Carbonate Systems of the Mediterranean and Middle East: Stratigraphic and Diagenetic Reference Models*. Geological Society, London, Special Publications, 329, p. 63-85.

RPS Energy, 2018. Biostratigraphic analysis of selected intervals from the Cheshire L-97 & L-97a wells, offshore Nova Scotia, Canada, Report for Nova Scotia Department of Energy and Mines, 41p.

RPS Energy, 2018. Routine and Wellsite biostratigraphic analysis of the Monterey Jack E-43/E-43 A wells, license EL2424, Shelburne Subbasin, offshore Nova Scotia, Canada, Report for Shell Canada Energy, 65p.

Saint-Ange, F., Hawie, N., Marfisi., E., Colletta, B., Dimitri, S., Cuilhe, L., MacDonald., A., Luheshi, M. 2018. Exploration well failures and reservoir distribution along the Scotian Slope (Eastern Canada), Conjugate Margin Conference, Halifax August 19-22.

Sibuet, J.C., Stéphane, R., Srivastava, S. 2011. Plate tectonic reconstructions and paleo-geographic maps of the central and north Atlantic oceans, Final report, Annex PFA 2011

Van Noort, R., Descamps, G., Magee, W. 2017. Monterey Jack E-43/E-43A End of Well Report, Nova Scotia – Shelburne Basin, Shell Canada Energy, EP201701214300, 125p.

Wade J.A. and MacLean B.C. 1990. The geology of the southeastern margin of Canada, Chapter 5. In Geology of the Continental Margin of Eastern Canada, Geological Survey of Canada n°2, Keen, M.J. and Willians, G.L. Eds, p. 167-238**.**

Weimer, P., Zimmerman, E., Cossey, S. P., Hirsh, H., Snyder, B., Leibovitz, M., & Adson, J. 2017. Atlas of fields and discoveries, central Mississippi Canyon, Atwater Valley, northwestern Lloyd Ridge, and western DeSoto Canyon protraction areas, northern deep-water Gulf of Mexico. AAPG Bulletin, 101(7), 995-1002.

Weston, J.F., MacRae A.R., Ascoli P., Cooper M.K.E., Fensome R.A., Shaw D., Williams G.L. 2012. A revised biostratigraphic and well-log sequence stratigraphic framework for the Scotia Margin, offshore eastern Canada. Can J. Earth Sci 49, p. 1417-1462.

Zhang, Y., Pe-Piper, G., Piper, D.J.W. 2014. Sediment geochemistry as a provenance indicator: Unravelling the cryptic signatures of polycyclic sources, climate change, tectonism and volcanism, Sedimentology, 61, 383-410, doi: 10.1111/sed.12066.